CTU in Prague
Faculty of Mechanical Engineering
Department of Mechanics

PhD Thesis

Mapping of Fatigue Damages – Program Shell of FE-Calculation

Ing. Jan Papuga

Branch of study: Mechanics of Solids, Deformable Bodies and Continua

Doc. Ing. Milan Růžička, CSc.
Supervisor

Prague, August 2005

Title:	Mapping of Fatigue Damages – Program Shell of FE-Calculation
Author:	Ing. Jan Papuga

Department:	Department of Mechanics
Faculty:	Faculty of Mechanical Engineering
University:	Czech Technical University in Prague
Address:	Technická 4, 166 07 Prague 6, Czech Republic

PhD Programme:	Mechanics of Solids, Deformable Bodies and Continua

Supervisor:	Doc. Ing. Milan Růžička, CSc. Department of Mechanics Faculty of Mechanical Engineering Czech Technical University in Prague

Number of pages:	115
Number of figures:	37
Number of tables:	20
Number of appendices:	9
Printed:	August 2005

Keywords:

multiaxial fatigue, critical plane criteria, integral criteria, fatigue postprocessors, mean stress effect, phase shift effect

ANNOTATION

The project described here is focused on multiaxial fatigue calculation in high cycle fatigue. The phenomenon of multiaxial fatigue, some basic assumptions and formulas are given first. Then the set of contemporary commercial fatigue postprocessors utilizing FE-data is reviewed in short. Since the postprocessors are aimed at commercial use, a possibility to use them for research is very limited. Therefore a PragTic software package, which is presented here, was developed. A set of experimental data (129 experiments altogether) was compiled from references. Thanks to the PragTic software, they could be evaluated using 12 existing high cycle fatigue criteria. Fruitfulness of the individual criteria is commented and also the effects of phase shift and mean stress can be examined separately. These results serve as a basis for design of two new criteria. First of them is of integral nature, the second one is based on a search for the critical plane. The integral version demands great computational effort. The critical plane criterion is thus emphasized too, though it leads to slightly worse prediction and its mathematical basis embodies some problems commented here. Nevertheless, the both proposed criteria give results which largely overcome results of any other criterion gathered here. The both criteria were generated from a set of 26 other versions. Here the advantage of PragTic was taken, because it can evaluate more criteria and load regimes together simultaneously.

ANOTACE

Tento projekt je zaměřen na multiaxiální výpočet únavy ve vysokocyklové oblasti. Nejprve je zde popsán fenomén multiaxiální únavy, některé zde platné předpoklady a základní vztahy. Poté jsou tu zhodnoceny současné komerční únavové postprocesory MKP dat. Jelikož jsou zaměřeny na komerční využití, je možnost jejich využití pro výzkum velmi omezená. Proto byl vyvinut softwarový balík PragTic, který je zde představen. Z literatury byl shromážděn soubor experimentálních dat (dohromady 129 testů). Díky PragTicu mohla být tato data vyhodnocena při použití celkem 12 existujících kritérií pro vysokocyklovou oblast. V dalším textu jsou jednotlivá kritéria vyhodnocena a také jsou odděleně posouzeny vlivy fázového posuvu a středního napětí. Všechny tyto výsledky pak slouží jako základ pro návrh dvou nových kritérií. Jedno z nich je z podstaty kritériem integrální, druhé je založeno na konceptu kritické roviny. Jelikož je integrální verze značně výpočetně náročná, je zdůrazňováno i ono kritérium kritické roviny a to přesto, že vede k mírně horším výsledkům a některé jeho matematické vlastnosti nejsou zcela korektní. Je nutno poznamenat, že obě kritéria poskytují výsledky, které jsou výrazně lepší než výsledky kteréhokoli kritéria zde posuzovaného. Obě byla nalezena jako optimum mezi 26 jinými verzemi. Zde právě mohla být plně využita schopnost PragTicu vyhodnocovat únavovou životnost pro více kritérií a zatěžovacích režimů zároveň.

ACKNOWLEDGEMENTS

I would like to thank doc. Milan Růžička who led me through my years spent on the PhD study. His advice and his help in intermediation of interesting contacts and contracts during these years were invaluable. The PragTic software described here in Chap. 4 would not be equipped with the native database without help of doc. Miroslav Španiel. His persuasion as a devil's advocate forced me to extend the work consumed on programming by at least one year more. Truly said, it looked in these times that some bigger project with more active programmers was arising, so I accepted his idea. I hope it was worth while although I was left alone with my PragTic code at last. I thank him for his great help as well, because he proposed concepts of the data_vector, data_base and memory pool and a core of their source codes too.

I would like to thank to the representatives of the ŠKODA VÝZKUM s.r.o. – namely to Ing. Miloslav Kepka, CSc and Ing. Marek Hejman, PhD. who made the finish of the PhD thesis possible with granting some spare time for it. Skoda Research Ltd. was also the company which ordered the state of the art survey evaluating and describing fatigue postprocessors of the FE-solution available. Parts of the survey are presented here with their kind permission.

My thanks belong to my parents. They supported me at the beginnings of the work and even when the work started to prolongate I found a suitable quiet office room at their home. I cannot imagine finish of the PhD thesis without their offer. My father spent a lot of time as a proof reader. I thank him for his patience.

At last, I would like to thank my wife. Even though we often argued if such a long-distance goal makes any sense, she at last accepted my viewpoint and tried to help me. Her parents helped us notably when they offered her an asylum in periods, when I needed to work all days long.

CONTENTS

LIST OF APPENDICES

NOMENCLATURE

SYMBOLS:

1, 2, 3	[-]	principal directions
b	[-]	fatigue strength exponent
b_{-1}	[MPa]	fatigue limit in fully reversed bending
b_0	[MPa]	fatigue limit in repeated bending
c	[MPa]	fatigue ductility exponent
C	[MPa]	shear stress on given plane
δ	[deg]	phase shift
ΔFI	[%]	fatigue index error
e	[-]	normal strain on given plane
E	[MPa]	elasticity modulus in tension
ε'_f	[-]	fatigue ductility coefficient
ε_n	[MPa]	normal strain
F	[N]	external force
f_{-1}	[MPa]	fatigue limit in fully reversed push-pull
f_0	[MPa]	fatigue limit in repeated tension
φ, ψ, χ	[-]	Euler angles between a global coordinate system and an examined plane
g	[-]	shear strain on given plane
G	[MPa]	elasticity modulus in torsion
γ	[-]	shear strain
γ	[-]	material parameter in Walker MSE formula
γ'_f	[-]	fatigue ductility coefficient in torsion
J_i	[MPa^i]	i-th invariant of stress tensor deviator
K	[MPa]	cyclic strength coefficient
κ	[-]	fatigue limits ratio $\kappa = f_{-1} / t_{-1}$
LLR	[-]	logarithmic lifetime ratio
LR	[-]	lifetime ratio
M	[-]	weight given to examined plane
M_B	[Nm]	bending moment
M_T	[Nm]	twist moment
N	[MPa]	normal stress on given plane
n'	[-]	cyclic strength exponent
ν	[-]	Poisson's ratio
P	[s]	period of cycle
ρ_c	[-]	factor of multiaxiality constraint (Ellyin)
S_f	[MPa]	true fracture stress
S_u	[MPa]	ultimate strength
S_y	[MPa]	yield strength
$\boldsymbol{\Sigma}$	[MPa]	stress tensor
σ_n	[MPa]	normal stress
σ'_f	[MPa]	fatigue strength coefficient
σ_H	[MPa]	hydrostatic stress
T	[MPa]	resolved shear stress
T_χ	[MPa]	mean resolved shear stress amplitude on examined plane
$t_{A,B}$	[MPa]	fatigue limit in fully reversed torsion according to type of induced crack (McDiarmid)
t_{-1}	[MPa]	fatigue limit in fully reversed torsion
t_0	[MPa]	fatigue limit in repeated tension
τ	[MPa]	shear stress
w	[-]	slope of S-N curve
W	[J]	local deformation energy

INDEXES:

a	amplitude
e	elastic component
eff	efficient
eq	equivalent
m	mean value
max	maximum value
p	plastic component
t	total value
1, 2, 3	indexes of principal stresses ($\sigma_1 > \sigma_2 > \sigma_3$)

ABBREVIATIONS:

CP	critical plane
CPA	critical plane approach of solution
Cross	Crossland criterion
CS	coordinate system
CSM	method by Carpinteri & Spagnoli for localisation of the critical plane
DV	Dang Van criterion
FE	finite element
Fin	Findley criterion
GAM	criterion according to Gonçalves, Araújo & Mamiya
HCF	high-cycle fatigue
IA	integral approach of solution
KCP	Kenmeugne et al. critical plane criterion
KIA	Kenmeugne et al. integral criterion
LCF	low-cycle fatigue
LCM	longest chord method
LHS	left hand side of equation
LPM	longest projection method
Mat	Matake criterion
MCCM	minimum circumscribed circle method
MCEM	minimum circumscribed ellipse method
MD	critical plane set according to Maximum Damage criterion
McD	McDiarmid criterion
MS	mean stress
MSE	mean stress effect
MSSR	critical plane set according to Maximum Shear Stress (or Strain) Range criterion
nMS	without mean stresses
NP	non-proportional loading
P	proportional loading
Ppd	Papadopoulos criterion
PB	plane bending
PSE	phase shift effect
RB	rotating bending
RHS	right hand side of equation
SpaC	Spagnoli method with modified MSE and CSM approach
SpaM	Spagnoli method with modified MSE and MD approach
SWT	1) Smith, Watson & Topper method of uniaxial fatigue damage calculation 2) Smith, Waston & Topper method of MSE inclusion
Ten	tension / compression
To	torsion
Z&L	Zenner & Liu criterion

NOTE

Tensors and vectors can be distinguished from scalar values by **bold letters** used in all formulas.

1 INTRODUCTION

1.1 PREAMBLE

Significant development in simulation of real behaviour of loaded components could be seen throughout last 30 years. This does not mean only the finite element methods and multibody systems. A continuing effort is applied to the development of fatigue damage computation. As the performance of computer components increases, there appear many levels of depth, at which the damaging process can be pursued in order to obtain correct simulation. An excellent representative at this point is the multiaxial solution of fatigue damage.

Pursuit to acquire an approach that allow description of damaging arising from simultaneous loading with more channels (e.g. bending and twisting) that needn't be correlated started at the 30's of the last century with Gough and Pollard. A tendency to reduce the loading to a uniaxial one was visible from the beginning, because the solution in the uniaxial category seemed to be mastered. As the time went on, another idea appeared – the damage is generally defined by some specific direction or by a specific surface of the crack incurred. An idea of a critical plane governing appearance of a crack thus originated. Later on, this solution was charged to be erroneous - the crack in its embryonic phase does not appear to follow one definite direction. It may be true later, throughout the phase of crack growth. There are too many statistical influences in the initiation phase (e.g. size of grains, possible inclusions, grains orientation). Perhaps it should be more appropriate to integrate (i.e. average) arising damage or other important parameters over all planes…

There is no generally accepted criterion for multiaxial fatigue until now. Nevertheless, there is market demand strong enough that leading fatigue software producers are forced to incorporate multiaxial modules into their fatigue postprocessors. There is great risk involved in it, thus these manufacturers usually apply more or less dated criteria. They believe that their old age together with a casual appearance in scientific reports as comparative criteria is sufficient cover for their incorporation. Some newer methods as e.g. the integral methods are moreover so computation time demanding that producers seem to hesitate if their incorporation among other technically usable methods is justified by their possibly higher predictive capability. Short introduction of features that are offered in commercial fatigue solvers is given in Sec. 4.1.

The software producers cannot afford to implement criteria, which are not satisfactorily proven or are not widely known at least. Besides, they do not spend time with enhancing potential of their software through e.g. an inclusion of a macro-language, which would enable testing of variations of criteria already implemented. This disables use of such software for any research. At the same time, each year further multiaxial criteria are published. Their presentation is justified by results of predictions reached under conditions or for loads given by their appropriate authors. Unfortunately, since their solution is more and more complicated, their complete testing under another load types and for another materials is scarce.

1.2 GOAL OF THE PHD THESIS…

The goal of this thesis is a new proposal of a multiaxial fatigue damage criterion that would be suitable for calculation in the high-cycle fatigue region. The existing criteria are very often tested on a very small batch of experimental data, thus its significant extension covering all possible load influences has to be reached. The new criterion will be tested on this enlarged experimental batch and compared with existing criteria so that its better behaviour could be proven.

1.3 …AND HOW IT WAS ATTAINED

As will be shown in Chap. 2, there are numerous effects that complicate the passage to the multiaxial solution (see e.g. [70], [73] or [66]). In order to evade them, the focus in this research was aimed at high-cycle fatigue. Here at least one of the degrees of freedom arising from too many parameters affecting the damaging process can be wiped off. No constitutive equations (see [56]) between tensors of stress and strain have to be tested. None the less, there are still enough of the possible effects, which should be covered better than existing criteria allow.

As regard the present state of the art, the existing multiaxial criteria are summed in Chap. 3. The emphasis is put mainly on criteria intended for the use in the HCF region and also on the criteria, which are embedded into the PragTic. The present situation in fatigue postprocessors of FE-results is shortly introduced in the Sec. 4.1. As is clearly shown, the use of such commercial software packages is wholly unsuitable, since these software tools do not implement necessary criteria and do not allow enough of variations of the computational procedures.

The starting point for the presented PhD thesis with the title "Mapping of Fatigue Damages – Program Shell of FE-calculation" originated in the reflection given in the Preamble above. A build-up of in-house software was set out as a distant goal. Thus the solutions of multiaxial methods could be compared and their predictive quality could be evaluated as a result of it. The ability to work with FE-data was set as necessary condition. This was mainly because of the critical place where the final damage could appear needn't be easily retrievable by previous examination of separate load channels. Through the subsequent development (starting with the diploma thesis [55] and continuing with LPSAFat [72], [74], [75] or MAXA [59], [62], [63] software later on), the **PragTic software** fulfilling such demands has been built. The PragTic fatigue postprocessor is described in its present version in Chap. 4 with its potential inputs and outputs. Further possible development is outlined too.

High-cycle fatigue tests are very demanding financially, because the time spent on loading is long. The determination of fatigue limits, with which the high-cycle fatigue criteria operate, is even more expensive. Though I participated in programs that lead to results falling into the high-cycle region ([6], [76] and [77]), these results were not representative enough to be utilized here in the test batch. They operated with number of cycles to the final damage whereas the benchmark data, which are compiled from data found in references, process fatigue limits. Chap. 5 is dedicated to description of the experimental data used.

Chap. 6 concerns results of all the analyses and shows the strengths of PragTic software, which lie in fast integration of new criteria, together with ability to broadly change their parameters in order to cover all influences arising. All the criteria are commented in separate sections. Afterwards a synthesis of separate effects influencing the damage calculation is given.

This forms the basis for the final design of new two criteria, which are proposed in Chap. 7 and lead to substantially better results. Their features, behaviour and results are commented there.

Conclusion in Chap. 8 closes the given theme. Possibilities of further development concerning the fatigue criteria, application of other material data and potential evolution of the PragTic software package are sketched there.

2 MULTIAXIAL FATIGUE PHENOMENON

Most of load states arising in service of mechanical components are multiaxial ones. How it is possible that mechanical engineers were able to avoid this question for so long while utilizing simple formulas suitable only for uniaxial load states? Is it necessary to complicate fatigue life computation with a further burden consisting in evaluation of changes of all load state components?

2.1 MULTIAXIAL STATE OF STRAINING

2.1.1 LOAD TYPES AND THEIR PRODUCTS

There is a few of basic load modes – tension, torsion, bending (see Fig. 1). They are distinct one from the other by the local load states, which they evoke in the loaded component. Except for the tension, every time the loaded component has another cross-section other than circular, the arising load state is a multiaxial one. Moreover, such simple load cases occur very rarely. One can usually find some combination of them. In expectation of wholly elastic response to the loading, these local load states induced by separate load channels can be superposed.

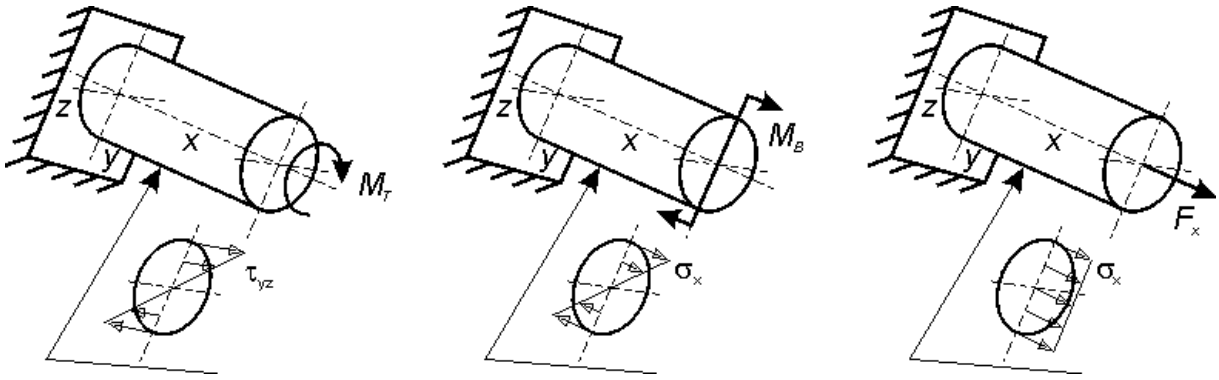

Fig. 1 Basic load modes and response on them – torsion, plane bending, tension from left to right.

Another matter of importance is worth mentioning. It is likely that the maximum local load will be observed on the surface of the component. Any other behaviour can be expected only under very special conditions – the contact areas where the load transfer takes place, inhomogeneity in material, places affected with high residual stresses induced with technological operations.

Except for these special cases, the load state on the surface is specific, because some components of stress tensor are zeroed (see Fig. 2). The load state on the surface tends to be a **plane stress state**. The Mohr's circles depicted in Fig. 2 show where the breakage can be expected according to different hypotheses of static strength. According to Tresca, the static strength should be tested towards maximum shear stress. The hypothesis of maximum normal stress says that the maximum principal stress has the highest effect. Both states are described in Fig. 2, which is no more general because of the presumption that $\sigma_x > \sigma_y$. If this presumption is loosened, it can be stated that the rupture is related either to maximum shear stress occurring on some plane with normal line inclined by 45 degrees to the normal line of surface or to the maximum principal stress which is likely to be found on some plane with normal line lying in the surface plane. All these presumptions and conclusions are fully used in **critical plane approaches** and in the CP filter proposed by Bannantine & Socie [7] particularly.

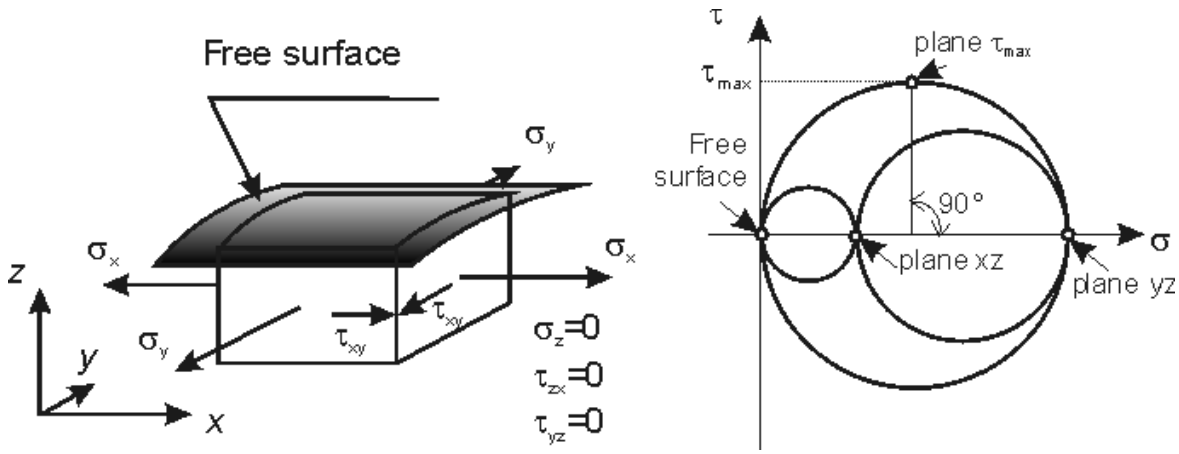

Fig. 2 The plane stress state on the surface under common conditions (left) and Mohr's circles (right) corresponding to it if the normal stresses are coincident with the principal ones.

2.1.2 LOAD COMBINATIONS

As stated in the last paragraph, the position of final breakage can be expected on some specific plane. Important fact should be that the multiaxial state can be transformed to a uniaxial load state in this way (or e.g. by von Mises hypothesis). The uniaxial state is defined by one local load value only.

However, what will happen if the ratio between σ_x and σ_y is variable throughout the service loading? One of these two components can even be negative and resulting maximum shear stress can lie on the circle defined by these two values. Then another Mohr's circles can be drawn for every point of load history and the maximum loading is defined on another plane. Which of them is the critical one?

Here we get the multiaxiality in all its beauty and awe. If the load channels are not linked in some specific way, not only the values of principal stresses, but even the principal directions change. Usually it is said that they rotate. The loaded material responds to the rotation of principal directions with strengthening or softening, which results in significantly different fatigue damages.

The reader can deduce from the previous text, how the specific conditions of any potential link among load channels should look, so that the problems with rotating principal directions could be evaded. The channels have to reach the local maximum and minimum at the same time in the load history. More locally, the changes of individual components of the tensor should be **proportional** throughout the loading. Thus loading fulfilling these conditions is defined as **proportional loading**. On the other hand, whenever such condition is not satisfied, the loading is denoted as **non-proportional**.

Reflection upon the low-cycle fatigue where the influence of plasticity is high leads to a correct suspicion that the low-cycle fatigue embodies locally all marks of non-proportional loading, although the external loads are proportional.

The term of non-proportional loading is very broad. It can be a random loading where the principal directions rotate over very large number of planes, or it can be simultaneous loading by two load channels even with the same frequency, but with different positions of maximum load. Here a **phase shift** of load channels is usually defined. Service conditions of technical components are closer to the random type of loading, but here the multiaxial solution still remains in early stages of development and evaluation. Thus the prevalent data summed on the problem of a multiaxial non-proportional loading are connected to the simple non-proportional loading usually with the same frequency and various phase shifts.

Finally, the **multiaxial loading** and **multiaxial solution** should be understood as broad categories, to which even the uniaxial items belong. Nevertheless, their true multiaxial meaning will be kept in view in the further text.

2.1.3 CRITICAL PLANE CONCEPT

One of the first proposals for a **critical plane concept** was given by Findley [21]. It was already mentioned in 2.1.1 that there are some specific planes, which the maximum load acts on. Since the arising crack is expected to be of planar character, direct conjunction of these two separate phenomena leads to an assumption that the plane with a maximum load or maximum load effect is the one along which the material is likely to break into a crack. The loads applied onto any plane can be separated into two components – shear and normal. At least from Brown and Miller [4], it is a widely accepted idea that the cracking process is led by the **shear component** of loading, whereas the **normal component** has only a secondary, although indispensable, effect in opening the tip of the arising crack and allowing the shear component to increase its devastating impact.

Two distinct expectations constituted throughout years. First – the critical plane is a plane where **Maximum Shear Stress or Strain Range** (**MSSR concept**) is located. Another approach expects that not only the shear component but the whole load effect is decisive, thus the maximum value of the damage parameter is related to the critical plane. A plane with **Maximum Damage** (**MD concept**) is the critical plane.

Based on pure logic, the MD concept should be preferred over the MSSR concept. When one cycle with the highest shear stress range in one plane is followed by many other with only a little lesser shear stress range in another plane, it is almost sure that the MSSR concept will fail. However, since some criteria show inappropriate behaviour in MD concept expectation, there still can be seen preference of the MSSR concept over the MD one (see [52] in Matake and Findley criteria comparison – here in Secs. 3.1.4 and 3.1.5 as well). Therefore, where the MSSR concept is native to a criterion embedded into the PragTic software, an option to shift meaning of the criterion to the MD approach is added.

Bannantine and Socie [7] defined the directions of prospective critical planes on the basis of the plane stress state expectation, which was already mentioned above (Sec. 2.1.1 and Fig. 2). There are two rupture modes expectable (normal and shear based). The planes with normal line deviated at $\psi = 90$ deg and $\psi = 45$ deg from the free surface normal line (see Fig. 3) are therefore believed to cover the possible directions of any critical plane. Such assumption significantly reduces the number of planes that have to be checked.

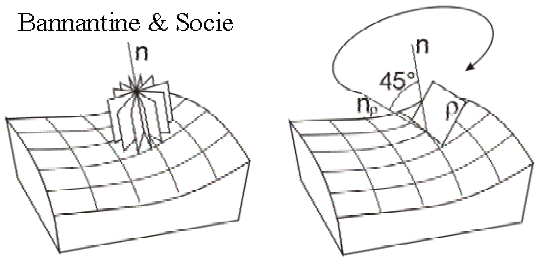

Fig. 3 Planes likely to break (to be critical) according to the assumption of Bannantine & Socie. Their normal lines are deviated at 90 deg (left) or 45 deg (right) from the surface normal line.

There is one more critical plane definition that was developed by a team of authors where the names of Carpinteri & Spagnoli appear most often. Thus it will be here denoted as **Carpinteri & Spagnoli method** (**CSM**). The method is based on a definition of weighted mean principal stress concept, first introduced in [10] and [11]. Note that the focus of the report is aimed at random loading. The concept utilizes Euler angles φ, ψ, χ between a global coordinate system and three principal directions 1, 2, 3 as an appropriate parameter for averaging throughout the cycle. The report [11] describes derivation of the three Euler angles from the 1, 2 and 3 principal directions. Once the angles are derivated, they are averaged with specific weights:

$$\overline{\varphi} = \frac{1}{M}\sum_k \varphi_k \cdot M_k ,$$
$$\overline{\psi} = \frac{1}{M}\sum_k \psi_k \cdot M_k , \qquad (1)$$
$$\overline{\chi} = \frac{1}{M}\sum_k \chi_k \cdot M_k .$$

The subscript k corresponds to the k-th time instant, at which the φ_k or the other two angles were derivated. The M_k parameter is the weight given to the current k-th load state, whereas M is the sum of all weights throughout the one cycle:

$$M = \sum_k M_k , \qquad (2)$$

Carpinteri et al. proposes two different weight systems. As first, the common arithmetic average can be reached by setting $M_k = 1$. The second proposal is much more complicated:

$$M = 0 \quad \text{if} \quad \sigma_{1,k} < c \cdot f_{-1}$$
$$M = \left(\frac{\sigma_{1,k}}{f_{-1}} \right)^w \quad \text{if} \quad \sigma_{1,k} \geq c \cdot f_{-1} , \qquad (3)$$

Here the c parameter is given to be lying somewhere in the range $0 < c \leq 1$. Exponent w is the exponent of the S-N curve. The more damaging planes are selected for averaging only by this weight, moreover the exponent w allows observing the S-N curve by such a weight and accentuate more the most damaging planes.

Spagnoli [82] and Carpinteri & Spagnoli [13] generalized the use of the described concept to the localization of the critical plane as well. They define that the critical plane should be deviated by an angle:

$$\psi = \frac{\pi}{4} \cdot \frac{3}{2}\left[1 - \frac{1}{\kappa^2} \right] \qquad (4)$$

from the weighted mean first principal direction. The search angle is built in such a way that the critical plane is coincident with the plane of which the weighted mean first principal direction is the normal for brittle materials ($\kappa \to 1$), whereas for ductile steels with $\kappa = \sqrt{3}$ the deviation angle is $\pi/4$.

A search procedure over all possible planes obeying such deviation angle has to be run. For search of the weighted mean first principal direction, the authors of [13] propose use of the weights defined in (3) with a parameter $c = 0.5$ without any further explanation or testing. The use of the parameter (3) is a little questionable in the given context, because the authors are assessing the HCF region – more precisely fatigue limits. There is a discussion open on the use of Palmgren-Miner rule in this region, but utilization of the original w exponents of the S-N curve valid for the LCF region should be checked.

2.1.4 INTEGRAL APPROACHES

The critical plane approach has its opponents. It cannot distinguish if some plane is solitary in being the most loaded or whether there are other planes as well, which are equally loaded. See [89] as an example – it shows a case of a MSSR concept, which under given conditions gives infinite number of possible critical planes). Surely, one can argue back if the uniqueness of the critical plane is really necessary. MD approaches moreover do not suffer from mentioned multivalency.

Well, another reasoning – let's have two different cycles leading to two different planes set as the critical planes. Under CPA concept, there is only slight interconnection between both damaging effects, to which the critical place is exposed. Is not there any major interaction expectable – as the observable branching and connecting of micro-cracks could suggest?

Micro-cracks that appear on some damaged grains need not to extend in size but can remain stopped on grain boundaries. At the same time, nearly for any cycle and plane orientation there are enough of the grains that can break at their preferred slip system. An idea that either stress components or directly the arising damage should be integrated over all existing planes is based on all these facts. The **integral approach** is formed. The integration has the same effect as the averaging - therefore the integration usually takes form of a spatial average, which is mathematically expressed through integration:

$$\bar{f} = \frac{1}{4\pi}\int_{\varphi=0}^{2\pi}\int_{\psi=0}^{\pi} f(\varphi,\psi)\sin\psi d\psi d\varphi \,. \tag{5}$$

The local extremes of loading are suppressed by this procedure. This is the main reason, why the expectation of IA suitability is related mainly to the area of random loadings with large rotation of principal directions (see [34]).

2.2 LOAD COMPONENTS DESCRIPTION

Multiaxial fatigue computation is almost at all cases based on stress or strain components on particular planes. Thus it is necessary to define values of these components, so that an analytic solution of given criteria could be found. When it is possible, such an analytic solution is a perfect tool for check of the proper installation into the PragTic software.

The second reason for analytic evaluation of criteria is the search for a definition of included material parameters. The uniaxial load conditions are usually used for derivation of their values – see e.g. Appendix VII and Appendix VIII here.

2.2.1 GENERAL CASE

DESCRIPTION OF POSITION OF EXAMINED PLANE

It is necessary to describe correctly the transformation of load values, when the tensor is projected to some specific plane. Since there are particular directions (see e.g. Fig. 3), in which the planes searched should be oriented towards the surface normal line, a model that covers whole description of desired orientation has to be found. The transformation from the p_i coordinate system (CS in further) to the r_i CS is achieved in two steps (see Fig. 4):

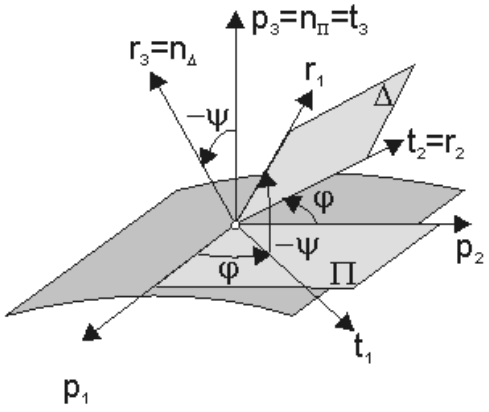

Fig. 4 Description of changes of coordinate systems from CS denoted p_i towards the r_i CS throughout a double rotation by angles φ and ψ. The original surface of component is the twisted one with darker grey colour. The corresponding coordinate system is here mainly defined by the surface normal line.

1) rotation around the surface normal line by angle φ, new CS is denoted as t_i;
2) rotation around the t_2 axis, which leads to the desired deviation of normal line of examined plane from the normal line to the surface. Final CS is denoted as r_i.

This double rotation can be written as:

$$\mathbf{r}_1 = \begin{bmatrix} r_{11} \\ r_{12} \\ r_{13} \end{bmatrix} = \cos\psi \cdot \left(\begin{bmatrix} p_{11} \\ p_{12} \\ p_{13} \end{bmatrix} \cdot \cos\varphi + \begin{bmatrix} p_{21} \\ p_{22} \\ p_{23} \end{bmatrix} \cdot \sin\varphi \right) - \begin{bmatrix} p_{31} \\ p_{32} \\ p_{33} \end{bmatrix} \cdot \sin\psi = \tag{6}$$
$$= \cos\psi \cdot (\mathbf{p}_1 \cdot \cos\varphi + \mathbf{p}_2 \cdot \sin\varphi) - \mathbf{p}_3 \cdot \sin\psi,$$

$$\mathbf{r}_2 = \begin{bmatrix} r_{21} \\ r_{22} \\ r_{23} \end{bmatrix} = -\begin{bmatrix} p_{11} \\ p_{12} \\ p_{13} \end{bmatrix} \cdot \sin\varphi + \begin{bmatrix} p_{21} \\ p_{22} \\ p_{23} \end{bmatrix} \cdot \cos\varphi = -\mathbf{p}_1 \cdot \sin\varphi + \mathbf{p}_2 \cdot \cos\varphi, \tag{7}$$

$$\mathbf{r}_3 = \begin{bmatrix} r_{31} \\ r_{32} \\ r_{33} \end{bmatrix} = \sin\psi \cdot \left(\begin{bmatrix} p_{11} \\ p_{12} \\ p_{13} \end{bmatrix} \cdot \cos\varphi + \begin{bmatrix} p_{21} \\ p_{22} \\ p_{23} \end{bmatrix} \cdot \sin\varphi \right) + \begin{bmatrix} p_{31} \\ p_{32} \\ p_{33} \end{bmatrix} \cdot \cos\psi = \tag{8}$$
$$= \sin\psi \cdot (\mathbf{p}_1 \cdot \cos\varphi + \mathbf{p}_2 \cdot \sin\varphi) + \mathbf{p}_3 \cdot \cos\psi.$$

Equation (8) describes direction of normal line of examined plane in dependency on the two defined angles φ and ψ. These two angles are expected to be in the following range (see (5) too):

$$\varphi \in \langle 0°;180° \rangle, \quad \psi \in \langle 0°;90° \rangle. \tag{9}$$

DESCRIPTION OF LOCAL LOAD COMPONENTS ON EXAMINED PLANE

When the local load state **ν** on some particular plane Δ is observed, it can be divided into two components – normal stress **N** and shear stress **C**.

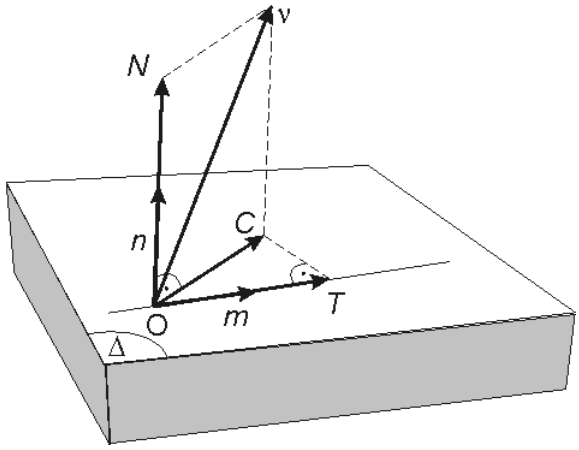

Fig. 5 Description of a local load state on a general plane Δ.

The complete acting stress is defined as:

$$= \boldsymbol{\Sigma} \cdot \mathbf{r}_3 . \tag{10}$$

The normal component can be easily detected both in direction and size:

$$\mathbf{N} = (\mathbf{r}_3 \cdot \ \ ) \cdot \mathbf{r}_3 \Rightarrow \mathbf{N} = (\mathbf{r}_3 \cdot \boldsymbol{\Sigma} \cdot \mathbf{r}_3) \cdot \mathbf{r}_3 , \tag{11}$$

$$N = (\mathbf{r}_3 \cdot \boldsymbol{\Sigma} \cdot \mathbf{r}_3) . \tag{12}$$

The normal stress has one unique feature. No matter how the input load history looks, it does not change its direction. Thus its mean and amplitude value can be easily set as values defined from maximum and minimum values throughout the load history:

$$N_a = \frac{1}{2} \cdot \left\{ \max_{t \in T} \left(\mathbf{r}_3 \cdot \boldsymbol{\Sigma}(t) \cdot \mathbf{r}_3 \right) - \min_{t \in T} \left(\mathbf{r}_3 \cdot \boldsymbol{\Sigma}(t) \cdot \mathbf{r}_3 \right) \right\}, \tag{13}$$

$$N_m = \frac{1}{2} \cdot \left\{ \max_{t \in T} \left(\mathbf{r}_3 \cdot \boldsymbol{\Sigma}(t) \cdot \mathbf{r}_3 \right) + \min_{t \in T} \left(\mathbf{r}_3 \cdot \boldsymbol{\Sigma}(t) \cdot \mathbf{r}_3 \right) \right\}. \tag{14}$$

There are other definitions possible too as can be seen e.g. in [9] where the integral mean value is proposed.

An equal simplicity in definition of behaviour of the shear component is possible only in cases where the loading is proportional. If it is not the case, the shear vector rotates on the examined plane and its end-tip creates some general curve. There are several methods of decomposition of the shear stress cycle into its mean and amplitude component. The first three of them are described by Papadopoulos in [53] . Here they are:

- **Longest projection method:** The longest projection of the shear stress path is searched throughout all possible direction (see Fig. 6). Here the false mean shear stress can be read as can be seen in Fig. 6.

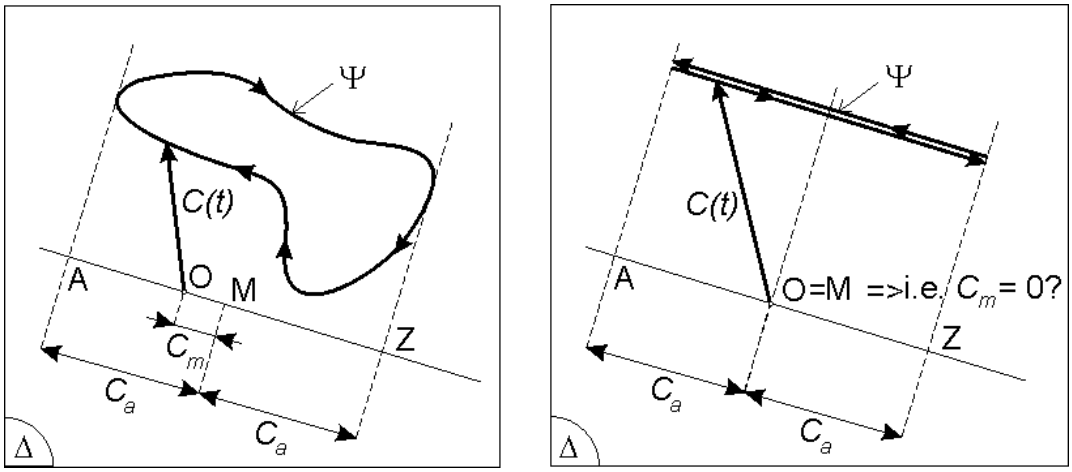

Fig. 6 Longest projection method (on left side) and case when it leads to evidently wrong definition of mean shear stress (picture on the right).

- **Longest chord method:** See Fig. 7 for its definition and the case when the resulting value of mean shear stress cannot be unambiguously determined.

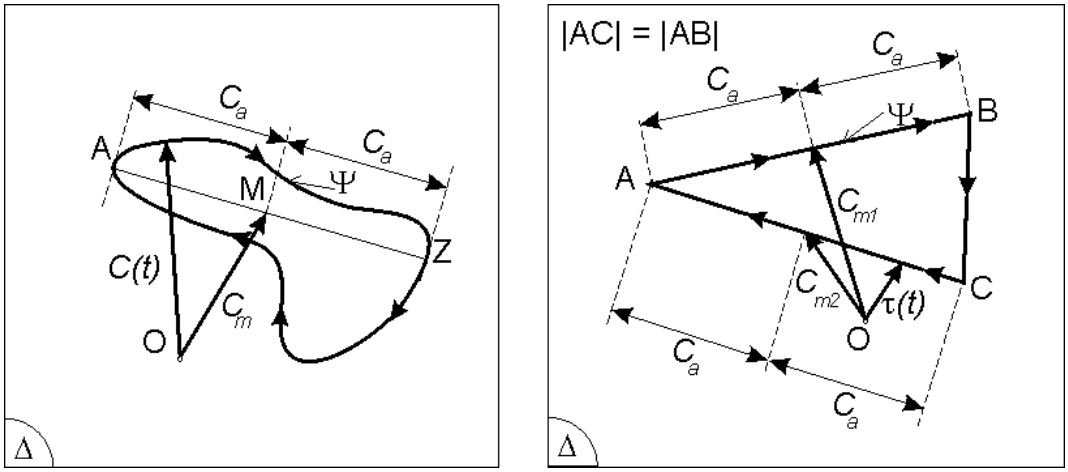

Fig. 7 Longest chord method (left) and the case when it leads to ambiguous definition of mean shear stress.

- **Minimum circumscribed circle method (MCCM):** This method was first presented by Papadopoulos in [51]. Its major feature is its explicitness in determination of mean shear stress (see Fig. 8). Papadopoulos later in [53] shows that such minimum circumscribed circle can be obtained by a search through all pairs and triads of points in the shear stress path, but such an approach can be very lengthy. Bernasconi in [8] presents and confronts other methods for its quicker evaluation.
- Another method called **minimum circumscribed ellipse method (MCEM)** can be found in other references [68]. The contrast in comparison with MCCM is clear – it should offer a better solution of phase shift effect problems. Nevertheless, as regards the definition of mean shear stress, it does not offer any new approach.

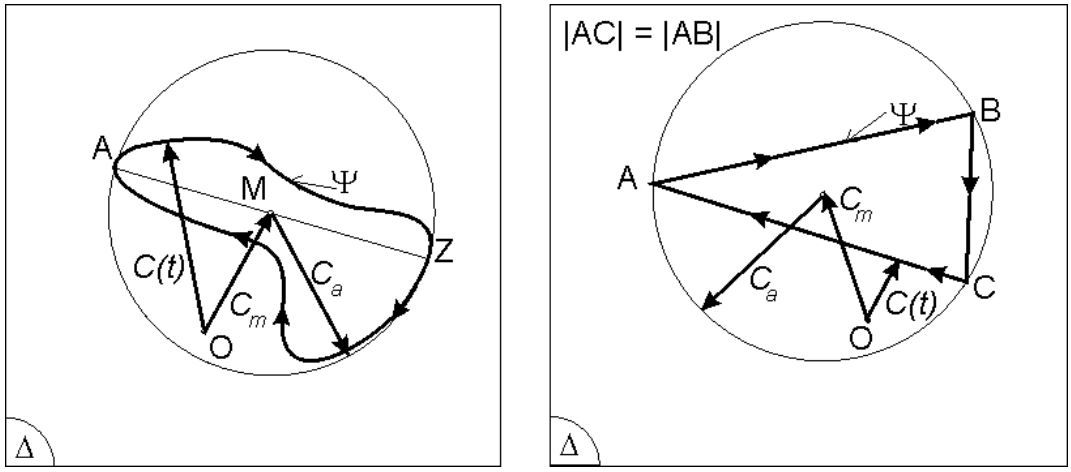

Fig. 8 Minimum circumscribed method and definition of shear tensor components for the case, in which the LCM fails in Fig. 7.

There is one interesting point worth mentioning. The first three methods are above all related to the search for a correct C_m definition. Nevertheless, the number of criteria utilizing this parameter is very limited (I know only one – the Zenner & Liu criterion described here in Sec. 3.1.12). Since the construction of MCCM is of artificial nature (what should it represent?) and is developed mainly in order to find the right value of the C_m parameter, its suitability can be doubted. The step towards the MCEM is therefore more logical or better stated – more rightful – because it gives reason why to do so complicated analysis.

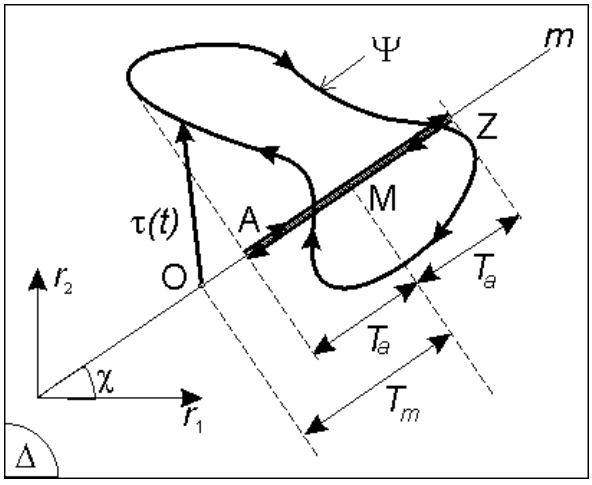

Fig. 9 Decomposition of resolved shear stress $T(\chi)$ in the m direction.

Another shear variable of interest is resolved shear stress T as defined by Papadopoulos in [51]. It is determined as a projection of the shear stress path to some specific direction **m**. Such projection simplifies its definition throughout the load history (see Fig. 9):

$$\begin{aligned} T_a &= \frac{1}{2}\cdot\left\{\max_{t\in P}[\mathbf{m}\cdot\mathbf{C}(t)] - \min_{t\in P}[\mathbf{m}\cdot\mathbf{C}(t)]\right\}, \\ T_m &= \frac{1}{2}\cdot\left\{\max_{t\in P}[\mathbf{m}\cdot\mathbf{C}(t)] + \min_{t\in P}[\mathbf{m}\cdot\mathbf{C}(t)]\right\}. \end{aligned} \tag{15}$$

2.2.2 HARMONIC BENDING & TORSION

As already stated before, the case of a smooth specimen loaded with a synchronous two-channel iso-frequency loading with an axial component (plane bending, rotating bending, tension) and shear component with phase shift δ is very fruitful for any prospective comparison of analytic and numerical solutions. Thus this specific case has to be completely mathematically mastered. Most of the derivation presented here is taken from [52]. Let the local loads be given as functions of external axial stress $\{\sigma_a, \sigma_m\}$ and shear stress $\{\tau_a, \tau_m\}$. Then the complete stress tensor is:

$$\boldsymbol{\Sigma} = \begin{bmatrix} \sigma_a\cdot\sin(2\pi t/P)+\sigma_m & \tau_a\cdot\sin(2\pi t/P-\delta)+\tau_m & 0 \\ \tau_a\cdot\sin(2\pi t/P-\delta)+\tau_m & 0 & 0 \\ 0 & 0 & 0 \end{bmatrix}. \tag{16}$$

NORMAL STRESS

To determine the history of normal stress, the equations (8), (12) and (16) should be combined:

$$N(t) = \sin^2\varphi\left\{\left[\sigma_a\cdot\sin\left(\frac{2\pi t}{P}\right)+\sigma_m\right]\cdot\cos^2\psi + \left[\tau_a\cdot\sin\left(\frac{2\pi t}{P}-\delta\right)+\tau_m\right]\cdot\sin 2\psi\right\}. \tag{17}$$

Further elaboration enables to derive both components of harmonic loading:

$$N_m = \sin^2\varphi\cdot\left(\sigma_m\cdot\cos^2\psi + \tau_m\cdot\sin 2\psi\right), \tag{18}$$

$$N_a = \sin^2\varphi\cdot\sqrt{\sigma_a^2\cdot\cos^4\psi + 4\tau_a^2\cdot\sin^2\psi\cdot\cos^2\psi + 2\sigma_a\tau_a\sin(2\psi)\cos^2\psi\cos\delta}\,. \tag{19}$$

SHEAR STRESS

Changes of shear stress can be evaluated in the plane defined by coordinate axes $\mathbf{r}_1$ and $\mathbf{r}_2$ from equations (6) and (7). Thus the shear stress components in both directions will be denoted as C_1 and C_2 (see Fig. 5, Fig. 9 and equation (10) for derivation):

$$\begin{aligned} C_1 &= \mathbf{r}_1\cdot\boldsymbol{\Sigma}\cdot\mathbf{r}_3, \\ C_2 &= \mathbf{r}_2\cdot\boldsymbol{\Sigma}\cdot\mathbf{r}_3. \end{aligned} \tag{20}$$

When the coordinate axes from the (6) - (8) are used, the description of these two parameters is:

$$\begin{aligned} C_1(t) &= -\frac{1}{2}\left[\sigma_a\cdot\sin\left(\frac{2\pi t}{P}\right)+\sigma_m\right]\sin\varphi\sin 2\psi + \left[\tau_a\cdot\sin\left(\frac{2\pi t}{P}-\delta\right)+\tau_m\right]\sin\varphi\cdot\cos 2\psi, \\ C_2(t) &= -\frac{1}{2}\left[\sigma_a\cdot\sin\left(\frac{2\pi t}{P}\right)+\sigma_m\right]\sin 2\varphi\cos^2\psi - \frac{1}{2}\left[\tau_a\cdot\sin\left(\frac{2\pi t}{P}-\delta\right)+\tau_m\right]\sin 2\varphi\cdot\sin 2\psi. \end{aligned} \tag{21}$$

In order to decompose both values into its mean and amplitude values, further simple but lengthy operations are necessary. They result in an ellipse described with two parameters:

$$C_1(t) = f \cdot \sin\left(\frac{2\pi t}{P}\right) + g \cdot \cos\left(\frac{2\pi t}{P}\right) + \left(-\frac{\sigma_m}{2} \cdot \sin 2\psi + \tau_m \cdot \cos 2\psi\right) \cdot \sin\varphi,$$
$$C_2(t) = p \cdot \sin\left(\frac{2\pi t}{P}\right) + q \cdot \cos\left(\frac{2\pi t}{P}\right) + \left(-\frac{\sigma_m}{2} \cdot \cos^2\psi - \frac{\tau_m}{2} \cdot \sin 2\psi\right) \cdot \sin 2\varphi. \quad (22)$$

The following substitutions are used:

$$f = \sin\varphi\left(-\frac{\sigma_a}{2} \cdot \sin 2\psi + \tau_a \cdot \cos 2\psi \cdot \cos\delta\right),$$
$$g = -\tau_a \cdot \sin\varphi \cdot \cos 2\psi \cdot \sin\delta,$$
$$p = -\frac{1}{2} \cdot \sin 2\varphi\left(\sigma_a \cdot \cos^2\psi + \tau_a \cdot \sin 2\psi \cdot \cos\delta\right), \quad (23)$$
$$q = \frac{\tau_a}{2} \cdot \sin 2\varphi \cdot \sin 2\psi \cdot \sin\delta.$$

Finally, the description derived of mean shear stress from (22) looks like this:

$$C_m = \sqrt{\left[\left(-\frac{\sigma_m}{2} \cdot \sin 2\psi + \tau_m \cdot \cos 2\psi\right) \cdot \sin\varphi\right]^2 + \left[\left(-\frac{\sigma_m}{2} \cdot \cos^2\psi - \frac{\tau_m}{2} \cdot \sin 2\psi\right) \cdot \sin 2\varphi\right]^2}, \quad (24)$$

whereas the shear stress amplitude is given as the longer half-axis of the ellipse described by (22). The half-axes are:

$$a,b = \sqrt{\frac{f^2+g^2+p^2+q^2}{2} \pm \sqrt{\left(\frac{f^2+g^2+p^2+q^2}{2}\right)^2 - (fq-gp)}}, \quad (25)$$

from which the longer one is taken to be the amplitude of shear stress:

$$C_a = \sqrt{\frac{f^2+g^2+p^2+q^2}{2} + \sqrt{\left(\frac{f^2+g^2+p^2+q^2}{2}\right)^2 - (fq-gp)}}. \quad (26)$$

AMPLITUDE OF RESOLVED SHEAR STRESS

The resolved shear stress amplitude affects only the Papadopoulos criterion. Its mean component is not used anywhere. The amplitude can be defined for the given shear stress path in dependency on the χ angle (see Fig. 9) as:

$$T_a(\psi,\varphi,\chi) = \sqrt{a^2\cos^2\chi + b^2\sin^2\chi}. \quad (27)$$

where parameters *a* and *b* correspond to lengths of the half-axes of the elliptic shear stress load path defined here in (25).

AMPLITUDE OF SECOND INVARIANT OF STRESS TENSOR DEVIATOR

Under such specific conditions, the amplitude of second invariant of stress tensor deviator can be fully algebraically described. The transformation of stress tensor deviator components into a vector in the Ilyushin five-dimensional subspace (see [33]) is used:

$$S_1 = \sqrt{\frac{3}{2}}s_{xx} \quad ; \quad S_2 = \frac{1}{\sqrt{2}}(s_{yy} - s_{zz}),$$
$$S_3 = \sqrt{2}s_{xy} \; ; \; S_4 = \sqrt{2}s_{xz} \; ; \; S_5 = \sqrt{2}s_{yz}. \quad (28)$$

Formulas can be rewritten more specifically for given load conditions (see (16)):

$$S_1 = \sqrt{\frac{2}{3}}[\sigma_a \cdot \sin(2\pi t/P) + \sigma_m]; \quad S_3 = \sqrt{2}\tau_{xy} = \sqrt{2}[\tau_a \cdot \sin(2\pi t/P - \delta) + \tau_m]; \quad S_2 = S_4 = S_5 = 0. \quad (29)$$

The following equality is used in the computation of the second invariant of the stress deviator:

$$\sqrt{J_2} = \sqrt{\frac{1}{2}\mathbf{S}:\mathbf{S}}. \quad (30)$$

Since the S_i components define a two-dimensional ellipse under given loads, a derivation of the amplitude value of second invariant of stress deviator corresponding to the major semi-axis of this ellipse leads to:

$$\sqrt{J_{2,a}} = \sqrt{\frac{1}{2}\left[\frac{\sigma_a^2}{3} + \tau_a^2 + \sqrt{\left(\frac{\sigma_a^2}{3} + \tau_a^2\right)^2 - \frac{4}{3}\sigma_a^2\tau_a^2 \sin^2\delta}\right]}. \quad (31)$$

Note that this definition of amplitude of second invariant of stress tensor deviator as a radius of a circumscribed five-dimensional sphere is given by Papadopoulos in [52]. Other parameters are also proposed in a way similar to the shift from MCCM to MCEM in two-dimensional space. The GAM method [27] presented here in Sec. 3.1.13 corresponds to the second group analogical to the MCEM solution.

3 PRESENT TYPES OF SOLUTION

> **Motto:** *It is fairly traditional that each author develops his own criterion for fatigue life prediction and verifies it by his own experimental data. Then some other author's data are not satisfied by that criterion, and a new one is suggested. Thus too many proposed criteria have been accumulated ... Many criteria have remained isolated each from other, without comparison or competition.*
>
> *cited from [83], p. 42.*

The same feeling was the starting point for design of software suitable for a comparison of different proposed criteria. The work continued in such a way that a great majority of criteria presented further are already implemented into the software PragTic developed in-house, which is described further in Chap. 4.

3.1 HIGH CYCLE FATIGUE

Usual high cycle fatigue criteria have at least one common point. They simply state, whether the component withstands applied loads or not. Thus the most general form could be given as an inequality:

$$a \cdot f(C) + b \cdot g(N) \leq f_{-1}\,, \tag{32}$$

where a and b parameters are set from two uniaxial fatigue limits (e.g. t_{-1} and f_{-1}). The linear combination of C and N shear and normal stresses in (32) can be seen replaced by a quadratic version too. Separation of amplitude and mean values of C and N stresses is used as well. Criteria in high cycle fatigue are wholly dominated by evaluation of stresses. Nevertheless, a fully elastic response is expected, so strain inputs can be used too. Generally the shear component C is assumed to dominate the damaging process, whereas the normal component N is expected to have a secondary effect.

3.1.1 HCF PREDICTION SUITABILITY EVALUATION

Any usual dimensioning in high-cycle fatigue is based on assessment, whether the component sustains infinite loading by a given load history. The criterion for durability is thus set as an inequality (32). If the load data of left-hand side of (32) correspond to experimentally detected fatigue limit, the ideal state of equality should be achieved. The fatigue index error ΔFI shows the degree of deviation from ideal equality:

$$\Delta FI = \left(\frac{LHS(load) - RHS(material)}{RHS(material)} \right) \cdot 100\%\,. \tag{33}$$

The prediction for experimentally verified fatigue limits should lead to $LHS = RHS$, i.e. $\Delta FI = 0$. If the LHS is higher, it means that the criterion is conservative, because it predicts that the component would fail under lower loads. Papadopoulos [51] qualifies a prediction to be good if fatigue index error lies in the range of ±5% or at worst ±10%.

Altogether, 129 test results appear in the thesis totally, so some systematic evaluation is necessary. Statistical parameters used here for further examination are mean value, range and standard deviation. The parameters have their predicative strength in their synergic comparison. It is insufficient to

evaluate the criterion towards only one particular parameter. In contrast to Papadopoulos [52], I do not expect that the average of the test batch has necessarily be as close to zero as possible. If the other statistical parameters show that the prediction stays minimally scattered, then an overall trend shifting the mean value to the conservative or non-conservative prediction needn't hinder.

There is one more important point to be mentioned. When the prediction is evaluated, it is based on the (32) inequality and ΔFI fatigue index error indicates the deviation from ideal equality. Then a following behaviour has to be expected:

$$\Delta FI_a = \left(\frac{LHS_a - RHS_a}{RHS_a} \right) \neq \Delta FI_b = \left(\frac{LHS_a^2 - RHS_a^2}{RHS_a^2} \right), \tag{34}$$

because the power of two increases the differences between *LHS* and *RHS*. The worst is to use this form of a criterion:

$$LHS(load, material) \leq 1. \tag{35}$$

The intrinsic nature of the criterion is hidden here. One has to read it more carefully, so that to be sure, which is the basic variable of the criterion. In order to make a correct comparison, all the criteria have to be written in a form that corresponds to some unique variable. Thus the resulting form of the evaluated criteria has been set here to match with an equivalent stress or more specifically with the fatigue limit in fully reversed axial loading:

$$LHS(load, material) \leq f_{-1}. \tag{36}$$

3.1.2 CROSSLAND, SINES

Both Crossland [12] and Sines [79], [80] published their works throughout the fifties of the last century. Their criteria are very much alike, utilizing the amplitude of second invariant of stress tensor deviator (which corresponds to the von Mises stress) as the basis. Another term is added to the equation in order to cope with the mean stress effect – while Sines prefers the mean value of first invariant of stress tensor (i.e. hydrostatic stress):

$$Sines: \qquad a_S \cdot \left(\sqrt{J_2} \right)_a + b_S \cdot \sigma_{H,m} \leq f_{-1}, \tag{37}$$

Crossland recommends use of its maximum value:

$$Crossland: a_C \cdot \left(\sqrt{J_2} \right)_a + b_C \cdot \sigma_{H,\max} \leq f_{-1}. \tag{38}$$

The coefficients *a* and *b* in both equations can be set through evaluation of the formulas at fatigue limits in torsion and tension. The Sines formula does not allow alternating fatigue limit in tension to be used due to a singular solution. Thus another load condition – a repeated tension – has to be used. The appropriate values are:

$$\begin{aligned} a_S &= \kappa, \\ b_S &= \left(6\frac{f_{-1}}{f_0} - \sqrt{3}\kappa \right) \end{aligned} \tag{39}$$

for Sines whereas for Crossland:

$$\begin{aligned} a_C &= \kappa, \\ b_C &= \left(3 - \sqrt{3}\kappa \right). \end{aligned} \tag{40}$$

The fatigue limit in repeated axial loading necessary for the Sines formula can be unavailable. Papadopoulos in [52] proposes its substitution by Goodman formula (97), together with the use of the fact that under fully reverse bending the Sines formula leads to:

$$\kappa = \sqrt{3}\,. \tag{41}$$

This formula is clearly generally incorrect, nevertheless Papadopoulos applies it to the derivation:

$$b_S = 6\frac{f_{-1}}{f_0} - \sqrt{3}\kappa = \frac{6f_{-1}}{2}\left(\frac{1}{f_{-1}} + \frac{1}{S_u}\right) - \sqrt{3}\cdot\sqrt{3} = 3 + \frac{3f_{-1}}{S_u} - 3 = \frac{3f_{-1}}{S_u} \tag{42}$$

Under type of loads used in this report, the b_S parameter is necessary only in cases where there is a mean axial load. In such cases the f_0 fatigue limits are already derived in Chap. 5.2.

Both formulas can be seen used as sample criteria, but the Crossland's one is the one more successful (see [5], [13], [52]).

3.1.3 MCDIARMID

The McDiarmid criterion is widely used. It is implemented (MSC.Fatigue, FE-Fatigue) or at least commented (Fe-Safe) in commercial fatigue software. McDiarmid established its form on a basis of broad comparison of test data [41], [42] and [43]. The first developed form was especially complicated:

$$\frac{C_a}{\left(t_{-1} - \left(t_{-1} - b_{-1}/2\right)\cdot\left(\frac{2\cdot N_a}{b_{-1}}\right)^{1,5}\right)\left(1 - \left(\frac{2\cdot N_m}{S_u}\right)^{0,5}\right)} \le 1\,. \tag{43}$$

This older version is implemented in the PragTic program too, but not commented here any more, because its results are inappropriate and not worth mentioning. The final version of the McDiarmid criteria is:

$$\frac{C_a}{t_{AB}} + \frac{N_{\max}}{2\cdot S_u} \le 1 \tag{44}$$

or written in the convention used here generally:

$$\frac{f_{-1}}{t_{AB}} C_a + \frac{f_{-1}}{2\cdot S_u} N_{\max} \le f_{-1}\,. \tag{45}$$

The t_{AB} symbol stands for choice between t_A and t_B fatigue limits corresponding to load conditions leading to a creation of cracks in A and B system. These two types of cracks correspond to cracks parallel to the surface (A type) or inwards from the surface (B type). This is a significant complicacy, because such distinction is not usually recorded. The relation $t_{AB} = t_{-1}$ is generally fulfilled for plane bending combined with torsion ([13]).

At first [42], the criterion was designed with critical plane defined by maximum shear stress range. Later McDiarmid announced another proposal where the critical plane is set by maximisation of (44) criterion's left hand side, i.e. by maximum caused damage. Both versions are implemented in PragTic. The MD variant usually leads to slightly better results.

Wherever the criterion is used, its results are not very promising (see [13], [52]), nevertheless it was included among the tested criteria.

3.1.4 FINDLEY

The origin of the Findley criterion goes back to the fifties of the last century [21]. It is the first critical plane criterion:

$$a_F \cdot C_a + b_F \cdot N_{max} \le f_{-1}\,. \tag{46}$$

In contrast to the McDiarmid criteria where the coefficient in (45) were set on the basis of extensive test batch evaluation, here the coefficients are derived from pure uniaxial tests. The critical plane is set

by a maximization of the left hand side of the criterion (46). The computation of both material variables a_F and b_F is based on two maximizations performed in fully reversed tension and in fully reversed torsion, which lead to:

$$\begin{aligned} a_F &= 2\sqrt{\kappa - 1}, \\ b_F &= 2 - \kappa. \end{aligned} \tag{47}$$

Papadopoulos omits this criterion in his comparison set [52] due to its sensitivity to the mean torsion loading. Nevertheless, since this criterion is cited elsewhere [13] as well, it is included in PragTic.

3.1.5 MATAKE

The Matake criterion can be written in the same way as Findley one:

$$a_M \cdot C_{a,MSSR} + b_M \cdot N_{max,MSSR} \leq f_{-1}. \tag{48}$$

The difference stands in the definition of the critical plane, which is a plane with maximum C_a, i.e. with maximum shear stress range (MSSR method) as well. This change allows the criterion to behave correctly according to Papadopoulos under mean torsion loads in contrast to the Findley criterion. The parameters a_M and b_M are:

$$\begin{aligned} a_M &= \kappa, \\ b_M &= 2 - \kappa. \end{aligned} \tag{49}$$

The model is tested in [13] and [52] with relatively fair results, although it does not reach the best ranking.

3.1.6 KENMEUGNE ET AL. – CRITICAL PLANE APPROACH

Another approach closely related to the Findley criterion is this one. Kenmeugne et al. introduced it in [34] and [84] together with their own proposal for an integral criterion, in order to compare results of very similar damage parameters but with different computational philosophy. The critical plane criterion is defined as:

$$a_{Kc} \cdot C_a + b_{Kc} \cdot N_a + d_{Kc} \cdot N_m \leq f_{-1}. \tag{50}$$

The criterion is a maximum damage criterion, thus the result is obtained through maximization of (50) LHS. The similarity of (46) and (50) is clear after a short inspection. The same conditions must be fulfilled under fully reversed loading and thus:

$$\begin{aligned} a_{Kc} &= a_F = 2\sqrt{\kappa - 1}, \\ b_{Kc} &= b_F = 2 - \kappa. \end{aligned} \tag{51}$$

The last unknown parameter has to be set from one test value of repeated bending, i.e.:

$$d_{Kc} = \frac{2f_{-1}}{f_0} - \frac{f_0}{2f_{-1}}(\kappa - 1) - 2 + \kappa. \tag{52}$$

The final formula is not correctly described in [34], because the two last summands are written there with opposite signs. The derivation of the correct formula was done similarly to the concept described further in Appendix VIII. Except for the [34] report where the description of test results is very vague, no other author mentions testing of this criterion. Anyway, the criterion was implemented into PragTic, so that the comparison of CPA and IA approaches could be extended with more clear data, than the authors of [34] offer.

3.1.7 DANG VAN

The criterion was first presented in [17]. It started a branch of mesoscopic criteria, which found a continuation in the Papadopoulos and Morel criteria. The mesoscopic criteria have their common point

in an assumption that not the apparent macroscopic quantities, but their mesoscopic counterpart related to the least homogenous agglomerates of grains should be checked for fatigue evaluation. Dang Van initiated the solution and presented a way of transforming the mesoscopic quantities towards macroscopic stresses. The last version of the criterion [18] can be written as:

$$a_{DV} \cdot C_a + b_{DV} \cdot \sigma_{H,\max} \le f_{-1}, \tag{53}$$

where the critical plane is set by maximization of the left hand side of the equation (53). Since hydrostatic stress is independent from the cutting plane direction, the criterion can be seen both as MSSR and MD all in one. Variables in the criterion are set by maximization of the left hand side for cases of fully reversed torsion and tension. Resulting converters thus are:

$$\begin{aligned} a_{DV} &= \kappa, \\ b_{DV} &= 3 - \frac{3}{2}\kappa. \end{aligned} \tag{54}$$

The Dang Van formula is widely used, although its predictive efficiency is reported as not very good [5], [15]. The method is implemented in a number of the commercial software (Fe-Safe, LMS.Virtual Lab Component Durability), thus it was included into the PragTic too.

3.1.8 SPAGNOLI

The last CPA criterion implemented is that proposed by Spagnoli [13], [82]. In fact, I finished already testing of a combination of both load parameters in the quadratic form as an MD variant, when I found Spagnoli's text. The composition of the criterion looks like this:

$$\sqrt{a_S \cdot C_a^2 + b_S \cdot N_{\max}^2} \le f_{-1} \tag{55}$$

with material parameters derived from two simple uniaxial tests:

$$\begin{aligned} a_S &= \kappa^2, \\ b_S &= 1. \end{aligned} \tag{56}$$

Thus the criterion can be rewritten in another form:

$$\sqrt{\frac{C_a^2}{t_{-1}^2} + \frac{N_{\max}^2}{f_{-1}^2}} \le 1, \tag{57}$$

which can be read as an extension of Gough's work into the out-of-phase loading.

Spagnoli utilizes the CSM concept of the critical plane (see Sec. 2.1.3). He proposes the use of $c = 0.5$ and the weight formula (3) in [13]. The results of the criterion given in [13] are nice (smaller range than the Matake criterion, which is the second best). The results in [82] show again nice range of results, but the histogram is more toothed. It adverts to some unknown effect, which is not satisfactorily solved.

The implementation to the PragTic is not so straightforward. First, the criterion is implemented with both MD and CSM concept of the critical plane localization. Second, since the S-N curve exponent in the weight parameter (3) is not available for all the materials in the test batch and because of its use below the fatigue limit is disputable, another proposals for the weight are given and tested there.

The $c = 0.5$ parameter is accepted as a given value and is not adjustable by a user. Until now, there was not done any research concerning its changes with the use of PragTic.

The MD variant preserves the material parameters set in (56) – the parameters can be derived in the same way as shown in Appendix VIII. Nevertheless the maximization of the damage parameter under reversed axial loading shows according to the computed second partial derivations that the resulting plane is the MD for cases of materials with $\kappa < \sqrt{2}$ only. Higher values of κ (i.e. common ductile steels) lead to the plane with minimum damage. Reversed torsion loading leads to the correct MD plane. This aspect will be further elaborated in Sec. 7.3.1.

Thus the MD variant of the Spagnoli criterion is not mathematically correct for ductile steels, which dominate the test batch here. Nevertheless it is tested in a full scale as well, so that the symptoms of the mathematical problem could be analyzed.

3.1.9 PAPADOPOULOS

This is the first criterion here, which is of integral nature. Papadopoulos reassumed the Dang Van methodology in the mesoscopic branch, but decided to integer both input variables over all planes [49], [50], [51] and [52]. Such integration is understood as averaging the load manifestation over all planes. The solution is not based on the MCCM or any other methodology for obtaining the shear stress amplitude C_a, but on another integration of resolved shear stress (shear stress path projection) over all possible directions in the current examined plane.

$$\sqrt{\langle T_a^2 \rangle} = \sqrt{\frac{1}{8 \cdot \pi^2} \int_{\varphi=0}^{2\pi} \int_{\psi=0}^{\pi} \int_{\chi=0}^{2\pi} \left(T_a(\varphi,\psi,\chi)\right)^2 d\chi \sin\psi \; d\psi \; d\varphi} \,. \tag{58}$$

The integration of the normal component over all planes is expected too, but here the equality is followed up:

$$\sigma_H = \frac{1}{4\pi} \int_{\varphi=0}^{2\pi} \int_{\theta=0}^{\pi} N(\varphi,\psi) \sin\psi \, d\psi \, d\varphi \,. \tag{59}$$

The final form of the Papadopoulos criterion is:

$$\sqrt{a_P \cdot \langle T_a^2 \rangle} + b_P \cdot \sigma_{H,\max} \le f_{-1} \,. \tag{60}$$

Coefficients can be set on a basis of two uniaxial tests as:

$$\begin{aligned} a_P &= 5\kappa^2 \,, \\ b_P &= 3 - \sqrt{3}\kappa. \end{aligned} \tag{61}$$

The criterion leads to a very simple formula for the case of a pure combination of axial and torsion harmonic loadings (described by stresses σ and τ) with phase shift:

$$a_P \cdot \sqrt{\frac{\sigma_a^2}{3} + \tau_a^2} + b_P \cdot \frac{\sigma_a + \sigma_m}{3} \le f_{-1} \,; \tag{62}$$

see [52] for its derivation. The influence of phase shift is under defined loading condition zeroed, which Papadopoulos sees as a positive sign of quality of the criterion. It is not clear, how is it possible that although such an easy formula exists the results of the Papadopoulos criterion in [5] are rather inadequate. The same formula (62) can be obtained by Crossland method (38) in expectation of in-phase loading, whereas both methods differ under non-proportional loading.

The criterion is fully integrated into the PragTic. All the formulas presented previously in this section are usable according to Papadopoulos [52] for hard metals, i.e. metals where κ ratio is:

$$\frac{5}{4} \le \kappa = \frac{f_{-1}}{t_{-1}} \le \sqrt{3} \,. \tag{63}$$

3.1.10 PAPADOPOULOS – CRITICAL PLANE APPROACH

Morel in [45] cites another version of a Papadopoulos criterion [50]. According to [15], this version should be more suitable for mild steels:

$$a_{P2} \cdot T_\chi + b_{P2} \cdot \sigma_{H,\max} \le f_{-1} \,, \tag{64}$$

where T_χ is defined as a mean value of T_a over all directions on (φ, ψ) plane:

$$T_\chi = \sqrt{\frac{1}{\pi}\int_{\chi=0}^{2\pi} T_a(\varphi,\psi,\chi)\,d\chi}\,. \tag{65}$$

The material parameters can be found as:

$$\begin{aligned} a_{P2} &= \kappa, \\ b_{P2} &= 3-\frac{3}{2}\kappa. \end{aligned} \tag{66}$$

The κ ratio should lie in the range corresponding to mild steels:

$$\frac{5}{3} < \kappa = \frac{f_{-1}}{t_{-1}} < 2 \tag{67}$$

for this method. This type of solution has not been tested yet. There are only two mild steels of together 11 tests in the test batch presented here in Chap. 5, among which moreover no mean stress effect is induced. Such a small group of test results is not representative enough to evaluate strengths and weaknesses of any criterion.

3.1.11 KENMEUGNE ET AL. – INTEGRAL APPROACH

The second criterion presented in [34] and [84] is based on a spatial average of the damage parameter, i.e. it is an integral criterion. The damage parameter is very alike to that in Sec. 3.1.6, but its spatial square mean is taken:

$$\sqrt{\frac{1}{4\pi}\int_{\varphi=0}^{2\pi}\int_{\psi=0}^{\pi}\left(a_{kI}\cdot C_a + b_{kI}\cdot N_a + d_{kI}\cdot N_m\right)^2 \sin\psi\,d\psi\,d\varphi} \le f_{-1}\,. \tag{68}$$

The appropriate material parameters have to be set from three fatigue limits ([34]):

$$\begin{aligned} b_{Ki} &= f_{-1}\sqrt{\frac{15-3\sqrt{25-8\left[\kappa^2-3\right]^2}}{2}}, \\ a_{Ki} &= f_{-1}\sqrt{\frac{12\cdot\kappa^2-21+{b_{Ki}}^2}{2}}, \\ d_{Ki} &= f_{-1}\,\frac{-\left(3b_{Ki}+2a_{Ki}\right)+\sqrt{\left(3b_{Ki}+2a_{Ki}\right)^2+45\left[4\left(\frac{f_{-1}}{f_0}\right)^2-1\right]}}{3}. \end{aligned} \tag{69}$$

Alike in 3.1.6, no clear evaluation of this criterion is given anywhere, thus it was implemented into the PragTic.

3.1.12 ZENNER & LIU

The criterion given in [38] and [89] is even more complicated:

$$\sqrt{\frac{1}{4\pi}\int_{\varphi=0}^{2\pi}\int_{\psi=0}^{\pi}\left[a_{ZL}C_a^2\left(1+c_{ZL}C_m^2\right)+b_{ZL}N_a^2\left(1+d_{ZL}N_m^2\right)\right]\sin\psi\,d\psi\,d\varphi} \le f_{-1}\,. \tag{70}$$

Four different fatigue limits f_{-1}, f_0, t_{-1} and t_0 are needed for setup of all necessary material constants:

$$
\begin{aligned}
a_{ZL} &= \frac{3}{2}\left(3\kappa^2 - 4\right), \\
c_{ZL}\cdot a_{ZL} &= \frac{28}{3t_0^4}\left[f_{-1}^2 - \left(\frac{\kappa\cdot t_0}{2}\right)^2\right], \\
b_{ZL} &= 3\left(3-\kappa^2\right), \\
d_{ZL}\cdot b_{ZL} &= \frac{28}{15 f_0}\left[\left(\frac{2f_{-1}}{f_0}\right)^2 - \frac{4}{21}c_{ZL}\cdot a_{ZL}\cdot\left(\frac{f_0}{2}\right)^2 - 1\right].
\end{aligned}
\tag{71}
$$

The dependency of the criterion on four material parameters was criticized by Papadopoulos in [52] and led him to exclusion of the criteria from his comparison. Zenner et al. opposed his objections in [89] with a reference to common methods used for the derivation of fatigue limits in repeated loading from their fully reversed counterparts.

Authors of [89] show their own histogram of fatigue results concerning the Papadopoulos data, which seems to be very promising. Unfortunately, the necessary material inputs (b_0, t_0 fatigue limits in repeated loading) are not described anywhere in [89]. The criterion is implemented into the PragTic.

3.1.13 GAM (GONÇALVES, ARAÚJO & MAMIYA)

The criterion of this trio of authors is quite new [27]. It is based on a construction of minimum circumscribed ellipsoid over the load path in five-dimensional deviatoric Ilyushin space. The final measure of loading goes over the Freitas definition ([68]), because the ellipsoid is five-dimensional:

$$
f = \sqrt{\sum_{i=1}^{5} a_i^2}\ , \tag{72}
$$

where a_i correspond to length of semi-axes of the ellipsoid circumscribing the stress path in the deviatoric space. Under specific conditions – iso-frequency out-of-phase sinusoidal multiaxial loading – the following equality holds true:

$$
\sum_{i=1}^{5} a_i^2 = \sum_{i=1}^{5} d_i^2\ , \tag{73}
$$

where d_i are the distances of the centre of the ellipsoid to the faces of any arbitrarily oriented rectangular prism circumscribing the stress path in the deviatoric space [27]. Final criterion utilizes the highest principal stress over the load cycle as the second load input, so that the most damaging combination could be expected:

$$
a_G \cdot \sqrt{\sum_{i=1}^{5} d_i^2} + b_G \cdot \sigma_{1,\max} \le f_{-1}\ . \tag{74}
$$

The material variables are set from fatigue limits as:

$$
\begin{aligned}
a_G &= \frac{\kappa - 1}{\sqrt{2}\left(1 - \frac{1}{\sqrt{3}}\right)}, \\
b_G &= \frac{\sqrt{3} - \kappa}{\sqrt{3} - 1}.
\end{aligned}
\tag{75}
$$

The d_i parameters can be set from search for minimum and maximum values of the transformed deviatoric stress tensor:

$$
d_i = \frac{1}{2}\left(\max_t s_i(t) - \min_t s_i(t)\right). \tag{76}
$$

Results of the criterion in [27] on the Papadopoulos' batch of tests in [52] are of similar prediction quality to the Papadopoulos criterion, but the simplicity of the computation rapidly leading to fatigue results is amazing. Thus the criterion was added into the PragTic as well, but, until now, only in the simplified version resulting from the equality in (73).

Note that the high-speed computation concerns just only the mentioned iso-frequency harmonic loading. Under common condition the necessity to construct the minimum circumscribed ellipsoid would likely notably exceed the MCCM methods in the computation period.

3.2 LOW CYCLE FATIGUE

The low cycle fatigue area is marked by one important aspect. The critical place where the component breaks is likely to be plasticized at least at some moments of loading. When we talk about multiaxial loading, the condition of a formulation of a elastic-plastic behaviour leads to another unknown in the already strongly uncertain damage calculation. More on this point can be found in [56] and the problem was commented in Sec. 4.3.8 too.

The hypotheses presented here correspond to a chief segment in the field of low cycle fatigue. More can be found in [70].

3.2.1 LOW-CYCLE FATIGUE EVALUATION

When the low-cycle fatigue is analyzed, the resulting number of cycles, which the component can sustain, is computed as the main information. If the criterion's credibility has to be judged, the experimentally obtained number of cycles serves as a proper opponent. Fig. 10 shows how the simplest interpretation could look. It is obvious that the degree of deviation from the 45 deg line shows, how much the criterion is deviated from ideal behaviour.

When analysing more experimental data and testing separate effects, the main statistical parameters are suitable. The same parameters, i.e. mean value, range and standard deviation as in high-cycle fatigue are used, but it has to be defined which parameter should be analyzed in this way.

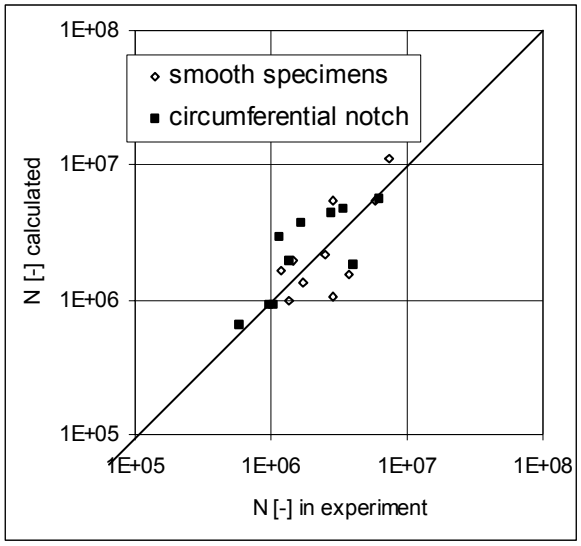

Fig. 10 A typical graphic tool for display of the prediction's quality.

The **Lifetime Ratio** *LR* corresponds well to the graphic analysis given in Fig. 10:

$$N_{measured} \geq N_{predicted} \rightarrow LR = \frac{N_{measured}}{N_{predicted}},$$
$$N_{measured} < N_{predicted} \rightarrow LR = -\frac{N_{predicted}}{N_{measured}}. \quad (77)$$

This definition was chosen in order to get the same properties as the ΔFI description. A positive value means a conservative prediction, while a negative value corresponds to a non-conservative prediction. Such proposal has at least one negative aspect, which is its discontinuity in the (-1; 1) range. Another proposal can correct it:

$$N_{measured} \geq N_{predicted} \rightarrow LR_b = \frac{N_{measured}}{N_{predicted}} - 1,$$
$$N_{measured} < N_{predicted} \rightarrow LR_b = 1 - \frac{N_{predicted}}{N_{measured}}. \quad (78)$$

It is usual to express the insufficient (not ideal) prediction as a *x*-multiple of the experimental value on conservative or non-conservative side. When the common logarithmic scale is used as in Fig. 10, both the LR and LR_b ratios show non-linear behaviour, which means that they are not suitable for the previously described statistical analysis. Much better behaviour can be obtained from the **Logarithmic Lifetime Ratio** (**LLR**):

$$LLR = \log\left(\frac{N_{measured}}{N_{predicted}}\right). \quad (79)$$

This criterion is continuous and the positive and negative values have the same meaning as the criteria above. The only problem is that the degree, how much the method is conservative or non-conservative, is not so easily recognizable for novice users.

3.2.2 SOCIE ET AL.

Socie proposed his method through the eighties and nineties of the 20th century [7], [25] and [81]. The method is based upon an observation that there are domains in fatigue life portions where different modes of cracking can be seen for materials examined. Thus two different modes of a crack initiation should be checked. One of them is the shear mode:

$$g_a \cdot \left(1 + k \cdot \frac{N_{\max}}{S_y}\right) = \frac{\tau_f'}{G} \cdot (2N)^b + \gamma_f' \cdot (2N)^c \quad (80)$$

and the second corresponds to the normal mode:

$$N_{\max} \cdot e_a = \frac{\sigma_f'^2}{E} \cdot (2N)^{2b} + \sigma_f' \cdot \varepsilon_f' \cdot (2N)^{b+c}. \quad (81)$$

The use of appropriately located planes examined (Bannantine & Socie proposal – see Sec. 2.1.3 or [7]) with each formula is expected – the shear variant (80) should be checked on planes with 45 deg deviation and on planes with 90 deg deviation for shear strains parallel to the surface and the normal variant (81) for the planes with the 90 deg deviation. The shear component of loading is checked only in its values in the direction parallel and perpendicular to the free surface.

Criterion is defined to be a MD approach, where maximum damage is the decisive parameter, whether in the normal or shear mode. Both formulas should thus be used simultaneously and the one with resulting lower number of cycles is the critical one. In some reports ([35], [54]) nevertheless, only the shear variant is tested or the both parts of the criterion are evaluated fully separately ([2] and [31]).

Moreover to that, Socie [81] proposes use of another criterion for cases of high cycle fatigue. This is a Findley based solution where the left hand side of Findley method (see (46)) is equal to equivalent shear stress. Since there is an assumption of wholly elastic behaviour, Socie proposes:

$$C_a + \beta_{FS} \cdot N_{\max} = \tau_f'(2N)^b . \tag{82}$$

Such HCF solution is rather anomalous, because here the resulting number of cycles is given.

The Socie's criterion of combined (80) and (81) formulas is validated in his [7] with results sufficient in the in-phase loading, whereas the lifetime ratio goes up to the value of four on the non-conservative side in the out-of-phase loading. Further testing e.g. in [36], with prevalent uniaxial or proportional data, shows successful prediction within the range of LR <-2; 2>.

All three formulas are implemented in PragTic. Formulas in (80) and (81) can be solved separately or the maximum damage can be looked for.

3.2.3 WANG & BROWN

CRITERION

Wang & Brown put up their criterion first in 1993 in [85]. The equivalent strain is a combination of the shear strain amplitude and efficient normal strain range:

$$g_a + S \cdot \Delta e_{eff} = [(1+\nu_e)+(1-\nu_e)S]\frac{\sigma_f'-2N_m}{E}(2N)^b + [(1+\nu_p)+(1-\nu_p)S]\varepsilon_f'(2N)^c . \tag{83}$$

The efficient normal strain range Δe_{eff} is the range between upper and lower values of normal strain in one shear strain half-cycle. Kim, Park and Lee [36] proposed another variation of (83) later on where the efficient normal strain range Δe_{eff2} corresponds to the whole shear strain cycle instead of its half. Testing of this criterion in [35], [36] and [85] show sensible results of $LR \in$ <-2; 2>, whereas [31] says that estimates under non-proportional loading tend to be conservative up to LR = 3.0.

Both variants of the efficient normal strain range definition are implemented into the PragTic, moreover with an option to switch on/off the MSE. The criterion is based on MSSR concept and thus its extension enabling the criterion to be run under an MD search was implemented too.

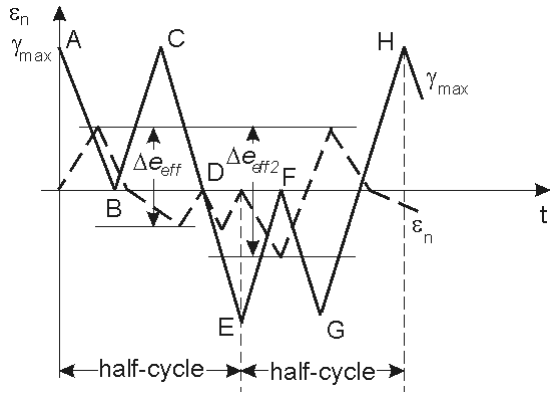

Fig. 11 Definitions of efficient normal strain range according to Brown & Wang ([85] – Δe_{eff}) and according to Kim, Park & Lee ([36] – Δe_{eff2}).

DECOMPOSITION

There are many proposals, how to decompose the complex load history into separate cycles. They are usually derived from the rain-flow method (see [65]). Brown and Wang introduced their specific way of load history decomposition in [86]. First the maximum value of equivalent strain has to be located in the load history. This value is chosen to be the starting point, and all previous data are moved to the end of the load history. The load history is than examined in search for the maximum value of the equivalent strain range relative to the present maximum:

$$\Delta\varepsilon_{eq}(t) = \max_{t} \varepsilon_{eq}\left(\varepsilon_{ij}(t) - \varepsilon_{ij}(t_{\max 1})\right). \tag{84}$$

Once such a value is found, the load history parts into two sections, which are decomposed independently with the same method. Decomposed cycles are managed with the common Wang & Brown method (83). An advantage of this approach is that under uniaxial loading it degenerates into to the common rain-flow method.

The described approach is fully integrated into the PragTic.

3.2.4 MOREL

The criterion by Morel uses parts of Dang Van's and Papadopoulos's works and shifts its focus towards the low-cycle fatigue. The plane examined here is the plane with maximum mean resolved shear stress T_χ. The equation (64) is the basis for definition of limiting state where the breakage in the meso-volume occurs:

$$T_{\chi,\lim} + \beta_{P2} \cdot \sigma_{H,\max,\lim} \le \Lambda_{P2}\,. \tag{85}$$

The limit state to the applied loading is defined by T_χ and $\sigma_{H,max} = \sigma_{H,a} + \sigma_{H,m}$ is (see Fig. 12):

$$T_{\chi,\lim} = \frac{\Lambda_{P2} - \beta_{P2} \cdot \sigma_{H,m}}{1 + \beta_{P2} \cdot \dfrac{\sigma_{H,m}}{T_\chi}}\,. \tag{86}$$

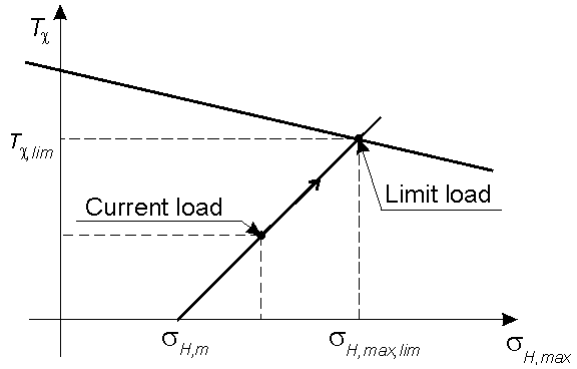

Fig. 12 Depiction of the correspondence between limit load and current load according to the Morel criterion.

If the coefficient of multiaxiality H is defined as:

$$H = \frac{T_\chi}{C_a} = \frac{T_{\chi,\lim}}{C_{a,\lim}}, \tag{87}$$

the limit amplitude of shear stress is found to be:

$$C_{a,\lim} = \frac{\Lambda_{P2} - \beta_{P2} \cdot \sigma_{H,m}}{H + \beta_{P2} \cdot \dfrac{\sigma_{H,m}}{C_a}}\,. \tag{88}$$

The number of cycles to the initiation of a fatigue crack is then defined to be:

$$N_i = p \cdot \ln\left(\frac{C_a}{C_a - C_{a,\lim}}\right) + q \cdot \frac{C_{a,\lim}}{C_a - C_{a,\lim}} - \frac{r}{C_a}, \tag{89}$$

where p, q and r parameters are functions of hardening parameters and can be set through least square method from one S-N curve – see [45]. Results of use of this criterion in [44] are within a band of

$LR \in$ <-3;3> (bending and torsion) or $LR \in$ <-6;6> (push-pull and torsion). Morel sustains this relatively high deviation by lack of suitable data for the determination of material parameters.

3.2.5 ELLYIN

The criterion by Ellyin took its final forms throughout the nineties of the 20th century [19], [20], [87]. It is an energetic criterion utilizing a sum of elastic and plastic terms of deformation energy as the damage parameter. The basic form of the criterion is:

$$\frac{\Delta W^t}{\rho_c} = \frac{\Delta W^p}{\rho_c} + \Delta W^{e+} = \kappa_E \cdot N^{w_E} + C_E \,. \tag{90}$$

The non-reversible dissipated energy in one cycle (from time t to $t+P$) is calculated as an increase in plastic deformation energy:

$$\Delta W^p = \int_t^{t+P} \sigma_{ij} d\varepsilon_{ij}^p \,. \tag{91}$$

Since the plastic term of deformation energy tends to be zero in HCF, the elastic term is added as well to include both potential categories. Here only the positive (i.e. crack opening) stresses and strains are evaluated:

$$\Delta W^{e+} = \int_t^{t+P} H(\sigma_i) H(d\varepsilon_i^e) \sigma_i d\varepsilon_i^e \tag{92}$$

through Heaviside function:

$$\begin{aligned} &H(x) = 1 \quad \text{if } x \geq 0, \\ &H(x) = 0 \quad \text{if } x < 0. \end{aligned} \tag{93}$$

The parameter ρ_c is a factor of multiaxiality constraint, which is defined to be:

$$\rho_c = \left(1 + \nu_{eff}\right) \left[\frac{\max\limits_i \left(\varepsilon_i\left(t_m\right)\right)}{\max\limits_{i,j} \left(\varepsilon_i\left(t_m\right) - \varepsilon_j\left(t_m\right)\right)} \right], \tag{94}$$

where t_m is the time where a maximum value of the denominator is reached and ν_{eff} is effective Poisson's ratio, which can be obtained e.g. with the following formula:

$$\nu_{eff} = \nu_p - \left(\nu_p - \nu_e\right) \cdot \frac{\Delta\sigma_{eq}}{E} \cdot \Delta\varepsilon_{eq} \,. \tag{95}$$

The parameters κ_E and w_E of (90) are material constants that can be set on a basis of two LCF tests, and C_E is the non-damaging elastic deformation energy, which has to be set from one HCF test.

The criterion prediction is tested in [19]. Here the data lying in the LCF region are suitably predicted, but when the fatigue process tends to come to the HCF (more than $2 \cdot 10^5$ cycles), the results of out-of-phase loading are very poor. LR reaching from -4 to -9 is seen here. Even worse, these badly predicted data-points lead to smaller differences between deformation energies set experimentally and by computation than the data-points with better accordance of fatigue damage results. This finding somewhat decreases credibility of the criterion.

4 PRAGTIC FATIGUE POSTPROCESSOR

The starting point for design of the software described in the further text was a requirement to have a control of all parameters of the fatigue life computation. Such requirement is not fulfilled by general commercial fatigue postprocessors, which are treated in Sec. 4.1 in short.

Although the design was based on a previously built *LPSAfat* and *MAXA* programs [57], [64] and [77], development took its time. This prolongation was caused mainly by work spent on a new native database for storage of FE-data. Expect for better access to FE-data, which was obtained in this way, the new solution was accepted as well for the reason of further expected branching of software as a common FE-postprocessor. The set of original expectations and requirements is stated and commented in Sec. 4.2. All features of the final programme are described in Sec. 4.3. Finally, proposals concerning further changes, improvements and implementation are commented in Sec. 4.4.

4.1 MARKET RESEARCH

I was able to find 5 commercially fatigue postprocessors available in the time of writing the thesis. An attempt at their more or less subjective comparison is given in this section and is closed by Tab. 1. The overview does not include separate extensions of FE-packages as they are included e.g. in COSMOS, ANSYS or the Fatigue Advisor of Pro/ENGINEER. Such solutions usually implement only some variation of S-N solution with uncomfortable input of computation parameters.

There is one of the five mentioned software packages, which can be marked as low-cost. This is WinLife. Prices of the other products are more than five times higher, reaching commonly the purchase price over 30 000 Euro. A usual annual maintenance costs somewhere between 15 and 25% percents of the purchase price.

The overview of features of individual software packages described further was done for ŠKODA VÝZKUM s.r.o., financial support of which is gratefully acknowledged.

4.1.1 WINLIFE

The program is developed by Steinbeis Technology Center in Ulm, Germany. It is distributed via the NEi-Nastran of Noran Engineering (http://www.nenastran.com) or separately (www.stz-verkehr.de). It has three separate modules – *Basic*, *Multiaxial* and *Gear Wheels and Bearings*, names of which apparently categorize their use.

The basic solution uses the S-N approach. The main disadvantage is the necessity to manually assign the S-N curve to each detail or notch, which prolongs the time necessary for finding the solution. Local uniaxial methods utilizing the e-N solution are implemented too – these are Smith, Watson & Topper method and newly the Bergmann method (for their description see e.g. [67] in Czech or [57]).

The multiaxial module is based on the S-N approach too. It uses damage computation on predefined planes. The maximum damage is the decisive criterion. The new version 2.3 (February 2005) has Findley's damage parameter implemented.

The program has no internal visualiser for display of the FE-mesh and results computed on it. Besides the Neuber's elastic-plastic solution the Mróz kinematic model is implemented as well in order to cover the multiaxial area. FE-data of less used FE-solutions IDEAS, SAMCEF and WTP-2000 can be imported directly. The only solver with direct import used more widely is Nastran, all other common programs need converters.

This is the only low-cost representative among fatigue FE-postprocessors, thus the prices should be mentioned too. The *Basic* module can be got for 3 400 Euro, *Multiaxial* for 4 200 Euro. The maintenance costs 1 500 Euro/year for both modules together.

4.1.2 FE-SAFE

Fe-Safe is being developed by Safe Technology in Sheffield, England. Fe-Safe is distributed via the Abaqus distribution network, and besides of it as a stand-alone product as well (see http://www.safetechnology.com). Fe-Safe incorporates another product of Safe Technology, which is the *Safe4Fatigue* aimed at signal processing and damage computation without FE-data. Additional modules *Rotate* for solution of axis-symmetric components and *TMF* for thermo-mechanical fatigue solution including creep effects are available.

All features except for the additional modules are integrated together. The program has not any internal visualiser of FE-data. The import options are wide: Abaqus, Ansys, Nastran, Beasy, Hypermesh, IDEAS, FEMSYS, CADFIX. In addition to the superposition of several FE-result files an option of definition of a sequence of FE-result files depicting e.g. transient behaviour can be used too. User can largely rule over load inputs through many implemented mathematical functions and block operations.

The multiaxial solution incorporates both S-N and e-N approaches. A representative of combined criteria with normal and shear strains is implemented too (Brown-Miller). Dang Van method is used for high-cycle fatigue. As regards the weld solution, each critical place has to be solved separately.

The product is furnished with a manual, which is at the top compared with other fatigue postprocessors. The context help is missing even here.

4.1.3 MSC.FATIGUE & FE-FATIGUE

These two products are described in one section, because they have the same core developed by nCode (Sheffield, England). Thanks to the strategic partnership with MSC.Software, these two companies cover all area of FE-processors. MSC.Software takes care of integrating the attachment to MSC.Nastran and of distribution of both software units (www.mscsoftware.com), whereas nCode develops the core unit and provides integration towards Ansys, Abaqus and IDEAS. The properties of MSC.Fatigue will be commented further.

The program is highly modular. It reaches the top concerning the prices. It is fully integrated into the Nastran environment, which is an interesting feature. If the Nastran is not available, the *Pre&Post* module must be bought to the *Basic* module in order to be able to use any FE-data. The multiaxial module is separated as well as modules *Vibration*, *Welds*, *Fracture* and *Utilities*.

The *Weld* module has its weakness in specific requirements on modelling of weld area, which considerably complicate work. Thus, e.g. the fillet weld of two perpendicular components has to be modelled with a row of elements connecting both sheets under 45°. The *Fracture* module is the only module of commercial products described, which computes the crack growth phase as well. This is in accordance with the Nastran‘s focus towards the airplane’s design.

The multiaxial solution comprises Mróz – Garud model of cyclic plasticity, Wang & Brown generalized rainflow decomposition and Socie’s criterion. The McDiarmid’s method covers the HCF region. One-parameter based calculations using only shear or normal strain are implemented as in other cases.

Though expensive, the program offers nearly all solutions except for the thermo-mechanical fatigue with creep. The only thermal effect incorporated is the change of S-N curves under specific high temperature.

4.1.4 FEMFAT

The program is developed by Engineering Center Steyer (ECS), which is a subsidiary of Magna Steyr located in St Valentin (Austria). Thanks to nearness, the program is distributed in Czech Republic directly from St Valentin. The program is highly modular, with moderate prices in comparison to MSC.Fatigue.

FemFat (http://www.femfat.com) is wholly based on the S-N solution. Even the multiaxial method is based on S-N curves, which are evaluated over specific planes. Unfortunately, only one reference [28] covering this type of solution was found in scientific area. There are not enough proofs in this reference to ensure the validity of the proposal used. Moreover, ECS does not offer complete clarification of its approach and leaves it as its know-how.

FemFat features one of the best weld modules for both spot and seam welds. The problem with the *Seam Weld* module is that although the solution is well developed the interface for the weld definition is not automated. Although no shape changes of the FE-model in the weld locality are required as by MSC.Fatigue, the user has to operate largely over the FE-data in order to define the weld shape by predefined numbers of coordinate systems and materials. The *Spot Weld* module has integrated a strong feature of mesh replacement around any defined spot weld. Since this re-mesh is automated, all necessary definitions of mesh properties are included, unlike to the seam weld solution.

Another strong point of FemFat is the existence of the *Heat* module with embedded thermal fatigue and creep model by Sehitoglu. The *Visualiser* module enables graphic inspection of results on FE-mesh, but it has only very basic functions.

4.1.5 LMS.VIRTUAL LAB COMPONENT DURABILITY

The LMS International (www.lmsintl.com) product range is very wide similarly with the MSC.Software. The Virtual Lab is the one unit of the whole product line where the Component Durability belongs. Some users can know its former name Falancs, which was changed after its acquisition by LMS International.

LMS contracted a settlement with Dassault Systemes. The arrangement allows the LMS to use the CATIA's interface for further development of its products. Thus the producer got enough room and time to facilitate more the postprocessing of obtained fatigue results.

The basic module incorporates the multiaxial solution. It is very basic, because only separated shear and normal strain component criteria are used. The Dang Van criterion is implemented for high-cycle fatigue.

The user can buy the spot weld and seam weld modules separately. Until now they are the only further modules. Module for random fatigue is to be incorporated at the end of this year. The seam weld module is built in the same way as it is in FemFat, but only British Standard method is implemented. Interesting is the automated detection of expected weld localities and offer of potential seam weld shapes. All FE-data inputs are managed with separately paid converters, which present a quite unpleasant additional fee.

The LMS overcomes other competitors with much better user interface, vast possibilities of further postprocessing and excellent seam weld module. The problem can be that it has not any thermal module until now.

4.1.6 OVERVIEW OF MULTIAXIAL SOLUTION

As regards the multiaxial solution, FemFat and WinLife utilize their specific approaches utilizing S-N curves evaluated on the planes examined. There are a number of methods implemented, predictive capability of which is not referred in any text I could find. Those are the methods utilizing e.g. von Mises stress, first principal stress, maximum shear stress amplitude (with no relation to normal stress), or other as the damage parameter. The damage parameter is often based only on one load parameter.

The other implemented multiaxial methods are:

- Dang Van criterion (LMS, Fe-Safe);
- McDiarmid criterion (MSC.Fatigue);
- Brown-Miller criterion (Fe-Safe);
- Findley criterion (WinLife);
- Socie criterion (MSC.Fatigue);
- Wang & Brown criterion (MSC.Fatigue).

The listing is very short and discloses that the implementation of new methods ended somewhere at the start of the nineties of the last century. Although since then many other new methods appeared, these criteria are not available.

criterion	WinLife	Fe-Safe	MSC.Fatigue	FemFat	LMS
basic solution	***	****	****	****	*****
seam welds	*	**	***	****	*****
spot welds			*****	*****	*****
PSD input		*****	*****		
modal input		*****	*****	*****	*****
thermal fatigue	*	*****	*	*****	*
creep		*****		*****	
multiaxial solution	***	*****	*****	****	****
transient solution (sequence of FE-calc.)		*****	*****	*****	*****
load history operation	*	*****	**	**	*****
manual	*	*****	****	***	*****
crack growth			*****		
intenal visualiser			*****	****	*****

Tab. 1 A comparison of features offered by commercial fatigue postprocessors. Maximum is marked with five stars, whereas none of them corresponds to no implementation. It is hard to define objective criteria for the comparison, therefore note that results are more or less subjective perception of mine.

4.2 REQUIREMENTS DEFINED

The previous work on *LPSAfat* (see [57], [61], [58]) and *MAXA* fatigue postprocessors([62], [74], [75]) was used as an initiation point, because their weaknesses were obvious. The target of the software development [64] was set as follows (the text in italics is nowadays commentary):

- An implementation of the methods defined with possibility to easily implement new methods.
- An ability to change a setup of different methods, to combine parts of their computation – in short to get a proper research instrument.
- An independent material database with integrated edit functions. *This point links to LPSAfat's material database, which had such functionality. Nevertheless the present solution is acceptably strong even without the material database. Thus its implementation was postponed.*
- Work with load history, its edition, composition, filtration & decomposition. *Done, except for the functions for internal composition of load history. They can be solved very easily e.g. with Excel or any other spreadsheet or even with very simple C programs. Anyway, an option to define the load history as a combination of simple mathematical formulas is implemented.*
- Enabling the load input from several load channels together. To define a proper definition of load system superposition.
- Reading FE-analysis results as the input data for the fatigue analysis.
- Building an inner data structure for description of whole FE-model. *This point was highly emphasized, because already MAXA had e.g. McDiarmid solution integrated. But the work with external data from FE-files was such a mess that the decision to build an inner database of the FE-data was adopted.*

- A visualisation of fatigue results through common FE-postprocessors. The *previous software packages operated over the ABAQUS ascii *.fil file, which could be visualised in the FEMAP postprocessor. Since this solution seemed to be too cumbersome, here the transfer of data back to origin FE-postprocessors was admitted as the best (=simplest) method.*
- A clear and readable user interface. *An attempt to facilitate the handling of program with minimum pop-up windows and integrate the inputs into the expectable places was made.*
- A help system. *The LPSAfat software had its own context help, so its existence inside the PragTic was presumed. When more users are expected, then it is very useful. It was postponed due to lack of time.*

4.3 FEATURES

The program is developed in C/C++ language. As in previous versions, the C++ Builder 5.0 was accepted for development. Due to lack of manpower and problems to keep an order over all calculation and input components from inside the console line, the idea of independent clean ANSI coding topped with either UNIX or Windows shell was abandoned. From November 2003, further implementation was directed to the use of full C++ Builder strength, which is in Windows based programming. Some features introduced here were already in less detail presented in other texts [61], [64], [77].

4.3.1 DATA STORAGE & MANIPULATION

A proper structure for data storage was looked for, so that the data could be quickly accessed and retrieved. Finally a schema of doc. Španiel from the Dept. of Mechanics of CTU was accepted. The concept is based on finding that nearly all FE-data and subsequent parts of computations can be decomposed into vectors with a uniform size of each component.

These entities are called **data_vectors** here. Each data_vector has its heading where description of its content, size of the component, number of items, etc. are placed. The data_vectors are saved in unique binary files. The binary form of files is the main reason for the described decomposition of data. It allows fast access to a desired component of a file, which is based on its relative position inside the data_vector and size of the data_vector component. The storage programmed to be file by file has another advantage, which is embodied in fast orientation throughout the data heap towards the desired type of the data_vector / file. Moreover, any change in the length of data_vector (add-on, deletion of components) does not take so much time, as if one file contending all data together was used.

The disadvantage of such a storage concept is that there are a huge number of files saved in one directory. Thus, there is another entity called **data_base** which is a class derived from the data_vector class. It consists of uniform components describing each data_vector, which belongs to the project being solved. The description takes over parts of the data_vector heading, but documents too, whether the data are saved in the file, which is currently not accessed, or the file is open and some part of it is read into the memory as the data_vector representation. The data_base is equipped with methods, which enable such opening and closing together with reading and writing of data.

The read and write functions are one of the most time demanding functions due to the access to the computer's hard disc. The data are cached in order to minimize the number of accesses. The user can open the data_vector through data_base method with some specified number of items concurrently read in one access to the hard disc representation – thus the cache is created. It can be expected that any query to the file is not a stand-alone process, but is a part of a sequence of queries. The size of data retrieved with one access does not prolongs the retrieval time so much as the access creation and termination, whereas the content of the cache is be used more than once for the given component.

The FE-data structure is linked together with pre-defined links. E.g. the element description refers to a number of defined real constants describing elements properties. Moreover, some items of the data description can have different sizes. An element is among others described by an element table of incidences, which shows all the nodes that form the element. Since there can be different element

types with a various number of nodes in one FE-model, the whole element description cannot be saved in one data_vector.

Thus the data_vector methods and properties are inherited to further data types, which have implemented defined possible links. As a result, the element description contains the element heading, with links to data_vectors of element groups, real constants, materials and to the element table of incidences. This last derivation of data_vector contains numbers of nodes of each element one after another, which are related with a reference in the element description. If some element is inserted into the structure, the insertion takes place only in the element description data_vector, which is an advantage. The element table of incidences data_vector is operated only through an addition to the end of the data_vector and a change of components number in the heading.

4.3.2 MEMORY POOL

At start, a port towards the UNIX system was expected as well. UNIX has speciality that two or more users can operate simultaneously. Each of potential users takes his part of system devices, which comprehends the memory too. If the memory residue available is too small to realize actions defined by the program, it can lead to its subsequent breakdown. The same problem can be found in Windows if there are more applications running simultaneously.

To prevent such a breakdown coupled with loss of not saved data, the **memory pool** was created. The memory pool is a space in the memory, which is pre-allocated at the start of the programme. Once pre-allocated, no other program or user can occupy it. Any further memory allocations necessary for the run of the program have to be done inside this memory pool.

The memory pool is defined as a class, equipped with methods enabling to document and manage the space already taken and the space inside the memory pool, which is still free.

Such solution prevents the breakdown caused by momentary excessive requirements on system devices. The loss of data caused by e.g. an outage is above all treated by the segmentation of processed data into the smaller files. Potential damage is minimized in both these ways.

4.3.3 FE-DATA INPUT

The previous software solutions were tightly connected to specific output formats of FE-solutions, generated by individual FE-solvers. It was e.g. the *.fil ascii file by Abaqus (see [57]). Such solution has its advantage in the fact that only one or at maximum two files (the topology of a FE-model and its results) have to be imported. The disadvantage is that the output formats can change during the development of these FE-solvers.

PragTic uses another concept. Since the FE-data can be considered as vectors, the common solvers (Ansys, Abaqus, Cosmos) allow the data to be reported in very similar formats consisting of comments, a header line describing the individual columns, and the information itself, which observes the rules of header line above. This information report can be interrupted by white lines or by repetitions of the header line (see the printout in the upper part of Fig. 13).

The information necessary for fatigue computation is usually well structured (description of nodes, elements, results). The biggest trouble is thus the recognition, which item in the file is currently being imported. This problem is solved with predefined names of columns that are usually used among FE-results.

The final implementation has these steps (see Fig. 13):

- The user selects which file is to be imported.
- A transcription of first 20 lines of the input file is shown in a dialogue window. User can add further lines by a right-hand click in a pop-up menu.
- Another choice in the same pop-up menu is to mark the header line. Once specified, the header line is scanned through and separate words are decomposed into the lines below. User then runs a trial analysis of imported data.

- If the column name is already mentioned in the database defined, a possible interpretation is proposed to the user (the fourth and fifth columns in Fig. 13). Minimum and maximum values in the given columns are written as well in order to present an overview of read data to the user.
- The user can change the interpretation proposed by a double click in the line examined. An option to eliminate some column and its data from the further conversion into the PragTic database is implemented too.
- If satisfied with the decoding proposed, the user runs the import. The import functions decompose the information read into the data_vector system used in PragTic and add the data_vectors into the data_base.

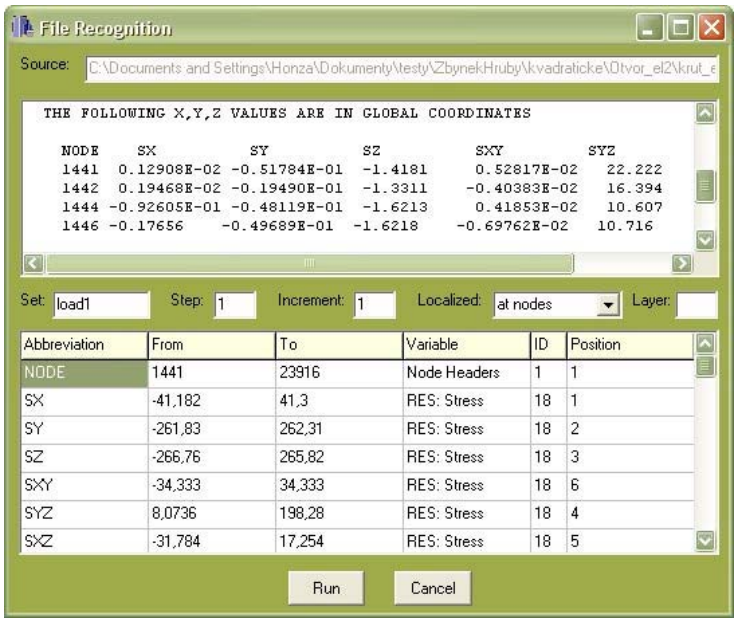

Fig. 13 The dialogue that enables import of formatted inputs as e.g. stress results created by Ansys here.

The disadvantage of the solution introduced here is that it takes more user's steps to import all data. Nevertheless, the user gets much better insight into the matter what he imports and he can check the data. It can be expected in addition that even FE-solvers, which were not until now tested, can generate files that would form an input sufficient for the PragTic analysis. Considering the intention of PragTic development, such solution looks much more handier.

4.3.4 LOAD HISTORY, MODES & REGIMES

The program was specialized in the multiaxial solution from the very beginning. This requirement posed claim to build up a system of load inputs that would be able to correctly simulate their interaction throughout the service. The following specialized data_vectors were created:

- A **load history** is a sequence of load data (forces, stress tensors or some other) which are either linked to a given time sequence or are freely ordered according to the time scale, but without its formal declaration. PragTic allows uploading the load history from an external source via the import system described in 4.3.3, editing it directly or creating it with simple mathematic formulations (see Fig. 14).
- A **load mode** is a combination of FE-results and the load for which they are obtained. To get the fatigue solution in one singular point instead of the FE-results, the user can set one stress tensor that has to be again linked to a specified external force.
- A **load regime** is a combination of the load mode and the load history. It completely defines service conditions of one type as e.g. the braking of a car can be.

In addition to the imported load history an option to define the load history by its generation from mathematically based signals is implemented. Here the option to define amplitude, phase shift and period is given for sinus, triangular and constant functions (see Fig. 11). The user can adjust sampling rate too, i.e. the number of data points in one period. The signals defined in the lines of Fig. 11 are not written to complete load history data_vectors, but only their definitions are saved. The final composition of the load regime history is done just before the fatigue computation itself.

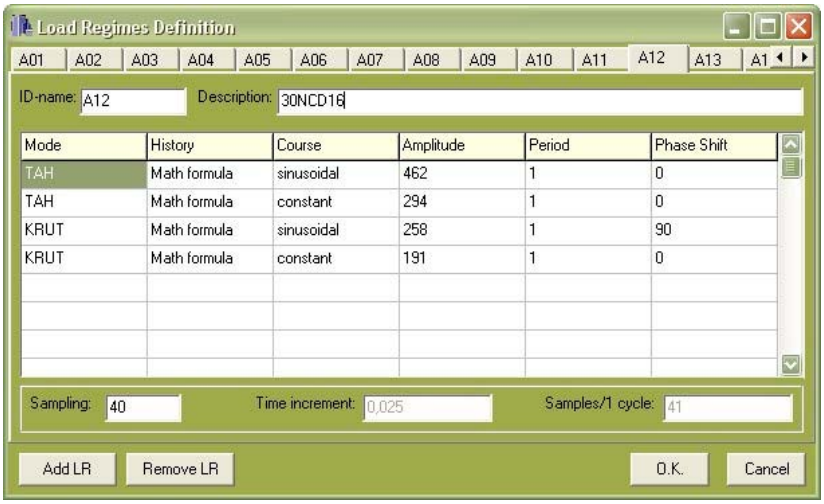

Fig. 14 Definition of the load regime as a superposition of several load channels described with mathematical formulas. The load regime given corresponds to the MPA12 test commented further.

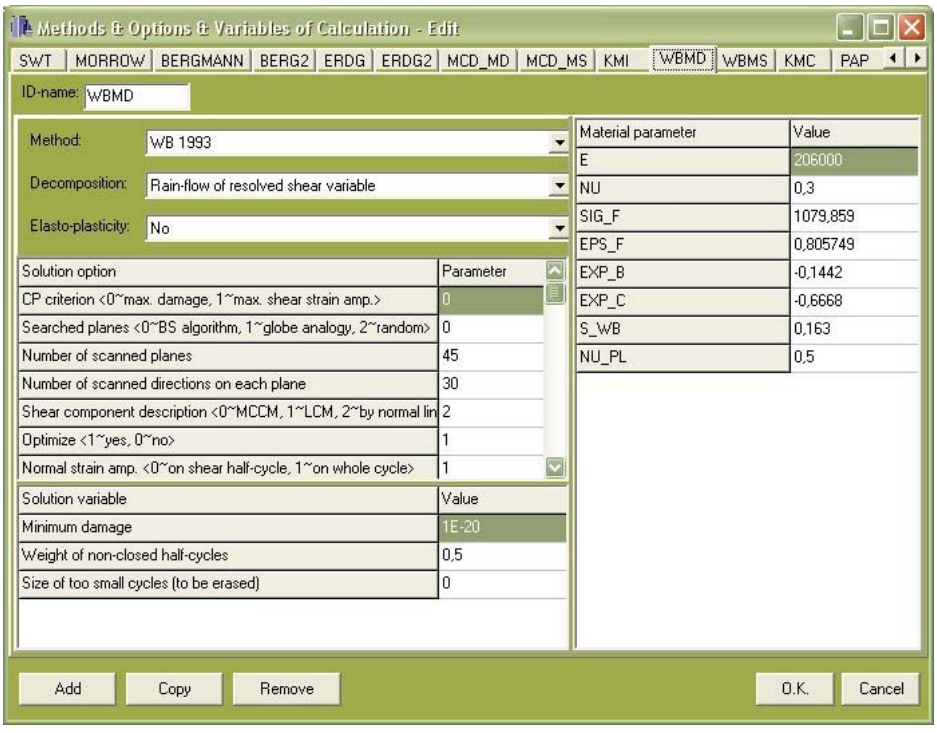

Fig. 15 Dialogue for description of used method, its setup and material parameters.

4.3.5 SYSTEM OF COMPUTATION OPTIONS

A set of optional parts of the computation process is defined for each calculation method – e.g. choice of the type of the load history decomposition belongs here. There are real and integer variables as well, which define the accuracy of computation, its speed, etc. All these options are defined for each

calculation method and are set in one common dialogue (see Fig. 15). The same dialogue takes in the setup of material variables, which are to be used in the computation.

Since setting of all these options and values is lengthy, an option to copy the setup of a desired method is implemented. This is the most tedious part of a solution's definition if more calculation types are necessary and therefore some further elaboration would be desirable. What is still missing to simplify the user interaction is an ability to upload the material data from a material database. An option to create a template of the setup of calculation methods would be comfortable too.

The PragTic program allows more calculation methods to be run in one analysis. It is optimised in such a way that once the local load history is built at some node it is used for all required methods of the computation. The final setup of what has to be calculated is done through the dialogue in Fig. 16, which appears after click on the *Run* button in the main menu (Fig. 17). This dialogue enables to combine defined computation methods, load regimes and limit the number of nodes for which the analysis has to be done.

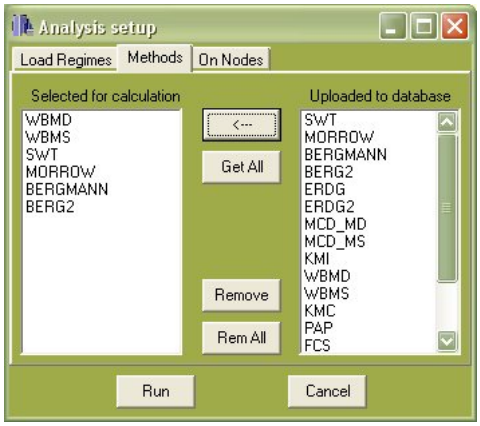

Fig. 16 The final selection of calculated load regimes, used methods and nodes for combinations of which the calculations are done.

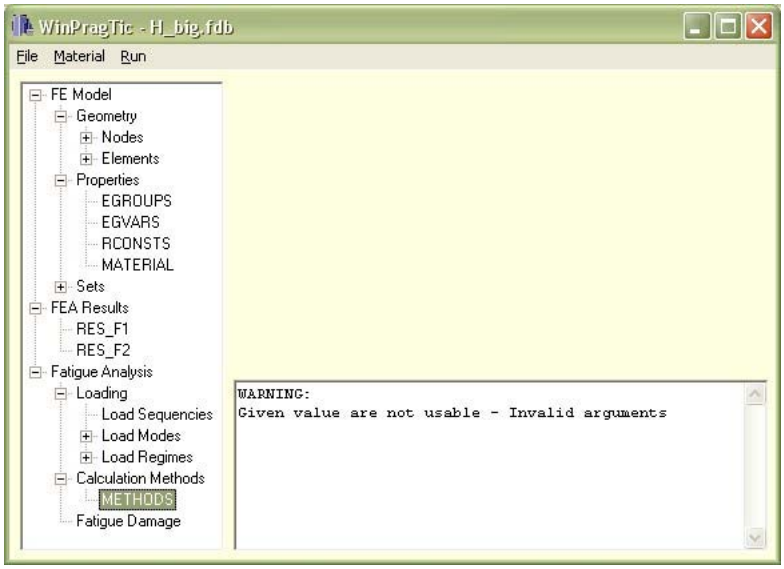

Fig. 17 Main window of the PragTic program. The overview of database items is on the left side, whereas the report window is on the right side.

4.3.6 USER INTERFACE

Parts of used dialogue windows were already presented in Fig. 13 – Fig. 16. The main user interface (Fig. 17) consists of three important items. These are the main menu, database tree and report window.

The main menu allows the current analysis setup to be saved, to save all the files under another name and to import new data. The *Material* option is not active now. The analysis is triggered by the click on the *Run* option of the main menu. The import allows also importing data_vectors used in another project. Such option can be very useful e.g. for a retrieval of the setup of methods (some compensation for missing templates commented in the previous section).

The database tree gives an overview of data_vectors / files that are already included in the project. Data_vectors are grouped according the variables they contain. A pop-up menu that appears after a right-hand click allows the user to view the items of given data_vectors or to edit them directly. The edit dialogue opened (Fig. 18) contains a *Fast Ascii Copy* button among others. The user can get the content of the spreadsheet into a formatted ASCII file by a click on it, which is the simplest way of any data export.

Other options of the database tree pop-up menu are the *Remove* and *Delete* options. The removal means exclusion of the data_vector from the data_base, whereas the deletion besides means a complete deletion of the appropriate file from the computer's hard disc.

There is an output window to document the state of computation and to show necessary notices. The warnings and errors are depicted here, as well as in a stand-alone warning/error window.

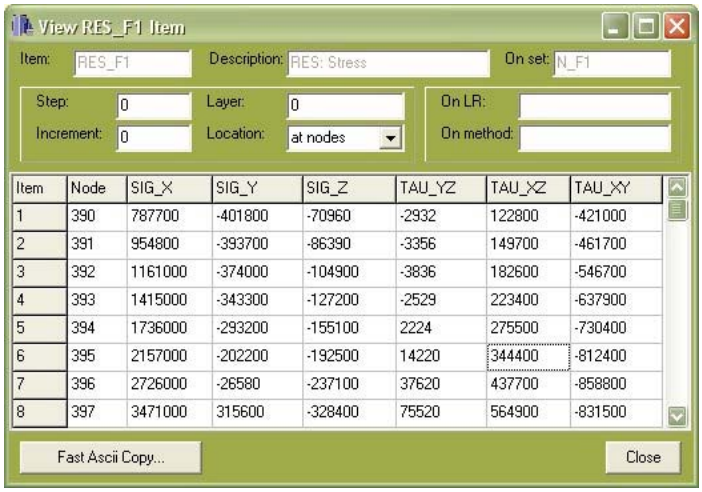

Item	Node	SIG_X	SIG_Y	SIG_Z	TAU_YZ	TAU_XZ	TAU_XY
1	390	787700	-401800	-70960	-2932	122800	-421000
2	391	954800	-393700	-86390	-3356	149700	-461700
3	392	1161000	-374000	-104900	-3836	182600	-546700
4	393	1415000	-343300	-127200	-2529	223400	-637900
5	394	1736000	-293200	-155100	2224	275500	-730400
6	395	2157000	-202200	-192500	14220	344400	-812400
7	396	2726000	-26580	-237100	37620	437700	-858800
8	397	3471000	315600	-328400	75520	564900	-831500

Fig. 18 The viewer and editor of data items. Notice the Fast Ascii Copy button in the left bottom corner.

4.3.7 CALCULATION METHODS IMPLEMENTED

Methods of the following authors are currently integrated:

- uniaxial (e.g. [67], [69], [71] in Czech or [57])
  - Smith, Watson & Topper
  - Morrow (also accredited to Landgraf)
  - Bergmann
  - Erdogan & Roberts
  - Heitmann
  - Morrow energetic
  - Feltner
  - Pospisil
- multiaxial – commented here in Chap. 3, also e.g. in [59], [60]:
  - HCF
    - McDiarmid v. 91

- McDiarmid v. 72
- Findley by Socie
- Papadopoulos
- Findley
- Kenmeugne et al. IA
- Kenmeugne et al. CPA
- Zenner & Liu
- methods proposed further in Chap. 7.

- LCF
  - Socie combined
  - Socie shear version
  - Socie tensile version
  - Wang & Brown

4.3.8 ELASTO-PLASTICITY

A computation of low-cycle fatigue remains disputable. Unlike in the HCF, where the completely elastic response can be expected, there are areas on the components loaded in the LCF region, where significant plasticity effects appear. Thus when the FE-model results have to be processed towards the fatigue damage calculation, the effect of plasticity has to enter somewhere on the way of computation. Its involvement further complicates the calculation, because the plastic response corresponds to a non-linear relation between stress and strain. Consequently, superposition of load modes, which could be effectively used in the HCF computation, cannot be used anymore.

There are two ways, how to get through this problem. The difference is based on the position, where the plasticity effect is introduced in the computation process.

First, when the load cycle is simple and not changing throughout the service history, the so-called **transient analysis** can be run. The load cycle is fully non-linearly simulated in the FE-solver and the results are mapped over the load cycle. An extensive introduction into the elastic-plastic constitutive relationships can be found in Czech in [56]. The fatigue solver can handle both stress and strain data and use this simulation of stress-strain behaviour through the load cycle directly. However, any further changes in the elastic-plastic behaviour through the cycle repetition as hardening, softening or ratchetting cannot be covered. It is clear as well that the results of FE-analysis cannot be used for any other combination of load channels.

The other way leads through a fully elastic FE-calculation. The plasticity effect is not introduced until the fatigue analysis is run. This solution uses e.g. the well known Neuber or Glinka method, which are both implemented in the PragTic as options for uniaxial analysis. Nevertheless, both these methods are verified and found acceptable only under uniaxial or proportional loading. There are other methods published, which are usable in the multiaxial area too – see e.g. [32], [40], [78].

Anyhow, the work on PragTic was until now focused on development of general computation line, with a specific goal set onto the high-cycle fatigue. The implementation and analysis of methods for full elastic-plastic description is expected in near future and only after the tool for transient analysis solution is implemented.

4.3.9 INTEGRAL METHOD IMPLEMENTATION

The integral methods are based on an integration of at least one load parameter over all planes in the examined point. The integration can be related to a unit sphere, surface of which is the result of integration if no other parameter is integrated:

$$\int_{\varphi=0}^{2\pi}\int_{\psi=0}^{\pi}\sin\psi d\psi d\varphi = 4\pi\ . \tag{96}$$

The integration has to be done in a discrete form. Thus a proper method of changes of φ and ψ angles had to be proposed. The following solution was implemented into the PragTic.

User sets the angular step of the search plane normal line lying in the plane tangent to the surface – i.e. he defines the basic $\Delta\varphi_B$ angular rotation (see Fig. 4). Length of the l_B circle arc between two points defined by this angular rotation in the tangent plane is computed and has to be preserved over the integration. The same as the basic $\Delta\varphi_B$ value is the $\Delta\psi$ angular rotation, which stays constant throughout the integration. Once the integration was performed on the tangent plane, the ψ angle is decreased from 90 deg by $\Delta\psi$. Here the evaluation is done what the angular rotation $\Delta\varphi_I$ should be in order to preserve utmost the l_B distance of points $(0; \pi/2\text{-}i\cdot\Delta\psi)$ and $(0+\Delta\varphi_i; \pi/2\text{-}i\cdot\Delta\psi)$ defined by these parameters on a unit sphere.

The reason for the preservation of arc length and not angular rotation is based on the description of the unit sphere. Weights of load effects entering the integration are approximately the same in this method, because the spherical area represented by the angular steps does not change significantly. There is much lesser number of planes being evaluated as well. And finally, the planes with higher $\Delta\varphi_I$ angular step are the planes where no significant damage can be expected (they are only slightly deviated from the plane tangent to the surface).

A trapezoidal method of integration is used throughout the discrete integration. The method was tested against the analytic solution given by Papadopoulos in [52] (here further in (62)) with a basic angular step of 2 deg. Results of fatigue index error (see (33)) were deviated at most by 0.11% for non-proportional loading and by 0.003% for proportional loading. Note, that the Papadopoulos method includes one more integration of resolved shear stress over all directions lying on the examined plane. This further integration was done with the same 2 deg step of angular rotation. Thus the described accuracy of computation seems wholly tolerable.

4.3.10 CRITICAL PLANE SEARCH

The three ways of the critical plane definition are described in 2.1.3, together also with the proposal of Bannantine & Socie for predefined directions of critical plane normal lines. This is one type of solution, which is offered. The problems given in the text further are not related to the CSM approach, which is dependent only on changes of loads, not on the meshed virtual model.

The position of the critical plane on the fictive meshed (i.e. discrete) surface of solid body is purely speculative. Although there is a uniaxial loading on sharp edges, any other smoother shape transition can generate an error if it is irregularly meshed. Moreover, some MD criteria tend to reach maximum damage on other planes, than those defined by Bannantine & Socie. And further, there are the cases of contact loading, where even the MSSR concept will fail if only the B&S planes will be examined.

Thus the same scan concept as described in the previous section was accepted for the search for planes that have to be evaluated. It will be referred as the **global search** in the text further. In order to shorten the computation time the basic angular step of 8 deg is accepted as the implicit value. Due to the discrete character of such a mapping, it is relatively sure that such a search will not reach the correct solution. To overcome this problem a further optimization can be run as a recommended option, which searches for the exact position of the critical plane.

The described optimization goes well for the MD methods where it is likely that the critical plane is unique. This is not the case of MSSR methods where more planes with MSSR can exist but with different normal stress. Then the final selection of the CP has to be done according to the whole damage parameter. The discrete record of the MSSR value throughout the scanning procedure can miss the potential CP and mark another plane, which is closer to the final MSSR value thanks to its lesser deviation from the normal line of the plane with the another MSSR. Then further optimization on such a plane can lead to erroneous (supposedly lesser) values of damage.

The solution accepted in PragTic utilizes the following concept. Once a value of MSSR higher than some given ratio of the present maximum is found, a maximization towards the plane of highest possible MSSR is done. If this one is reached a further maximization is aimed at maximization of the

whole damage parameter, while the MSSR value has to be maintained on the same level. If the search path gets too close to a plane which has been already marked as a potential CP, the maximization is abandoned and another plane of the original order is tested. It is expected here that further maximization would lead to a plane, which is already among the separated potential CPs. As a result, a set of potential CPs, which have a high MSSR and are oriented relatively different one another, is created. The final critical plane is chosen from them. The final choice is based on the highest MSSR at first. If more of the MSSR values on different planes coincide, then a second round of the selection is run according to the highest value of the damage parameter.

4.4 FUTURE DEVELOPMENT

Currently an extension of the PragTic program towards the import and use of results for transient analysis (i.e. both stress and strain data throughout the load history) is being implemented. Some other enhancements that would be useful were already commented. The majors are:

- Building of the material database. An option to upload some specific material from the material database has to be added into the Methods dialogue. Its properties should be still editable in the Methods dialogue and their saving back into the material library should be enabled.
- It could be useful to use predefined templates of calculation methods. The option to use default values for given methods seems interesting as well.
- Help system would be desirable. It is becoming more and more tedious to describe the solution, however is the interface simplified.
- The dialogue triggered by the click on the Run button that creates triplets of load regimes, calculation methods and selected nodes should be moved to the menu as a new "**analysis**" data_vector. The Run button would launch a dialogue, which analyses from the "analysis" data_vector have to be computed. This step would notably simplify further re-calculations of new methods and new load regimes. A perfect example for its potential efficient use is the subsequent derivation and testing of new methods in the Chap. 7.
- The implementation and testing of plasticity models that would enable to transform the fictive fully elastic solution into the elastic-plastic one.

5 SET OF EXPERIMENTAL DATA USED

The primary experimental data used in the comparison of a predictive capability of methods implemented in the PragTic fatigue postprocessor were completely extracted from the referred literature. All data concern the high-cycle fatigue.

There are methods in PragTic, which can cover low-cycle fatigue as well. Although there are many tests data available in this area, this fatigue category is not treated here. Further elaboration of elastic-plastic conversion from fictitious elastic stresses would be necessary. Since the situation in this category of solution is still not definite, inclusion of plasticity effects would increase the complexity of interacting effects and could confuse their interpretation.

5.1 TEST DATA AVAILABLE

The test data were gathered from several different sources. When the search was conducted, the target objects were specified to be fatigue limits occurring under an arbitrary combination of at least two load channels. It was clear soon that there is none among tested criteria that includes correctly both the mean stress and phase shift effects together. The demand was therefore broadened towards uniaxial fatigue limits with involved mean stress.

Most of the compiled data is corresponding to a combination of plane bending and torsion under the same frequency of loading and different phase shifts. The PragTic program allows further increase in complexity (different frequencies), but such data were unavailable.

5.1.1 DATA FROM CARPINTERI & SPAGNOLI

This collection of data can be found in [13] but all of them are references taken from original [47]. Three different groups can be separated according to material – hard steel, mild steel and grey cast iron (see Tab. 2, Tab. 3 and [13] in detail). All data correspond to a combination of fully reversed plane bending and fully reversed torsion with various phase shifts. Fatigue limits in fully reversed bending and fully reversed torsion and ultimate strength are given in each category, i.e. fatigue limits in repeated loading are missing. Since there are no mean loads, the fatigue limits in repeated loading are not necessary for any of the criteria used.

The data CS23-CS30 corresponding to grey cast iron were not included into the final test batch. Results of their solution can be seen separately in Appendix VI. The reason for their separation lies in very low ratio between fully reversed fatigue limits in bending and torsion, which are nearly the same ($\kappa \to 1$). Thus derivation of material parameters necessary for most of integral criteria leads to singularity (Kenmeugne et al. IA) or one of their material parameters becomes negative. The critical plane criteria achieve much better results.

Further, data concerning uniaxial results without any mean stress effect were removed from the test batch. These data could indicate differences between tabulated and measured fatigue limits at best, but they do not show any effect that is intended to be studied here.

Referred in - material	b_{-1} [MPa]	t_{-1} [MPa]	S_u [MPa]	b_{-1}/t_{-1} [MPa]
Nishihara, Kawamoto [47] - hard steel	313.9	196.2	704.1	1.60
Nishihara, Kawamoto [47]]- mild steel	235.4	137.3	518.8	1.71
Nishihara, Kawamoto [47] - grey cast iron	96.1	91.2	230	1.05

Tab. 2 Material parameters referred in Carpinteri & Spagnoli [13].

Material	Case	Remark	σ_a[MPa]	σ_m[MPa]	τ_a[MPa]	τ_m[MPa]	δ[deg]
Nishihara, Kawamoto - hard steel	*CS1*	*PB*	*327*	*0*	*0*	*0*	*0*
	CS2	PB+To	308	0	63.9	0	0
	CS3	PB+To	255.1	0	127.5	0	0
	CS4	PB+To	141.9	0	171.3	0	0
	CS5	*To*	*0*	*0*	*201.1*	*0*	*0*
	CS6	PB+To	255.1	0	127.5	0	30
	CS7	PB+To	142	0	171.2	0	30
	CS8	PB+To	255.1	0	127.5	0	60
	CS9	PB+To	147.2	0	177.6	0	60
	CS10	PB+To	308	0	63.9	0	90
	CS11	PB+To	264.9	0	132.4	0	90
	CS12	PB+To	152.5	0	184.2	0	90
Nishihara, Kawamoto - mild steel	*CS13*	*PB*	*245.3*	*0*	*0*	*0*	*0*
	CS14	PB+To	235.6	0	48.9	0	0
	CS15	PB+To	187.3	0	93.6	0	0
	CS16	PB+To	101.3	0	122.3	0	0
	CS17	*To*	*0*	*0*	*142.3*	*0*	*0*
	CS18	PB+To	194.2	0	97.1	0	60
	CS19	PB+To	108.9	0	131.5	0	60
	CS20	PB+To	235.6	0	48.9	0	90
	CS21	PB+To	208.1	0	104.1	0	90
	CS22	PB+To	112.6	0	136	0	90
Nishihara, Kawamoto - grey cast iron	*CS23*	*PB*	*93.2*	*0*	*0*	*0*	*0*
	CS24	*PB+To*	*95.2*	*0*	*19.7*	*0*	*0*
	CS25	*PB+To*	*83.4*	*0*	*41.6*	*0*	*0*
	CS26	*PB+To*	*56.3*	*0*	*68*	*0*	*0*
	CS27	*To*	*0*	*0*	*94.2*	*0*	*0*
	CS28	*PB+To*	*104.2*	*0*	*21.6*	*0*	*90*
	CS29	*PB+To*	*97.1*	*0*	*48.6*	*0*	*90*
	CS30	*PB+To*	*71.3*	*0*	*86.1*	*0*	*90*

Tab. 3 Test data referred in Carpinteri & Spagnoli [13]. The italicised load cases were not used in the survey – either they are simple uniaxial test without any mean load or they are related to the grey cast iron with $\kappa \to 1$.

5.1.2 DATA FROM PAPADOPOULOS

The batch of data first presented by Papadopoulos [52] attained great popularity, together with the histogram way of evaluation of prediction quality, which was introduced there. The data of four different materials (Tab. 4) and from various authors are gathered there (Tab. 5). The set covers all necessary effects, but is too small to evade statistical influences.

Referred in - material	b_{-1} [MPa]	t_{-1} [MPa]	S_u [MPa]	b_{-1}/t_{-1} [MPa]
Nishihara, Kawamoto [47] - hard steel	313.9	196.2	680	1.60
Lempp – reported in [88] – 42CrMo4	398	260	1025	1.53
Zenner et al. [88]– 34Cr4	410	256	795	1.60
Froustey, Lasserre [22] – 30NCD16	660	410	*1880*	1.68

Tab. 4 Material parameters referred in Papadopoulos [52]. The italicised data will not be used, because more appropriate seem to be data given directly by Froustey & Lasserre in [22], here in Tab. 6.

Again, the fatigue limits in repeated loading are not noticed in [52]. Although Nishihara and Kawamoto [47] are referred both in Secs. 5.1.1 and here, the extracted data are different. Thus, both these sets are used in the final batch. Be aware, that the tensile strength of 30NCD16 given by Papadopoulos significantly differs from values given elsewhere (even in the [22] reference) and supposedly should correspond to true fracture stress – see $S_f = 1880$ MPa given in [37]. The PF01 and PF02 tests are probably taken from other source than [22] where they are not mentioned at all ([24]?) .

Further, it has to be pointed out that the results of Crossland and Sines given in [52] are not appropriate. Papadopoulos et al. obviously misplaced the $\sin^2(\delta)$ by only $\sin(\delta)$ in the analytic formula for the $J_{2,a}$ computation according to (31). See Appendix I for correct results.

Material	Case	Remark	σ_a[MPa]	σ_m[MPa]	τ_a[MPa]	τ_m[MPa]	δ[deg]
Nishihara, Kawamoto, reported in McDiarmid [41] - hard steel	PNK01	PB+To	138.1	0	167.1	0	0
	PNK02	PB+To	140.4	0	169.9	0	30
	PNK03	PB+To	145.7	0	176.3	0	60
	PNK04	PB+To	150.2	0	181.7	0	90
	PNK05	PB+To	245.3	0	122.65	0	0
	PNK06	PB+To	249.7	0	124.85	0	30
	PNK07	PB+To	252.4	0	126.2	0	60
	PNK08	PB+To	258	0	129	0	90
	PNK09	PB+To	299.1	0	62.8	0	0
	PNK10	PB+To	304.5	0	63.9	0	90
Lempp, reported in Zenner et al. [88] - 42CrMo4	PL01	PB+To	328	0	157	0	0
	PL02	PB+To	286	0	137	0	90
	PL03	PB+To	233	0	224	0	0
	PL04	PB+To	213	0	205	0	90
	PL05	PB+To	266	0	128	128	0
	PL06	PB+To	283	0	136	136	90
	PL07	PB+To	333	0	160	160	180
	PL08	PB+To	280	280	134	0	0
	PL09	PB+To	271	271	130	0	90
Zenner et al. [88] - 34Cr4	PZ01	PB+To	314	0	157	0	0
	PZ02	PB+To	315	0	158	0	60
	PZ03	PB+To	316	0	158	0	90
	PZ04	PB+To	315	0	158	0	120
	PZ05	PB+To	224	0	224	0	90
	PZ06	PB+To	380	0	95	0	90
	PZ07	PB+To	316	0	158	158	0
	PZ08	PB+To	314	0	157	157	60
	PZ09	PB+To	315	0	158	158	90
	PZ10	PB+To	279	279	140	0	0
	PZ11	PB+To	284	284	142	0	90
	PZ12	PB+To	355	0	89	178	0
	PZ13	PB+To	212	212	212	0	90
	PZ14	PB+To	129	0	258	0	90
Froustey, Lasserre [22] - 30NCD16	PF01	PB+To	485	0	280	0	0
	PF02	PB+To	480	0	277	0	90
	PF03	PB+To	480	300	277	0	0
	PF04	PB+To	480	300	277	0	45
	PF05	PB+To	470	300	*270*	0	60
	PF06	PB+To	473	300	273	0	90
	PF07	PB+To	590	300	148	0	0
	PF08	PB+To	*565*	300	141	0	45
	PF09	PB+To	540	300	135	0	90
	PF10	PB+To	211	300	365	0	0

Tab. 5 Test data referred in Papadopoulos [52]. The data in the PF section in italic are different from the original set given by Froustey & Lasserre in the Sec. 5.1.3.

5.1.3 DATA BY FROUSTEY & LASSERRE

The experimental results were presented in [22], here they are re-interpreted in Tab. 7. They concern the harmonic bending and twisting of 30NCD16 steel with different phase angles. The tests are performed under mean axial load of value 300 MPa.

The tests correspond to tests PF03-PF10 cited in Papadopoulos ([52], here Tab. 5), but tensile strength differs; here the Froustey & Lasserre variant is taken as the right value (see the variations between Tab. 4 and Tab. 6). Papadopoulos sets aside the FL04 test for some unknown reason. Nevertheless, it should be there because it could oppose his expectation that there is no phase shift effect caused by combined harmonic bending and twisting. His statement (Fig. 10 in [52]) is based on evaluation of test batch results, which for small number of tests does not seem to be representative enough. On the other hand, if the data gathered here are evaluated, they can be interpreted in a way that the significance of phase shift increases with a decrease of σ_a/τ_a ratio. The other differences between Tab. 5 and Tab. 7 are of minor importance – the values of FL06 and FL10 tests will be used for PF08 and PF05 tests respectively.

Referred in - material	b_{-1} [MPa]	t_{-1} [MPa]	S_u [MPa]	b_{-1}/t_{-1} [MPa]
Froustey, Lasserre [22] – 30NCD16	660	410	1160	1.61

Tab. 6 Material parameters referred in Froustey & Lasserre [22].

Material	Case	Remark	σ_a [MPa]	σ_m [MPa]	τ_a [MPa]	τ_m [MPa]	δ [°]
Froustey, Lasserre – 30NCD16 [22]	FL01	PB+To	630	300	0	0	0
	FL02	PB+To	0	300	370	0	0
	FL03	*PB+To*	*211*	*300*	*365*	*0*	*0*
	FL04	PB+To	220	300	385	0	90
	FL05	*PB+To*	*590*	*300*	*148*	*0*	*0*
	FL06	*PB+To*	!563!	*300*	*141*	*0*	*45*
	FL07	*PB+To*	*540*	*300*	*135*	*0*	*90*
	FL08	*PB+To*	*480*	*300*	*277*	*0*	*0*
	FL09	*PB+To*	*480*	*300*	*277*	*0*	*45*
	FL10	*PB+To*	*470*	*300*	!271!	*0*	*60*
	FL11	*PB+To*	*473*	*300*	*273*	*0*	*90*

Tab. 7 Test data referred in Froustey & Lasserre [22]. The data in italic are already referred in the PF set in 5.1.2, thus the FL04 test and the specifications in tests FL06 and FL10 are the only used data from this set.

5.1.4 DATA BY PALIN-LUC

Here the data set found in [5] by Banvillet, Palin-Luc et al. and in [46] by Morel and Palin-Luc was used. Since Banvillet et al. tested hypothesis based on volumetric definitions, useful data in other load combinations are referred here too. The plane bending is replaced with rotating bending in two cases and with tension in three cases. None of the criteria presented here is volumetric or involves the effect of stress gradient in any way, thus the fatigue limits corresponding to these specific loads taken from [5] are used (see Tab. 8).

The majority of tests are loaded with a mean stress in one of load modes at least. The test denoted as MPA06X is the test No. 4 from [5] where it is apparently wrongly reproduced. The values given here in Tab. 9 are corrected thanks to personal correspondence with Mr. Palin-Luc. They can be found reproduced correctly e.g. in [15].

There were three tested materials:

- quenched and tempered 30NiCrMo16 steel (30NCD16 according to AFNOR, equivalent to BS 4S28-1964; tested by Froustey et al. [23]);
- annealed C20 mild steel (AFNOR standard XC18, equivalent to SAE 1017; tested by Galtier [26]);
- SG cast iron EN-GJS800-2 (AFNOR standard FGS800-2; tests done by Bennebach [1] and Palin-Luc [48]).

Material parameters of the test set of 30NCD16 steel show rather higher strengths in contrast to the material data given by Froustey & Lasserre (Sec. 5.1.3) or Papadopoulos (Sec. 5.1.2). Thus the sets of PF&FL and MPA test batches are separated and will be examined with their appropriate material parameters.

Further test data are proposed on quenched and tempered high strength 35CD4 steel (equivalent to SAE 4135) in [46], but only reversed fatigue limits can be found there. These data are therefore not used in the test batch here for the same reason as the similar uniaxial nMS tests given by Carpinteri & Spagnoli in 5.1.1. Note that the result values of Papadopoulos, Crossland and Dang Van criteria presented in [5] are incorrect for an unknown reason. See results in Appendix I for their right solution.

Referred in – material	b_{-1} [MPa]	f_{-1} [MPa]	br_{-1} [MPa]	t_{-1} [MPa]	S_u [MPa]	b_{-1}/t_{-1} [MPa]
Banvillet et al. – 30NCD16 – from [23]	690	560	658	428	1200	1.61
Banvillet et al. – XC18 – from [26]	332	273	310	186	520	1.785
Banvillet et al. – FGS800-2 – from [1] & [48]	294	245	280	220	795	1.34

Tab. 8 Material parameters referred in Banvillet et al. [5]. See again the differences of values in contrast to Tab. 4 and Tab. 6.

Material	Case	Remark	σ_a [MPa]	σ_m [MPa]	τ_a [MPa]	τ_m [MPa]	δ [°]
30NCD16 quenched and tempered - adopted from [23]	MPA01	RB+To	337	0	328	0	0
	MPA02	RB+To	482	0	234	0	0
	MPA03	Ten	235	745	0	0	0
	MPA04	Ten	251	704	0	0	0
	MPA05	Ten	527	222	0	0	0
	MPA06	PB	575	375	0	0	0
	MPA06X	PB	558	428	0	0	0
	MPA07	PB	627	273	0	0	0
	MPA08	PB	679	156	0	0	0
	MPA09	PB+To	519	0	291	0	0
	MPA10	PB+To	514	0	288	0	90
	MPA11	PB+To	451	294	250	191	0
	MPA12	PB+To	462	294	258	191	90
	MPA13	PB+To	474	294	265	0	45
	MPA14	PB+To	464	294	259	0	60
	MPA15	PB+To	554	287	135	0	45
	MPA16	PB+To	474	0	265	0	90
	MPA17	PB+To	220	199	368	0	90
	MPA18	PB+To	470	299	261	0	90
	MPA19	PB+To	527	287	129	0	90
	MPA20	PB+To	433	472	240	0	90
	MPA21	PB+To	418	622	234	0	90
	MPA22	PB+To	0	299	396	0	0
	MPA23	PB+To	0	486	411	0	0
	MPA24	PB+To	0	655	364	0	0
	MPA25	PB+To	482	0	268	0	0
	MPA26	PB+To	207	299	350	0	0
	MPA27	PB+To	474	294	265	0	0
	MPA28	PB+To	584	281	142	0	0
	MPA29	PB+To	447	473	252	0	0
	MPA30	PB+To	425	635	223	0	0
XC18 annealed – adopted from [26]	MPB01	PB+To	246	0	138	0	0
	MPB02	PB+To	246	0	138	0	45
	MPB03	PB+To	264	0	148	0	90
FGS 800-2 – adopted from [1] & [48]	MPC01	PB+To	228	0	132	0	0
	MPC02	PB+To	245	0	142	0	90
	MPC03	PB+To	199	0	147	0	0
	MPC04	PB	184	225	0	0	0

Tab. 9 Test data referred in Banvillet, Palin-Luc & Lasserre [5].

5.1.5 TEST DATA BY GOUGH

Although purely proportional, the data measured by Gough [29] and described later more completely in [30] are valuable for the mean stress effect incorporation. All data correspond to a combination of bending and twisting either with harmonic or constant course. The S65A steel material parameters are summed in Tab. 10, the test parameters in Tab. 11. The material parameters given in [29] are especially worth it, because fatigue limits in repeated torsion and plane bending are set too.

Referred in - material	b_{-1} [MPa]	b_0 [MPa]	t_{-1} [MPa]	t_0 [MPa]	S_u [MPa]	b_{-1}/t_{-1} [MPa]
Gough [29] – S65A	583.8	1065.7	370.7	687.3	1000.8	1.575

Tab. 10 Material data extracted from Gough [29]. The material was treated with the following procedures: normalized at 900°C, oil-hardened from 850°C, tempered to 640°C, air-cooled.

Material	Case	Remark	σ_a [MPa]	σ_m [MPa]	τ_a [MPa]	τ_m [MPa]	δ[°]
Gough - S65A normalized at 900°C, oil-hardened from 850°C, tempered to 640°C, air-cooled	G01	PB+To	552.90	266.41	0.00	0.00	0
	G02	PB+To	532.83	532.83	0.00	0.00	0
	G03	PB+To	0.00	0.00	339.00	169.89	0
	G04	PB+To	0.00	0.00	343.63	343.63	0
	G05	PB+To	549.82	0.00	0.00	169.89	0
	G06	PB+To	540.55	0.00	0.00	343.63	0
	G07	PB+To	555.99	266.41	0.00	169.89	0
	G08	PB+To	555.99	266.41	0.00	343.63	0
	G09	PB+To	469.51	532.83	0.00	169.89	0
	G10	PB+To	472.59	532.83	0.00	343.63	0
	G11	PB+To	0.00	266.41	311.97	0.00	0
	G12	PB+To	0.00	532.83	284.17	0.00	0
	G13	PB+To	0.00	266.41	304.25	169.89	0
	G14	PB+To	0.00	532.83	281.09	169.89	0
	G15	PB+To	0.00	266.41	308.89	343.63	0
	G16	PB+To	0.00	532.83	293.44	343.63	0
	G17	PB+To	547.50	0.00	155.99	0.00	0
	G18	PB+To	389.20	0.00	259.46	0.00	0
	G19	PB+To	168.34	0.00	335.91	0.00	0
	G20	PB+To	496.53	266.41	141.31	169.89	0
	G21	PB+To	374.52	266.41	249.42	169.89	0
	G22	PB+To	161.39	266.41	322.01	169.89	0
	G23	PB+To	428.58	532.83	121.24	343.63	0
	G24	PB+To	315.06	532.83	210.04	343.63	0
	G25	PB+To	126.64	532.83	251.74	343.63	0
	G26	PB+To	386.11	266.41	257.15	0.00	0
	G27	PB+To	383.79	0.00	255.60	169.89	0
	G28	PB+To	552.90	266.41	0.00	0.00	0
	G29	PB+To	532.83	532.83	0.00	0.00	0

Tab. 11 Test data set experimentally by Gough [29].

5.2 INCORPORATING MEAN COMPONENT OF LOAD

The previous section reports on test and material data, which formed the test batch for the comparative analysis. No fatigue limits in repeated loading can be found here, except for the Gough's S65A steel, which is the only one perfectly diagnosed. To overcome this problem, often the Goodman relation is used (see e.g. [89]). Nevertheless, the test data show behaviour strongly deviated from such relation, thus here another forms of derivation will be accepted.

The determination of repeated fatigue limits is done only there where it is really necessary. The sets of tests where no mean stress value figure are left out, because the mean stress component will not appear at all. The fatigue limits in repeated loading serve in the computation as dummy inputs only.

5.2.1 RELATIONSHIPS TO INCLUDE MSE

There are more empirical formulas besides the Goodman's one, which have the goal to transform loading with mean value to a fully reversed one. A list of them can be seen in Tab. 12 and also in a comparison for the S65A steel (Fig. 19), for which sufficient input data can be found in [29].

author	formula		recommended use
Goodman	$\frac{\sigma_a}{\sigma_{a,eq}}+\frac{\sigma_m}{S_u}=1,$ i.e. $b_0=\frac{2S_u b_{-1}}{S_u+b_{-1}}$	(97)	ductile materials
Gerber	$\frac{\sigma_a}{\sigma_{a,eq}}+\left(\frac{\sigma_m}{S_u}\right)^2=1,$ i.e. $b_0=\frac{S_u^2}{b_{-1}}\left[\sqrt{1+\left(\frac{2b_{-1}}{S_u}\right)^2}-1\right]$	(98)	ductile materials
Soderberg	$\frac{\sigma_a}{\sigma_{a,eq}}+\frac{\sigma_m}{S_y}=1,$ i.e. $b_0=\frac{2S_y b_{-1}}{S_y+b_{-1}}$	(99)	brittle materials
Morrow	$\frac{\sigma_a}{\sigma_{a,eq}}+\frac{\sigma_m}{S_f}=1,$ i.e. $b_0=\frac{2S_f b_{-1}}{S_f+b_{-1}}$	(100)	general ductile materials
Morrow	$\frac{\sigma_a}{\sigma_{a,eq}}+\frac{\sigma_m}{\sigma_f'}=1,$ i.e. $b_0=\frac{2\sigma_f' b_{-1}}{\sigma_f'+b_{-1}}$	(101)	steels (better than (100)), not suitable for the aluminium alloys
SWT	$\sigma_{a,eq}=\sqrt{\sigma_a(\sigma_a+\sigma_m)},$ i.e. $b_0=\sqrt{2}b_{-1}$	(102)	general use in ductile metals, acceptable for aluminium alloys, for steels worse than (101)
Walker	$\sigma_{a,eq}=\sqrt{\sigma_a^{\gamma}(\sigma_a+\sigma_m)^{1-\gamma}},$ i.e. $b_0=2^{\gamma}\cdot b_{-1}$	(103)	thanks to further material parameter γ superior to any other formula if only is the γ parameter available

Tab. 12 Methods for b_0 derivation from the MSE formulas. The recommendations given for the use of Morrow, SWT and Walker formulas are excerpts from Dowling [16].

The MSE diagram is formed by one of the formula line (Goodman, Gerber, Soderberg, Morrow or SWT) together with a yield line, which borders the region so that the yield limit would not be overcome. A quadrant axis is depicted too, because the amplitude and mean stress of any fatigue limit in repeated loading are the same. The S65A steel has specific behaviour (as already Gough in [29] mentions), because its repeated fatigue limit in bending is even higher than the yield limit.

As regards validity of the criteria, the Goodman formula is often accepted, because its use is at least conservative. Another commonly used assumption is that the correct value lies somewhere between curves defined by Goodman and Gerber formulas. Dowling states in [16] that the Goodman formula is largely conservative and should be replaced e.g. for steels by Morrow or SWT formula.

The Dowling's report compares the criteria by Goodman, Morrow, SWT and Walker, i.e. the Gerber's one is not included in his report. Dowling recommends the Walker's solution as the best choice for all types of materials. Unfortunately, tunning of the γ parameter cannot be used here because it needs more data. Thus the Morrow formula or SWT formula will be used where possible or needed.

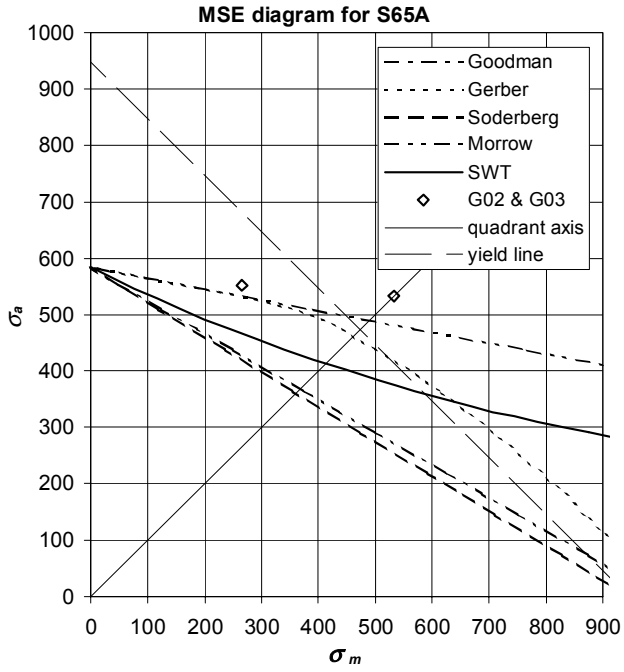

Fig. 19 Possible interpretations of the mean stress effect on S65A steel together with two measured tests by Gough.

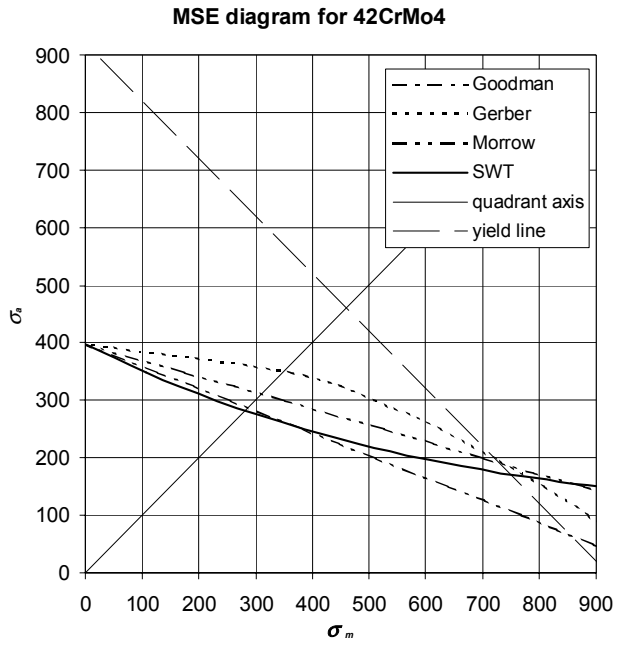

Fig. 20 The MSE diagram of 42CrMo4 steel draw from data taken from Papadopoulos [52] and Boller [3].

The case of 42CrMo4 steel was solved with a use of data given by Boller in [3] (S_f = 1525 MPa, S_y = 998 MPa, S_u = 1111 MPa). Because there is a significant difference between ultimate strengths

given by Papadopoulos in [52] and Boller cited here, a linear shift was used leading to final values (S_f = 1407 MPa, S_y = 920.7 MPa). Use of the Morrow formula leads to b_0 = 620.5 MPa (see Fig. 20).

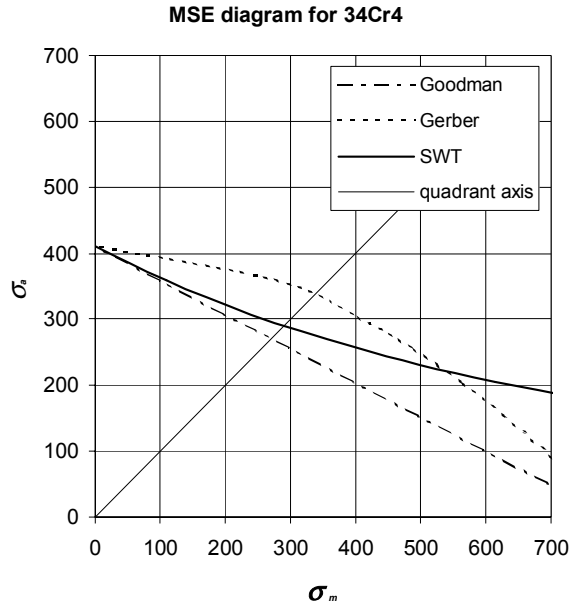

Fig. 21 The MSE diagram of 34Cr4 steel draw from data taken from Papadopoulos [52].

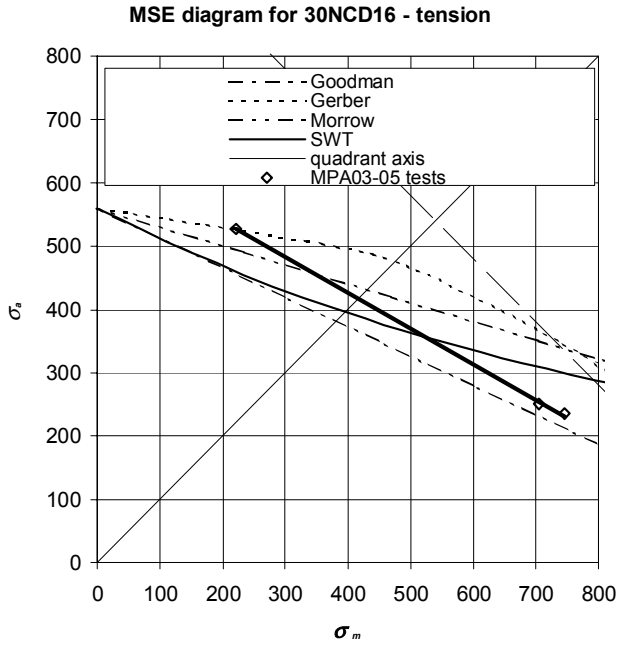

Fig. 22 The MSE diagram of 30NCD16 steel loaded in tension. Parameters of tests MPA03 – MPA05 are added.

The material data given by Papadopoulos are very brief. Unfortunately, any other relevant source of material properties of 34Cr4 steel was not found. Thus only the three formulas in Fig. 21 could be derived. An approximate value b_0 = 600 MPa is used in further computations.

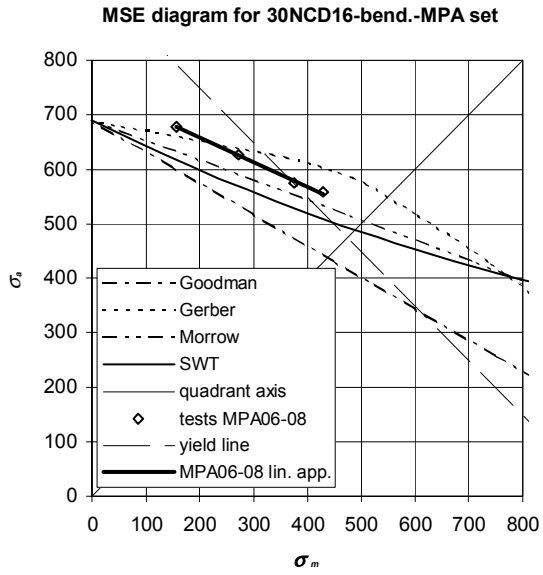

Fig. 23 The MSE diagram for 30NCD16 steel of the MPA test series under bending load. The test data MPA06, MPA06X, MPA07 and MPA08 are added. Material data used for drawing of the diagram are taken from Morel & Palin-Luc (see 5.1.4).

Determination of fatigue limits in repeated loading for 30NCD16 steel is mostly based on test data given by Banvillet et al. in [5]. The test data MPA03 – MPA05 and MPA06-MPA08 are linearly approximated. True fracture stress S_f = 1880 MPa commented already in Sec. 5.1.2 is used to draw the Morrow formula, yield stress S_y = 950 MPa and tensile strength S_u = 1200 MPa are taken from [5]. Resulting values of one interpolation (tension, Fig. 22) and one extrapolation (bending, Fig. 23) are b_0 = 833.6 MPa and b_0 = 1030.7 MPa respectively.

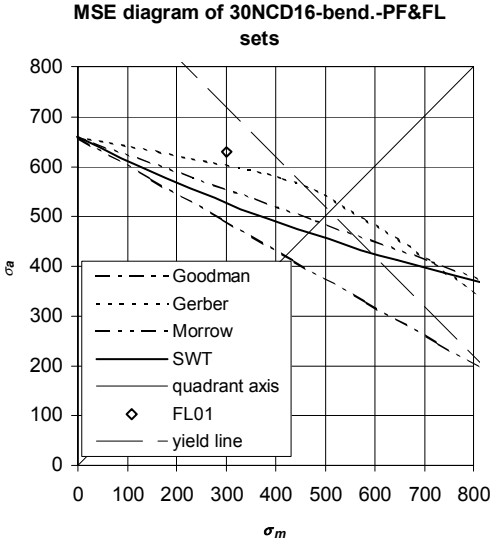

Fig. 24 The MSE diagram for 30NCD16 steel under plane bending of the PF & FL test sets. The only usable set is the FL01 one lying above the formula lines.

The results and material properties of tests of Froustey and Lasserre (FL batch) and of their tests summarised by Papadopoulos (PF batch) are used for new validation of b_0. The only test point FL01 lies even above the line of linear approximation in Fig. 23, whereas all the formula curves except for the yield line lie lower (see Fig. 24). Fatigue limit b_0 = 985.9 MPa is finally set. It is derived from

linear decrease of the b_0 value given for the MPA test. The shift is done in linear dependency with tensile strengths of both batches. The final value lies bellow yield stress S_y = 1020 MPa given by Froustey & Lasserre in [22].

The solution of the MSE problem for FGS800-2 is not straightforward. All proposals previously used (even the Goodman formula) are too non-conservative to the only test with MSE in the batch (MPC04). The result is thus obtained through interpolation between MPC04 and fatigue limit in fully reversed bending. The result is b_0 = 394.9 MPa. The other curves in Fig. 25 are defined by material data referred in Tab. 8 and S_y = 462 MPa and S_f = 815 MPa given in [46].

A sum of possible fatigue limits in repeated bending or tension is depicted in Tab. 13. It is obvious that the results of Morrow formula were either directly used or were at least the closest ones to the final value. Where the Morrow formula could not be used (an absence of S_f value), the SWT took its role. The only exception is the SG cast iron FGS800-2, which is obviously too brittle for formulas proposed (formula by Soderberg reaches b_0 = 359.3 MPa).

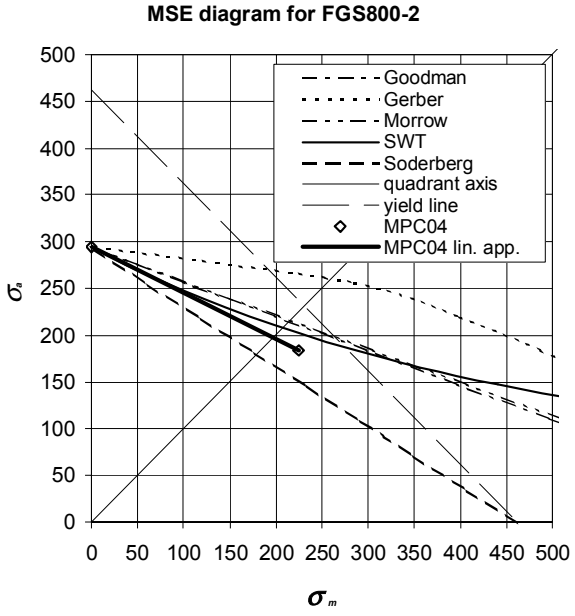

Fig. 25 MSE diagram of FGS800-2 cast iron. The linear approximation between the load case MPC04 and the fully reversed fatigue limit in bending is used.

Values of b_0 or f_0 in MPa according to formulas						
	Goodman	Gerber	Morrow	SWT	**final value**	commentary
42CrMo4	573.4	702.5	620.5	562.9	**620.5**	Morrow formula
34Cr4	541.0	673.1	-	579.8	**600.0**	estimated mean value
30NCD16 – tension	763.6	946.0	863.0	792.0	**833.6**	derived from tests
30NCD16 – bend. – MPA	876.2	1093.5	1009.5	975.8	**1030.7**	derived from tests
30NCD16 – bend. – PF&FL	841.3	1049.7	977.0	933.4	**985.9**	lin. decrease from MPA set
FGS800-2	429.3	524.1	432.1	415.8	**394.9**	derived from tests
S65A	737.4	920.6	979.1	825.6	**1065.7**	set experimentally

Tab. 13 Summarized proposals for fatigue limits in repeated axial loading. The values closest to the selected final value have greyed background.

5.2.2 FATIGUE LIMIT IN REPEATED TORSION

If the search for fatigue limits in repeated bending and tension was speculative, here it is even more. Fortunately, the repeated fatigue limit in torsion is necessary only for the Zenner & Liu criterion. The complication in obtaining fatigue limits in repeated loading is something what Papadopoulos in [52]

emphasizes with a clearly negative meaning, when concerning properties of different criteria. Zenner in [89] protests against the Papadopoulos' criticism. He proposes the use of common approximate formulas based on tensile strength for calculation of fatigue limit in repeated axial loading and of the following equation for the fatigue limit in repeated torsion:

$$t_0 = \frac{4t_{-1}}{2\frac{b_{-1}}{b_0}+1}. \qquad (104)$$

The fatigue limit in repeated torsion is not used in any other criterion than the Zenner & Liu, thus their recommendation (104) can be taken without any further reconsidering.

6 ANALYSIS OF HCF RESULTS

The methods ofr HCF analysis presented in Sec. 3.1 are tested on fatigue data compiled in Chap. 5. The results of individual methods are commented in the following sections. The two major observable effects – the mean stress effect and phase shift effect – are analyzed.

6.1 RESULTS OF PRESENT METHODS

All the results of individual tests in the form of ΔFI fatigue index errors are gathered in Appendix I. The groups of materials (subdivided by the load type in the case of 30NCD16 as well) are evaluated statistically in the tables of Appendix I and their statistical evaluations are transferred to the summaries in the first part of Appendix II. This subdivision is made so that the ranges of results of appropriate methods could be analyzed separately, because here the effect of insufficiently set material properties could be caught. The summary of each statistical parameter is accompanied with its further statistical evaluation over all materials. Although such an extra evaluation could look weirdly, it again proposes an interpretation, how the statistical results are distributed.

The summary given in the second part of Appendix II offers another type of subdivision. The separate analyses of data affected by mean loads, non-proportionality or their mixtures are done there. The majority of the groups formed are large enough (at least 20 values), but two groups are still lacking more data. These are the group with mean load in torsion and the group of non-proportional loading without mean load and phase shift different from 90 degrees. Both of them have over 10 values, which is more than some other interpreters evaluate (see the phase shift effect in [52]), but still not enough in contrast to the other groups formed here.

6.1.1 SINES METHOD

The analytic solution given in [52] was utilized for computation of the Sines formula (37). A warning is necessary, because Papadopoulos in his results gives inappropriate values due to misinterpretation of computational formula given here in (31). He mistaken the squared phase shift cosine with only a linear term. Correct results can be thus found in Appendix I. The reader can found the histogram of the Sines method in Fig. 26.

The presented results are computed with the originally derived b_S parameter from (39) utilizing fatigue limit in repeated bending. A test was performed too, which used the b_S parameter (42) derived by Papadopoulos from Goodman formula. As could be expected, the results are worse than those obtained with the (39) formula – the overall range of ΔFI increases to 73% and the overall standard deviation goes up to 15.6%. Detailed data of this test are not reported here more extensively, because the Sines formula leads to inferior prediction anyway.

The Sines solution does not offer any property, which would top the other criteria. It has very large scatter of results due to the too strong phase shift effect, which is further increased by the improper mean stress effect. Interesting results reached for the Gough's test batch are not confirmed for other proportional data.

6.1.2 CROSSLAND METHOD

The Crossland method is closely related to the Sines' one, because it differs only in the imposition of the mean hydrostatic stress effect (see 3.1.2). It is thus interesting to watch the differences in the

quality of prediction – see Fig. 26. The Crossland solution forms notably nicer histogram in contrast to the Sines one.

The median of the histogram is shifted to the right side. When the summaries in Appendix II are closely viewed, one can see that this inclination is likely caused by an interaction of two distinct categories – proportional loading with mean value of –3.8% and non-proportional one with mean value of –12.5%. Because the scatter of the non-proportional loading is significantly higher than that of the proportional one, the histogram is skewed to the right side, with left slope not so inclined.

The summary is that the improper phase shift effect incorporation does not allow the Crossland criterion to behave correctly under out-of-phase loading. If only the proportional loading is analyzed, the results are relatively good and increase of scatter with mean load is not so excessive as in other criteria. Reduction of applied harmonic loading to an in-phase group leads to the same analytic formula as it is in Papadopoulos solution (compare (38) and (62)).

Results of the Crossland criterion given in Papadopoulos [52] are inadequately computed as was mentioned in the previous section. Results given in [5] are not correctly computed as well, but here the reason is unknown.

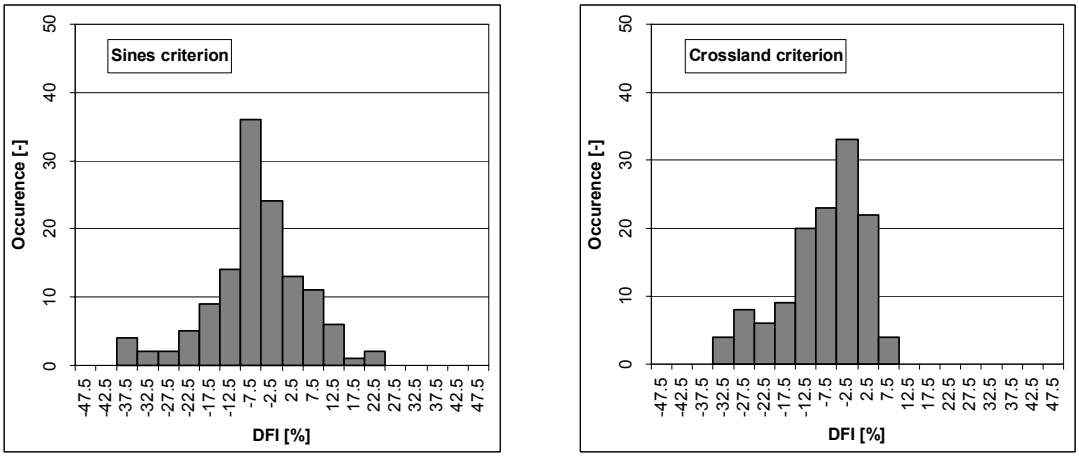

Fig. 26 Histograms of results of the Sines and Crossland criteria.

6.1.3 MCDIARMID METHOD

The McDiarmid method (see Sec. 3.1.3) was tested both in the MD and MSSR variants. The results of the maximum damage variant are slightly better. Their average value is about 1.5% closer to the zero and their scatter is lesser, but the difference is not so significant. This is the reason why the MD variant of the McDiarmid method is the only one completely enumerated in Appendix I and Appendix II. The depiction of MSSR results is limited only to the comparison made in Fig. 27.

The methods were tested with the assumption of Bannantine & Socie on predefined directions of the critical plane. Possible critical locations were scanned with a step of 8 deg and afterwards a maximization was run towards the highest MD or MSSR.

The method offers results which do not excel in any category. The results of uniaxial loading with the mean value higher than the amplitude show the worst behaviour in more detailed examination. Well, the cases MPA03 and MPA04 could be interpreted as a result of a bad input of material data. It is a pure tensile loading where the crack A type initiation (see Sec. 3.1.3) is not documented as it is under plane bending and torsion. Nevertheless, the result of the MPC04 plane bending test, which has very close value, testifies that the problem is really in badly defined MSE.

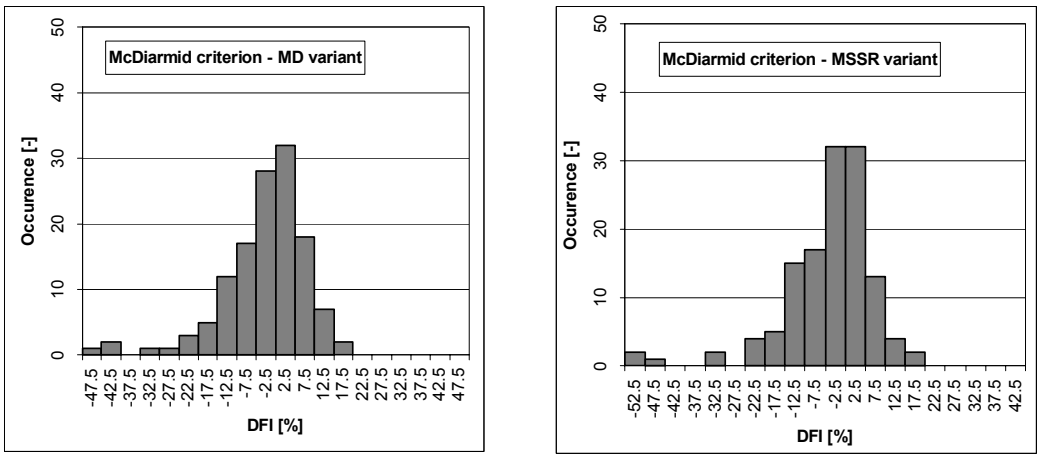

Fig. 27 Histograms of results of the McDiarmid method – in MD and MSSR variants.

6.1.4 FINDLEY AND MATAKE METHODS

Both these methods have the same damage parameter – see (46) and (48). The only difference here is the type of search for the critical plane. Findley proposes the MD method, whereas Matake prefers the MSSR one.

Both methods were run with a general search for the critical plane (for explanation see Secs. 4.3.9 and 4.3.10). The basic step for scanning was chosen to be 8 deg in Findley method, afterwards the maximization was run. The Matake took the same basic angular step, but the method is more complicated for numerical solution. The MSSR maximization leads to more possible critical planes, from which the final one has to be chosen by the highest LHS of (48). For closer information about the algorithm of the search process see Sec. 4.3.10 above.

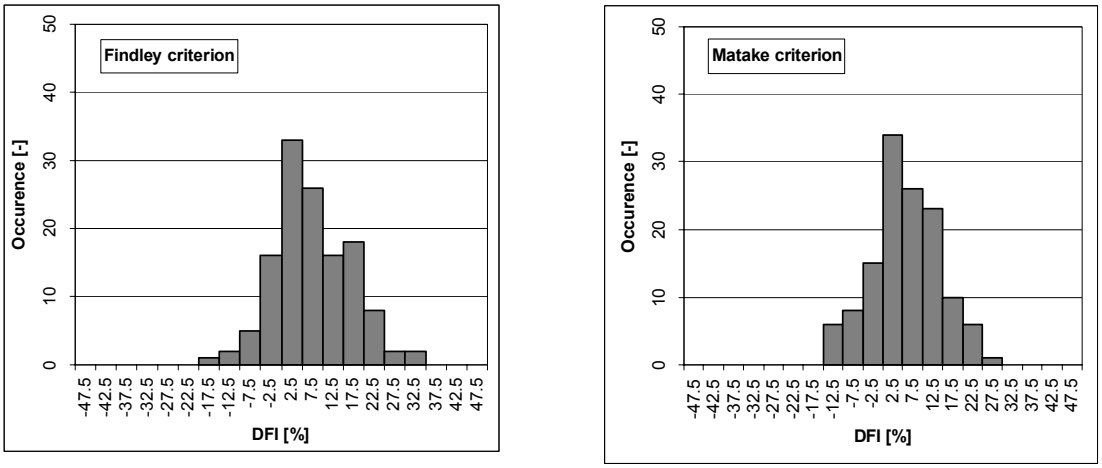

Fig. 28 Histograms of results of the Findley and Matake criteria. The formulas are the same, but Findley uses the MD variant, whereas Matake the MSSR.

The procedure is mentioned here again in order to explain the arising problem, because e.g. Carpinteri & Spagnoli in [13] recognize it in a different way. Let's study the CS30 test case as an example. Its results are given in Appendix VI. It is chosen because the problem is clearly visible and the result given here is largely different in contrast to the result given by [13]. The MSSR plane is found on two positions – first it is the plane perpendicular to the specimen axis, the second time it is the plane perpendicular both to it and to the surface of the specimen too. The planes have the same C_a = 86.1 MPa amplitude, but the $N_{\max}$ is largely different – it is $N_{\max}$ = 71.3 MPa in the first case, but zero in the

second case. Spagnoli & Carpinteri chose the second case, which led to ΔFI = -5.6%. They most likely missed the other MSSR plane with the much higher loading giving ΔFI = 64.6%. The results of Matake criterion in [13] are thus often deviated from correct values (Appendix I) just due to this error.

Although the range and standard deviation of the Matake criterion are lesser than those of the Findley criterion in the whole test batch, the subsequent groups seem to be covered better with the latter. Its worse appearance in histogram and statistics is caused above all by fluctuation of average values, which reaches twice of the range given by Matake for all groups. The differences between average values of P and NP or MS and nMS groups by Findley are large.

The complete set of the test batch is better covered with the Matake criterion, which is with the Dang Van method the best of the critical plane criteria evaluated here.

6.1.5 DANG VAN METHOD

The Dang Van method leads to results with very similar characteristics as that by Matake. It was run with the general search of the critical plane using a base angular step 8 deg followed by further maximization in this test.

What seems to be significant for such a good behaviour is that the criterion gives results with the smallest scatter of the average value for all materials. The criterion shows only small difference of results statistics in comparison of {MS} and {nMS} group, but the contrast of all characteristics of {P} and {NP} groups is very strong. The difference between these two groups forms the criteria histogram with steep right and gentle left slopes similarly as in the Crossland criterion.

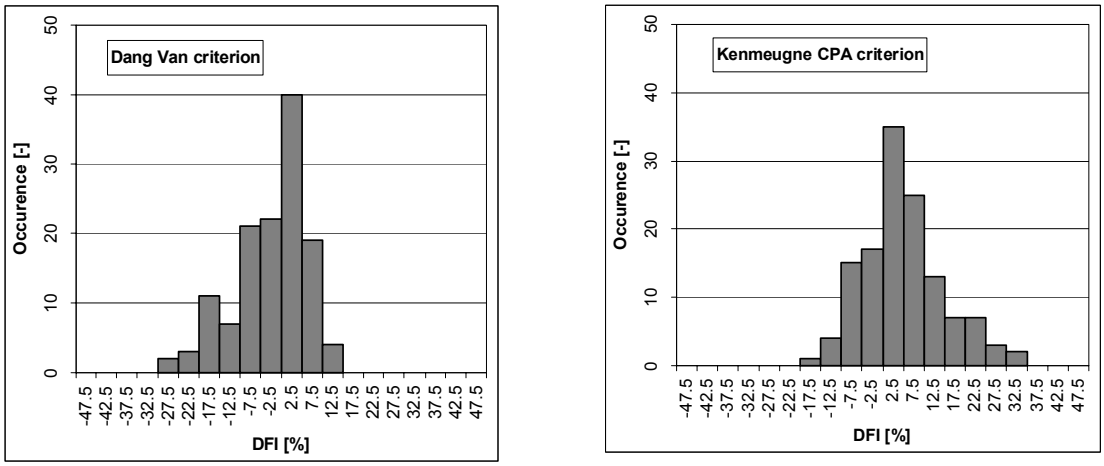

Fig. 29 Histograms of Dang Van and Kenmeugne critical plane criteria.

The overall average value is slightly shifted to the non-conservative side, but close to zero. The gentle slope of the histogram's left side (higher scatter of non-proportional data), which goes down to the ΔFI error of –28.9%, is unpleasant. Such a non-conservative prediction is not suitable. If the choice between the Matake and Dang Van methods was made, the conservativeness of the Matake criterion should be preferred.

Be aware that results of the Dang Van method presented in [5] are not correct. Some negative expectations, which were based purely on these bad results, were reported in 3.1.7. The right results disprove them and the criterion can be ranked highly among other methods.

6.1.6 KENMEUGNE ET AL. CPA METHOD

Kenmeugne et al. separate effects of mean and amplitude values of normal stress and add a third material constant. All of this is done in order to improve the mean stress effect in contrast to the other (two-parameter) criteria. The criterion is MD based and was run under similar conditions as all the

previous ones, i.e. with global search for the critical plane at 8 deg base angular step followed with the further maximization.

The proper rival to this criterion is the Findley method. They both tend to the same solution under nMS loading. Both of them have the overall range very close, the average value is closer to zero in the KCP approach, whereas the overall scatter is lesser by Findley method.

The conclusion is that the separation of normal stress components in the KCP model is not justified. All MS groups of test data have better statistics for the Findley method.

6.1.7 SPAGNOLI METHOD

The Spagnoli criterion was broadly tested as regards the parameters of computation. The focus was set onto the comparison of CSM and MD approaches. Since this is the only criterion with the CSM method applied, its features were tested more extensively, than any other criterion was. Results of individual variants can be seen separately in Appendix III. The results gathered in this appendix are limited to the material groups, in which values of the *w* exponent for description of S-N curves are available (Tab. 14).

material	test group	*w* [-]
hard steel	CS01-12	8.7
mild steel	CS14-22	18.2
grey cast iron	CS24-30	19.4
34Cr4	PZ	20.9
30NCD16	PF, FL, MPA	13.2

Tab. 14 Values of the *w* exponent for description of S-N curves. All of the values cited here are taken from [82].

First of all, the overall insufficiency of the criterion as regards its MSE was found. A look at the histogram in Fig. 30 where the MD approach is summed is sufficient to prove it. Large scatter with a range approximating the McDiarmid criterion was found even in the CSM variant. Spagnoli does not show any detailed results, only histograms are depicted. He does not mention any unsuitable behaviour, although he uses the same data as Zenner ([88], here the PZ test batch) and as Froustey & Lasserre [22], the FL test batch) where the mean loads are too. In fact, he obtained acceptable results, because the MSE in both these test groups is not as pronounced as e.g. in the MPA group. A simple test with fatigue limit in repeated tension is enough to check that the criterion in the current form cannot pass. Under such condition it is sure that the second ratio in (57) occurring on the plane perpendicular to the axial loading is $f_0 / f_{-1} >> 1$. It is sure that the squared shear stress term does not decrease it.

The weight parameter of the CSM variant was largely examined. As shown in Tab. 14, not all materials have the exponent *w* defined. A question can be raised moreover, if its use is rightul (see 2.1.3). The test result in the CSM variant and weight parameter as described in (3) are thus given in Appendix III as the SpaC1 method. Another two variants, in which the *w* material parameter is not used, were proposed – SpaC2:

$$\begin{aligned} M_2 &= 0 \quad \text{if} \quad \sigma_{1,k} < c \cdot f_{-1} \\ M_2 &= 1 \quad \text{if} \quad \sigma_{1,k} \geq c \cdot f_{-1} \end{aligned} \tag{105}$$

and SpaC3

$$\begin{aligned} M_3 &= 0 \quad \text{if} \quad \sigma_{1,k} < c \cdot f_{-1} \\ M_3 &= \sigma_1 \quad \text{if} \quad \sigma_{1,k} \geq c \cdot f_{-1} \end{aligned} . \tag{106}$$

The constant c was held to be 0.5 for all M parameters. When the results of all three methods are observed, there is no pronounced winner. The SpaC2 and SpaC3 methods lead to similar results with better ranges than the SpaC1 offers, nevertheless their standard deviation is higher in contrast to the SpaC1. Nevertheless, no clear reason for introduction of the w parameter into the calculation is visible.

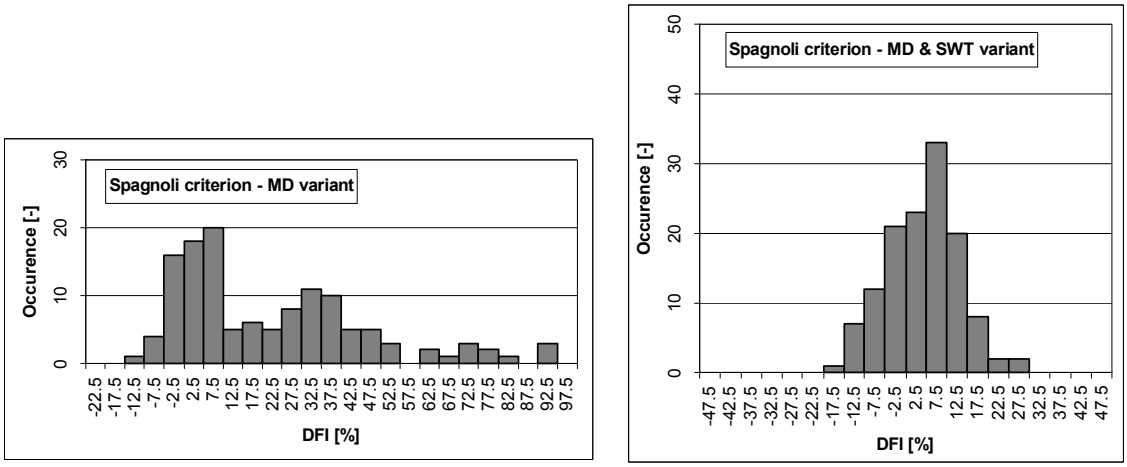

Fig. 30 Histograms of the Spagnoli criterion in the MD variant. The left histogram concerns the original form of the criterion given in (55), the right corresponds to the solution SpaM utilizing the MD and MSE by SWT (107).

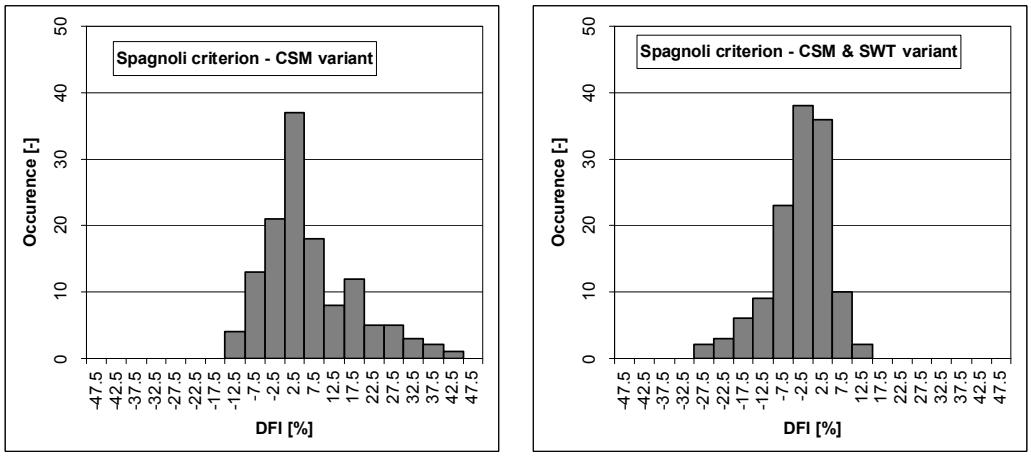

Fig. 31 Histograms of the Spagnoli's CSM variant. The reduction of the mean stress effect is obviously too strong.

Elaboration of a new fatigue criterion is given in Chap. 7. Any intervention into existing criteria presented here is thus slightly inconsistent. Anyhow, the source of problems in formula (55) can be removed easily with a more acceptable mean stress term according to SWT:

$$\sqrt{a_S \cdot C_a^2 + b_S \cdot N_a \cdot N_{\max}} \le f_{-1}. \tag{107}$$

The new definition observes the coefficients defined in (56). The histogram in Fig. 30 shows significant improvement for the MD variant. This form of the method is described in appendices as a SpaM solution. Nevertheless, even here its results are only slightly better than the Findley solution.

When the same damage parameter is applied to the CSM solution, the scatter of results largely improves as well, though it is obvious that the decrease of the MSE is too strong. The CSM solution is once again tested with the M_2 (SpaC2S) and M_3 (SpaC3S) weights, which both reach very similar results. The solution utilizing the M_2 weights is shown again in the overview in Appendix I and

Appendix II as the SpaC method. The CSM method was run with the angular step of 2 deg and then the optimization followed.

It can be concluded that the variant in the CSM & MSE combination reaches the best results from this Spagnoli group. Note the differences in the overview in Appendix II and Appendix III. The Gough's data, which are not present in Appendix III, greatly worsen results of the MD prediction.

6.1.8 PAPADOPOULOS METHOD

Only the integral method (see Sec. 3.1.10) is implemented in PragTic and tested here. The integration of resolved shear stress is done with the use of global search of planes with defined 2 deg angular step between evaluated planes (see Sec. 4.3.9).

The results are relatively close to the Dang Van criterion – the range and average value are similar. More promising is the standard deviation, which shows significantly lesser scatter of results of the Papadopoulos criterion. The Papadopoulos criterion has not the unsuitable behaviour of the Dang Van method, which lead to highly scattered results under non-proportional loading. Its histogram is thus more smooth and its form confirms that the differences in mean values are not so high.

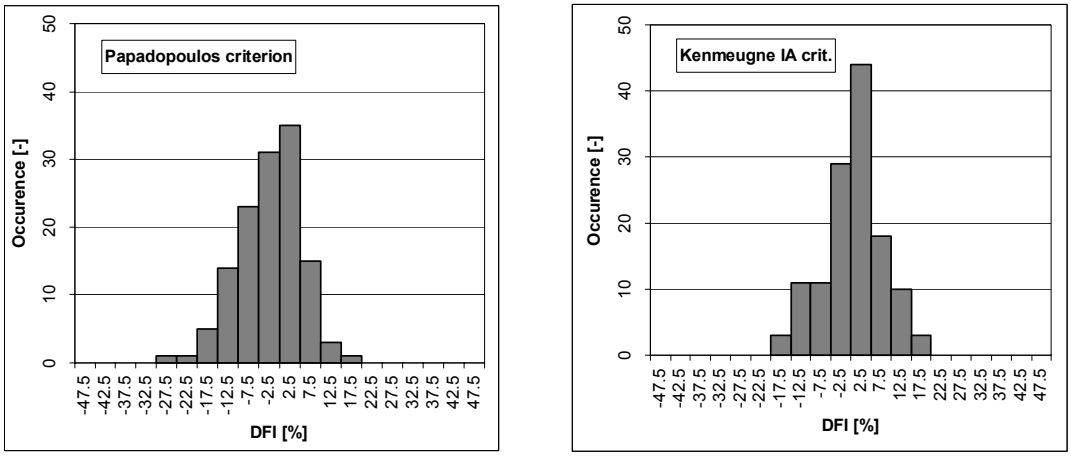

Fig. 32 Histograms of two integral criteria – that of Papadopoulos on the left side, whereas the Kenmeugne et al. criterion in the integral version is given on the right side.

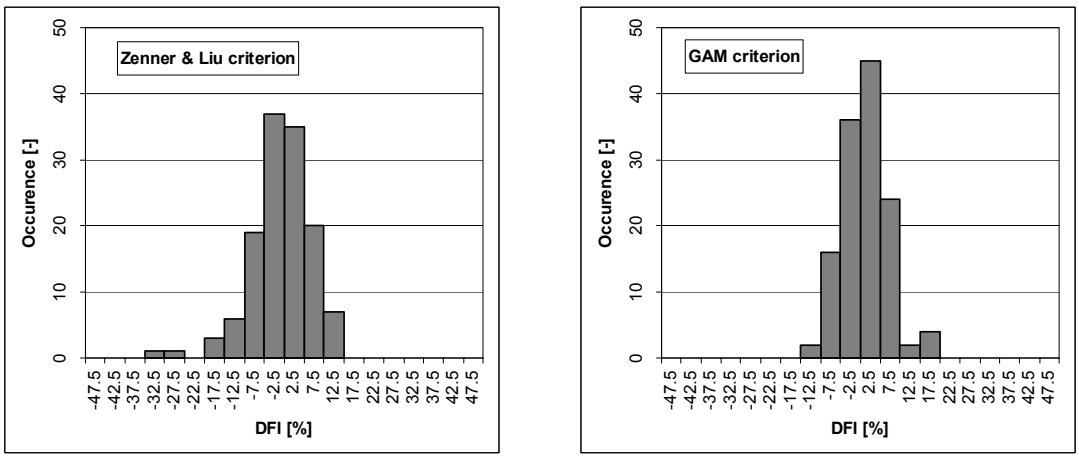

Fig. 33 Histograms of Zenner & Liu criterion (left) and GAM criterion (right).

6.1.9 KENMEUGNE ET AL. IA METHOD

If the results of the KCP criterion led to a conclusion that adding the third material parameter in order to cover the mean stress effect better apparently missed the mark, here the same change has a beneficial effect. The integration of the damage parameter took its place as described in 4.3.9 with the base angular step 2 deg.

The histogram is relatively nice shaped and can be denoted as symmetric. The mean value lies nearly exactly at zero, scatter and range are the best ones from criteria commented up to now. Challenge is that the mean stress effect could still be covered better. The mean load effect under axial loads is too high, resulting in too conservative average value in contrast to other examined groups.

6.1.10 ZENNER & LIU METHOD

This method is the only one utilizing four material parameters. The criterion is built in such a way that the load input appears there even in power of four. As follows, small input deviations (in load) lead to a higher output deviation (damage). This need not to be bad, but it surely affects the demand on accurately set material parameters. As was already stated in Chap. 5, the fatigue limits in repeated loading are fully derived from other material parameters. The histogram depicted in Fig. 33 shows two tests (MPA03 and MPA04) to be far away on the non-conservative side. One should mention the range of the MPA03-05 tensile test batch, which is very large. Since a change of the fatigue limits in repeated loading to lesser values (increasing thus the conservativeness of the method) would lead to a shift of the range to the right side of the histogram, the range would stay at best on the level of the Papadopoulos criterion. Thus again, the inclusion of two more material constants does not lead to any significant improvement of the prediction.

The data given by Gough are the only test batch where all four material parameters are experimentally set. To cover this topic more correctly the comparison of relative occurrence of this method for different test batches is given in Fig. 34 and Fig. 35. The results shown for the Gough data look great but it should be reminded that these test data are completely of in-phase nature. Such limitation needn't be negative nevertheless, because the non-proportional solution looks to be covered even better with the Z&L method.

Another comparison can be made from data on the Papadopoulos [52] test batch of tests (PNK, PL, PZ and PF tests). Zenner, Simbürger and Liu present very good results for such batch in [89], unfortunately without appropriate material data, which were used there. Since there are four different materials included, which offers very large variety of results, such a practice should be criticized.

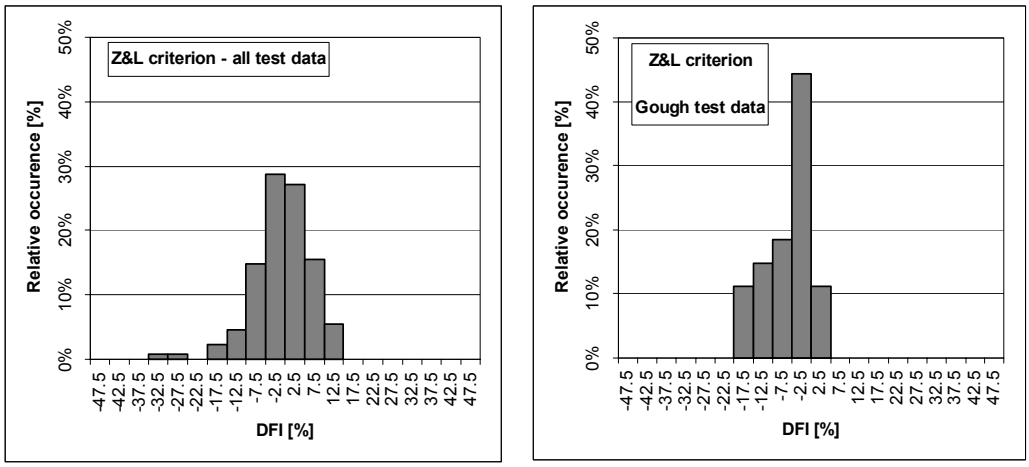

Fig. 34 Histograms of relative occurrences of the Z&L criterion. Gough test data are the only ones supplied with all material parameters necessary for perfect computation.

The criterion was tested here with the standard 2 deg angular rotation. Results are not very decisive, because the insecurity over input material data is too large. A tendency can be seen that the prediction could be at most of similar predictive capability as the Papadopoulos criterion where only two material parameters are necessary. Thus the usability of the criterion has to be further checked with more complete material data.

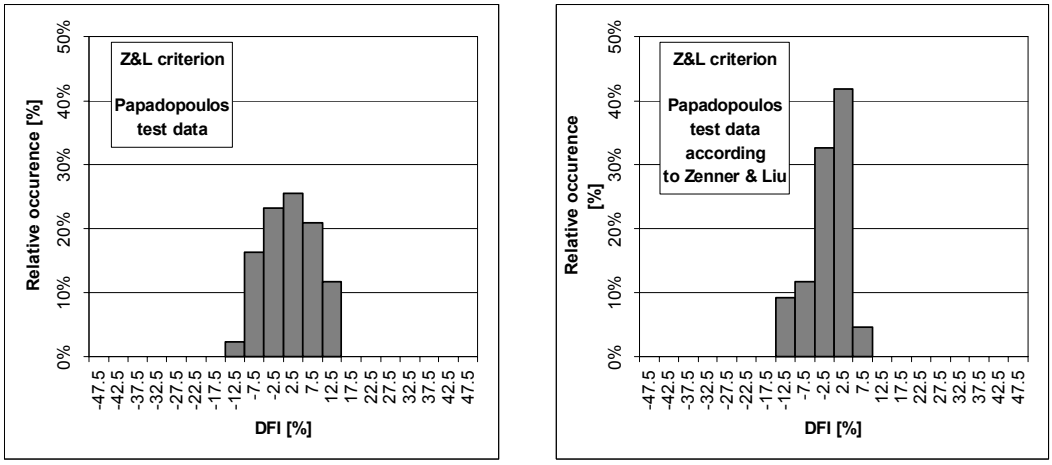

Fig. 35 Histograms of relative occurrences for the 43 tests given by Papadopoulos in [52]. The left histogram is the one computed with material data defined here previously, whereas the right histogram is taken over from [89].

6.1.11 GAM METHOD

Clearly, this is the best criterion available. The results are really convincing. What has to be challenged, is its complexity if the loading does not comply with the requirements defined in Sec. 3.1.13. The method was incorporated into this PhD thesis very lately and thus no work on its further elaboration (both MSE and PSE show some room for improvements) was done. In fact, the results seem to be in so far satisfactory that not being the proposals given here further one could say it is perfect.

One notice has to be added. Authors of the criterion made a mistake in their own computation presented in [27]. They obviously have not expected a change of maximum principal stress with the applied phase shift. Thus, the results given in [27] are more conservative and scattered than the correct solution would give.

6.2 EFFECTS

Due to very poor predictive capabilities, the McDiarmid and Sines methods will not be commented in the further text. Also, the other methods based on evaluation of load effects in the Ilyushin 5-dimensional space (Crossland and GAM methods) will not be evaluated in some special way. The interesting results of the GAM method were not expected at the start of my work. The basic research was thus focused mainly on further elaboration of CPA and IA methods.

6.2.1 PHASE SHIFT EFFECT

Surely, the ranges of methods are not so different for the CPA and IA methods. More decisive is the significantly lesser scatter found in IA methods, together with much better behaviour under non-proportional loading. The assumption stated by Kenmeugne et al. in [34] that the IA methods are above all suitable for random loading with a high degree of rotation of principal directions is too limiting. Simply, when the loading is out-of-phase, the HCF region seems to be covered better if an integral method is used.

The differences of methods concerning the phase shift effect incorporation can be seen from the separated {P, nMS} and {NP, nMS} groups. As regards the range of average values, the smallest value is obtained in KIA and Z&L methods. GAM and Matake methods are good as well. On the other hand the Crossland and Dang Van methods show differences that look very odd – as if the damage parameter was built in a way which does not allow any correlation of data.

The Crossland and Dang Van method show high increase of range with applied non-proportionality too. The same shows the Matake method, but the smaller difference in average value helps here. Acceptable values of range increase are obtained by Papadopoulos and Z&L methods, whereas the Kenmeugne KIA method shows nearly the same but high range for both groups.

Very similar behaviour can be found for the standard deviation parameter as well. The conclusion regarding the phase shift effect is:

1) The composition of Crossland, Dang Van and Matake criterion is unsuitable for non-proportional loading.
2) The Kenmeugne KIA criterion shows nearly the same scatter for in-phase and out-of-phase loading, but its degree seems too big. The quadrate of a linear combination of shear and normal stresses does not seem to allow any further improvement.
3) Both Papadopoulos and Zenner & Liu methods (i.e. linear and quadratic combination of load parameter respectively) show the best behaviour, although the increase of scatter with non-proportionality stays extensive.
4) The GAM method appears to be slightly worse than these both best methods.

Based on the evaluation given by Papadopoulos in [52], an examination was also focused on tests with different value of phase-shift. There is unfortunately a too small group of the results {nMS, NP different from 90 deg}. The group has only some 13 tests, which is a higher number than the Papadopoulos examines, but much smaller in comparison to other groups {nMS, P}, {nMS, NP 90 deg}. Thus the strange effect showing much higher scatter of data in both these groups in contrast to the group of NP data with phase shift different from 90 deg cannot be taken as really holding true. More data of similar setup have to be processed. If such suspicion is verified, then the result would cast doubts on the shear components decomposition.

6.2.2 MEAN STRESS EFFECT

The high scatter of data induced due to improper PSE sets aside the Crossland and Dang Van methods. To pursue the quality of MSE incorporation, the {P} and {P, nMS} groups have to be watched:

1) The increase of scatter by Findley, KCP and Matake under mean loads is obviously too high. This is the reason which disqualifies the Findley and KCP method.
2) Results of the KIA method appears to be too scattered already within the {P, nMS} category and thus its high scatter in any other category is not very surprising.
3) The problem of improper behaviour of Z&L method was already commented in Sec. 6.1.10.
4) Use of maximum hydrostatic stress is promising – both Papadopoulos and Dang Van criteria work well. Dang Van's implementation is even better, but its PSE takes it down.
5) The GAM criterion shows superb quality, with the same average value of both categories and only slight increase of scatter.

When the {NP} and {NP, nMS} groups are compared, too strong PSE does not allow making any proper evaluation.

The effect of mean load given on the torsion channel cannot be examined fully, because the number of tests is too small – there are only 12 tests.

6.3 CRITICAL PLANE DEFINITION

There are three approaches of the critical plane definitions. The critical plane can be set according to the maximum shear stress range (MSSR – here e.g. the Matake criterion), maximum damage (MD –

here by the Findley or Spagnoli MD variant) and Carpinteri & Spagnoli method of deviation from weighted mean first principal direction (CSM – tested here as a variant of the Spagnoli criterion).

According to effects separated in Appendix II, there is too great influence of inadequately defined mean stress inclusion. This is the reason, why the {nMS} group has to be examined as the most important category and why the validation comparing the MD and CSM variants of the Spagnoli criterion in 6.1.7 is not taken as definite (here the CSM variant largely overcome the MD – mainly due to MD's unsuitable behaviour with Gough's data). Since the CSM generally produce a less loaded plane, it is expectable that the same damage parameter (and the same mean stress effect inclusion above all) will not produce analogical results.

When the Findley (MD) and Matake (MSSR) criterion are compared in this category, the Findley's reaches clearly better results under non-proportional loading. The differences between MD and MSSR variants by the McDiarmid criterion are not so pronounced.

The MD and CSM variants of the Spagnoli criterion do not show such a big difference, though it seems to be large enough. At least for the data gathered here, the CSM variant reaches better results. Nevertheless, I hesitate to accept this point. The CSM method originated at first as a tool for description of random loading effects. It defines the directions of weighted mean principal stresses in an acceptable way.

Well, but the next step – the search for the critical plane based on these mean principal directions does not seem to be so clear. The method is relatively fast, independent of potential problems during determination of normal lines to the surface of the specimens. The deviation angle (4) is based on a more or less correct assumption concerning steel and cast iron. Nevertheless, I cannot fudge the question whether the method for CP definition should not degenerate to the MD approach, when the loading is harmonic and not random. This is based on expectation that if there is a plane which is more loaded than the other ones, there are likely enough of the grains oriented in coincidence with that plane predisposed to break. Since the results are contradicting this expectation, more testing has to be done, so that the definite answer could be found.

7 NEW PROPOSAL AND ITS EVALUATION

The previous chapter presented results, which were obtained on the test batch defined in Chap. 5 with current methods. The only recently added GAM method gives the best results there. The GAM method is quite new, so the design of a new criterion was based on the analysis of the other methods made in 6.2 where the separate effects are evaluated.

The final solution was searched in two steps. First a basic composition of the damage parameter was evaluated without any MSE inclusion. I expect that if any progress in evaluation of out-of-phase loading can be reached, then it will be related to changes done in this basic composition.

7.1 CARRIER

The **carrier** represents a fatigue damage parameter, which intentionally operates with amplitudes of local loads only. The work with {nMS} data only leaves aside the MSE problems and thus the form of the criterion can be evaluated as regards the phase shift effect only. There are several points that form the basis of this search:

- The suitable damage parameter processes the load description on a specific plane – this is the shear and normal stresses for HCF.
- The influence of these two parameter is not the same – the primary effect has the shear stress component.
- The torsion mean stress effect in combination of pure axial and torsion loading is debatable (see [14]). Only slight interaction should be expected, if any.
- Although results up to now show that the integral approaches have better behaviour a critical plane methods are tested as well. Here the MD approach is preferred over the MSSR, because the comparison of Findley and Matake shows its better behaviour (see {P, nMS} and {NP, nMS} groups), when mean loads are not active. The CSM approach is not included into the design of the new criterion

7.1.1 PROPOSALS

Tab. 15 sums all new tested proposals together with carriers of existing criteria. There are three groups of criteria examined. First group are the integral methods utilizing the C_a shear stress amplitude parameter. A linear combination of stress components is added in the PZ1 proposal, whereas the quadratic combination in PZ3 tries to use the maximum hydrostatic stress.

There is a difference between maximum hydrostatic stress and the spatial integral average of maximum normal stress:

$$\sigma_{H,\max} \neq \frac{1}{4\pi}\int_{\varphi=0}^{2\pi}\int_{\psi=0}^{\pi} N_{\max}\sin\psi d\psi d\varphi\,, \tag{108}$$

although the equality of (59) is fulfilled. That is because maximum hydrostatic stress is assessed at each time point, whereas $N_{\max}$ is found at different time moments when the loading is non-proportional.

Mark	Carrier formula		a	b	Commentary
Z&L	$\sqrt{\frac{1}{4\pi}\int_{\varphi}\int_{\psi}\left(a\cdot C_a^2+b\cdot N_a^2\right)\sin\psi d\psi d\varphi}\le f_{-1}$	(109)	$\frac{9}{2}\kappa^2-6$	$9-3\kappa^2$	standard Zenner & Liu criterion
PZ1	$\sqrt{\frac{1}{4\pi}\int_{\varphi}\int_{\psi}a\cdot C_a^2\sin\psi d\psi d\varphi}+b\cdot\sigma_{H,a}\le f_{-1}$	(110)	$\frac{5}{2}\kappa^2$	$3-\sqrt{3}\kappa$	
PZ3	$\sqrt{\frac{1}{4\pi}\int_{\varphi}\int_{\psi}a\cdot C_a^2\sin\psi d\psi d\varphi+b\cdot\sigma_{H,a}^2}\le f_{-1}$	(111)	$\frac{5}{2}\kappa^2$	$9-3\kappa^2$	
PZ4	$\sqrt{\frac{1}{4\pi}\int_{\varphi}\int_{\psi}\left(a\cdot C_a^2+b\cdot N_a\right)\sin\psi d\psi d\varphi}\le f_{-1}$	(112)	$\frac{5}{2}\kappa^2$	$f_{-1}\left(3-\kappa^2\right)$	
PZ9	$\sqrt{\frac{1}{4\pi}\int_{\varphi}\int_{\psi}a\cdot C_a^2\sin\psi d\psi d\varphi+b\cdot\sigma_{H,a}}\le f_{-1}$	(113)	$\frac{5}{2}\kappa^2$	$f_{-1}\left(3-\kappa^2\right)$	
Fin	$a\cdot C_a+b\cdot N_a\le f_{-1}$	(114)	$2\sqrt{\kappa-1}$	$2-\kappa$	standard Findley criterion
Mat	$a\cdot C_a+b\cdot N_a\le f_{-1}$	(115)	κ	$2-\kappa$	standard Matake criterion (MSSR approach)
DV	$a\cdot C_a+b\cdot\sigma_{H,a}\le f_{-1}$	(116)	κ	$3-\frac{3}{2}\kappa$	standard Dang Van criterion
Spa	$\sqrt{a\cdot C_a^2+b\cdot N_a^2}\le f_{-1}$	(117)	κ^2	1	standard Spagnoli criterion
PC2	$\sqrt{a\cdot C_a^2+b\cdot\sigma_{H,a}^2}\le f_{-1}$	(118)	κ^2	$9\left(1-\frac{\kappa^2}{4}\right)$	
PC3	$\sqrt{a\cdot C_a^2+b\cdot\sigma_{H,a}}\le f_{-1}$	(119)	κ^2	$3f_{-1}\left(1-\frac{\kappa^2}{4}\right)$	
PC4	$\sqrt{a\cdot C_a^2+b\cdot N_a}\le f_{-1}$	(120)	$\frac{\kappa^2}{2}+\frac{\sqrt{\kappa^4-\kappa^2}}{2}$	f_{-1}	
Ppd	$\sqrt{\frac{1}{8\pi^2}\int_{\varphi}\int_{\psi}\int_{\chi}a\cdot T_a^2 d\chi\sin\psi d\psi d\varphi}+b\cdot\sigma_{H,a}\le f_{-1}$	(121)	$5\kappa^2$	$3-\sqrt{3}\kappa$	standard Papadopoulos criterion
PP1	$\sqrt{\frac{1}{8\pi^2}\int_{\varphi}\int_{\psi}\int_{\chi}\left(a\cdot T_a^2+b\cdot N_a^2\right)d\chi\sin\psi d\psi d\varphi}\le f_{-1}$	(122)	$9\kappa^2-12$	$15\left(3-\kappa^2\right)$	
PP2	$\sqrt{\frac{1}{8\pi^2}\int_{\varphi}\int_{\psi}\int_{\chi}a\cdot T_a^2 d\chi\sin\psi d\psi d\varphi+b\cdot\sigma_{H,a}^2}\le f_{-1}$	(123)	$9\kappa^2-12$	$15\left(3-\kappa^2\right)$	
PP3	$\sqrt{\frac{1}{8\pi^2}\int_{\varphi}\int_{\psi}\int_{\chi}\left(a\cdot T_a^2+b\cdot N_a\right)d\chi\sin\psi d\psi d\varphi}\le f_{-1}$	(124)	$5\kappa^2$	$f_{-1}\left(3-\kappa^2\right)$	
PP4	$\sqrt{\frac{1}{8\pi^2}\int_{\varphi}\int_{\psi}\int_{\chi}a\cdot T_a^2 d\chi\sin\psi d\psi d\varphi+b\cdot\sigma_{H,a}}\le f_{-1}$	(125)	$5\kappa^2$	$f_{-1}\left(3-\kappa^2\right)$	
PP5	$\sqrt{\frac{1}{8\pi^2}\int_{\varphi}\int_{\psi}\int_{\chi}a\cdot T_a^2 d\chi\sin\psi d\psi d\varphi}+\frac{1}{4\pi}\int_{\varphi}\int_{\psi}b\cdot N_a\sin\psi d\psi d\varphi\le f_{-1}$	(126)	$5\kappa^2$	$3-\sqrt{3}\kappa$	

Tab. 15 A list of tested carrier formulas together with their material variables.

Even if the loading is strictly proportional, there is a change of placement of N_{max} at time by a direction of the examined plane – where once N_{max} was, N_{min} is now after some further rotation. The $\sigma_{H,max}$ concept integrates the N_{max} and N_{min} together in one time instant. Only afterwards, it determines the position at the time, at which the maximum value of $\sigma_{H,max}$ was reached. The N_{max} concept uses only N_{max} obtained at different time instants and the final value of $\sigma_{H,max}$ is derived directly from them.

This the reason, why Tab. 15 contains both definitions. There is open room for a reflection upon the meaning of both definitions. Whereas the maximum hydrostatic stress is defined as a maximum load throughout the cycle, the spatial average of maximum normal stress sums the maximum load effects on all separate planes, which is more similar to the way how the shear stress amplitude C_a is determined. Due to their definition the load calculated through the maximum hydrostatic stress is equal or lesser than the load resulting from the spatial average of maximum normal stress, which thus tends to generate more conservative solution.

The PZ4 proposal is of a hybrid form – the C_a parameter is powered by two in contrast to the linear N_a parameter. This composition took its form from the idea of a primary effect of shear stress and an only secondary effect of normal stress. This property can be sufficiently expressed by different size of *a* and *b* parameters where *a* would be the larger one. The same can be reached by the PZ4 proposal where the sensitivity to C_a changes will be surely higher than that of N_a parameter.

Second group is formed by methods utilizing the critical plane concept. They are the most frequently covered, thus only three different proposals are given (PC2, PC3 and PC4). The PC3 and PC4 carriers are of hybrid character. The PC2 and PC3 carriers test further use of hydrostatic stress in the damage parameter.

The way of setting the method parameters is shown for these two types of criteria in Appendix VII (PZ4 carrier) and Appendix VIII (PC4 carrier). The material parameters of other methods were derived in a similar way.

The third group is based on the concept of the mean resolved shear stress used by Papadopoulos. It is evaluated here with different forms of mutual relations of interacting parameters. There was some expectation hidden, whether this definition of the shear stress component influence is not more suitable for description of non-proportional loading.

7.1.2 RESULTS OF CARRIER PROPOSALS

Results of the testing are very interesting – see Tab. 16. The critical plane criteria were tested as the MD methods with the basic angular step 8 deg and afterwards the further maximization was run. The integral methods were calculated with the integrating angular step 2 deg between examined planes and between evaluated directions of *T* resolved shear stress as well.

First of all, existing criteria have to be commented once again. The Matake criterion is subjoined only to compare it with the Findley criterion, i.e. to make a comparison of MSSR and MD methods. Apparently, the MD method seems to reach better results.

Use of hydrostatic stress in the Dang Van criterion does not seem to be acceptable. Its use is almost certainly the reason of much higher deviation of results obtained with the Dang Van criterion when they are compared to the Findley criterion. The overall better results of the Dang Van criterion in the whole test batch have to be ascribed to a better behaviour of hydrostatic stress under mean loads. Since the carriers focused on the PSE are evaluated here, the ranking of the Dang Van criterion is significantly decreased. The negative properties of hydrostatic stress under non-proportional loading are projected into the PC2 and PC3 criteria as well.

Another point of interest is the difference between the integration of N_{max} and maximum hydrostatic stress. Here the test pairs are {PZ4, PZ9}, {Ppd, PP5} and {PP3, PP4}, where the second of the pair is the one using the maximum hydrostatic stress. While in the mixed combination, the integration of N_{max} seem to lead to better, less scattered results, the linear combination in the {Ppd, PP5} pair does not show any significant difference. Results can be thus interpreted that the maximization of N_{max} leads to

at least the same or slightly better results than the use of maximum hydrostatic stress. Increase of computation time in the case of N_{max} integration is not very high too, because the partition of load to the $\{C, N\}$ pair is necessary anyway.

The difference between the same concepts in the quadratic combination are much less pronounced, and it is visible in much smaller degree under non-proportional loading only. Under proportional loading, the changes of N_{max} to N_{min} and back under different directions of the examined plane do not influence the calculation as normal stress is squared.

There is a further discussion of the same problem in Appendix VI where results of grey cast iron are summed. Here the solution utilizing the maximum hydrostatic stress leads to significantly less scattered results. Since there is a very small number of tests, this aspect will need more care in future.

There is no great distinction if the damage parameters are defined in a linear or quadratic combination. In all cases the most promising parameter is the mixed one with the shear stress parameter in the quadratic form and the normal stress parameter as a linear function. The integral method with C_a parameter (PZ4) reaches really nice results, whereas the PP3 integral method with T_a parameter is significantly worse, although still superior inside its family of PP proposals. The CP concept (PC4) is of similar scatter as the PZ4, but its mean value is strongly shifted to the conservative side. These three carriers will be processed further in order to reach the final resulting criterion. The expectation concerning the split of load input sensitivity into a hybrid form was fulfilled.

The last two criteria of Tab. 16 are depicted just for broader comparison. The poor results of Crossland criterion in the nMS group were already commented in 6.1.2. The GAM method does not reach very interesting results as regards the {nMS} data. It seems that its overall results are strongly influenced with the unsuccessfully integrated phase shift effect. Its overall good result are based on the fact, that inclusion of {MS} loads increases its range in small scale only.

ΔFI	case	Z&L	PZ1	PZ3	PZ4	PZ9	Fin	Matake	DV	Spa	PC2
Average	nMS	-0.9%	1.8%	-1.3%	1.6%	0.0%	2.2%	3.2%	-1.9%	2.4%	-5.1%
	P, nMS	-0.5%	2.6%	-0.5%	2.3%	0.9%	3.6%	3.7%	3.6%	1.0%	-0.5%
	NP, nMS	-1.2%	1.2%	-1.8%	1.1%	-0.6%	1.2%	2.8%	-5.8%	3.3%	-8.3%
Range	nMS	23.4%	23.6%	24.4%	21.1%	21.9%	27.5%	33.4%	39.0%	27.4%	34.4%
	P, nMS	14.8%	16.7%	14.8%	15.1%	13.0%	15.4%	15.6%	15.4%	19.4%	14.8%
	NP, nMS	23.4%	22.2%	24.4%	19.9%	21.9%	27.5%	33.4%	35.2%	27.4%	30.7%
St. dev.	nMS	4.8%	4.6%	4.9%	4.2%	4.4%	5.8%	6.1%	8.9%	5.5%	7.9%
	P, nMS	4.2%	3.6%	4.2%	3.3%	3.5%	3.6%	3.7%	3.6%	5.1%	4.2%
	NP, nMS	5.1%	5.1%	5.3%	4.7%	4.8%	6.7%	7.3%	9.4%	5.6%	8.2%

	case	PC3	PC4	Ppd	PP1	PP2	PP3	PP4	PP5	Cross	GAM
Average	nMS	-1.8%	9.1%	2.9%	1.5%	1.5%	4.3%	2.7%	4.6%	-5.2%	2.0%
	P, nMS	2.7%	8.3%	1.1%	-0.5%	-0.5%	2.3%	0.9%	2.6%	1.1%	1.4%
	NP, nMS	-5.0%	9.7%	4.1%	2.9%	2.9%	5.7%	4.0%	6.0%	-9.5%	2.3%
Range	nMS	31.4%	20.4%	25.8%	27.3%	27.3%	23.0%	25.0%	23.9%	38.6%	28.8%
	P, nMS	13.2%	15.9%	14.1%	14.8%	14.8%	15.1%	13.0%	16.7%	14.1%	14.4%
	NP, nMS	28.8%	20.4%	25.8%	27.3%	27.3%	23.0%	25.0%	23.9%	34.5%	28.8%
St. dev.	nMS	7.4%	4.6%	4.8%	5.2%	5.2%	4.5%	4.7%	4.9%	9.3%	5.0%
	P, nMS	3.2%	4.6%	3.7%	4.2%	4.2%	3.3%	3.5%	3.6%	3.7%	3.7%
	NP, nMS	7.8%	4.5%	5.0%	5.4%	5.4%	4.8%	4.9%	5.1%	9.5%	5.8%

Tab. 16 Results of existing and proposed carriers obtained on the test batches mentioned.

7.2 MEAN STRESS EFFECT INCLUSION

To design a fully equipped damage criterion, the carrier is to be further extended with mean stress parameter, while maintaining the carrier's properties in nMS loading. Once the carrier is set, the

simplest MSE inclusion is replace the N_a parameter with $N_{\max}$. Such solution tends to $N_{\max} = N_a$ whenever the mean loads are zeroed and thus obeys the basic carrier formula. Moreover, there is no other material parameter necessary. The final three tested proposals are given in Tab. 17.

In order to preserve the negative influence of positive (opening) mean normal stresses, it is defined in all of the three proposals that:

$$\begin{aligned} N_m > 0 \quad &\Rightarrow \quad N_{\max} = N_a + N_m, \\ N_m \le 0 \quad &\Rightarrow \quad N_{\max} = N_a. \end{aligned} \tag{127}$$

The same definition ensures that the durability will not be decreased in cases of square of the negative mean normal stresses, which would be unsuitable.

Mark	Formula	a	b	Carrier
PZa	$\sqrt{\frac{1}{4\pi}\int_{\varphi}\int_{\psi}\left(a\cdot C_a^2 + b\cdot N_{\max}\right)\sin\psi d\psi d\varphi} \le f_{-1}$ (128)	$\frac{5}{2}\kappa^2$	$f_{-1}\left(3-\kappa^2\right)$	PZ4
PCa	$\sqrt{a\cdot C_a^2 + b\cdot N_{\max}} \le f_{-1}$ (129)	$\frac{\kappa^2}{2}+\frac{\sqrt{\kappa^4-\kappa^2}}{2}$	f_{-1}	PC4
PPa	$\sqrt{\frac{1}{8\pi^2}\int_{\varphi}\int_{\psi}\int_{\chi}\left(a\cdot T_a^2 + b\cdot N_{\max}\right)d\chi\sin\psi d\psi d\varphi} \le f_{-1}$ (130)	$5\kappa^2$	$f_{-1}\left(3-\kappa^2\right)$	PP3

Tab. 17 List of basic two-parameter formulas tested together with their material variables when the MSE is incorporated via the $N_{\max}$ parameter.

Results of all criteria proposed in this section can be seen in the Appendix IV, whereas their statistical evaluation in Appendix V. The PZa criterion markedly overcomes even the GAM method in the scatter of results. Results of the PPa method are more or less similar to those of the GAM method.

The PCa method shows unacceptable MSE behaviour. Group {MS} has much higher average value than the {nMS} group. A more suitable solution was found with utilization of the SWT mean stress inclusion as it was shown e.g. by the SpaM method derivation from the Spagnoli method – see Tab. 18.

Mark	Formula	a	b	Carrier
PCa2	$\sqrt{a\cdot C_a^2 + b\cdot\sqrt{N_a\cdot N_{\max}}} \le f_{-1}$ (131)	$\frac{\kappa^2}{2}+\frac{\sqrt{\kappa^4-\kappa^2}}{2}$	f_{-1}	PC4

Tab. 18 The PCa2 two-parameter formula tested together with its material variables. Here the MSE solution utilizes SWT equivalent stress.

Here the effect of negative mean stress is expected as defined in (127). The method PCa2 behaves worse than the PZa as regards all statistical parameters. In contrast to the GAM method it has lesser range of results, the standard deviation is the same, but the mean value is largely shifted towards the conservative side of prediction (as already its carrier is). Interesting is that the PCa2 method belongs to the CPA family and thus its computation time can be very small in comparison to other methods (and even to the GAM method under general conditions).

There is an option to implement the third material parameter with the N_m mean normal stress as it can be seen e.g. in the Kenmeugne criteria - see its derivations in Appendix VII and Appendix VIII. These options are depicted in Tab. 19.

Knowing the results of the Kenmeugne and Zenner & Liu criteria, results of the methods presented in Tab. 19 are not surprising. All methods tend to show worse results compared to the “a” variants. This applies even to the case of Gough's tests results where the b_0 fatigue limit was experimentally set.

Nevertheless the PZb, PPb and PCb are still better than any other tested method, except for the GAM solution where the PPb and PCb methods have slightly higher scatter.

Mark	Formula		d	Carrier
PZb	$\sqrt{\frac{1}{4\pi}\int_\varphi\int_\psi\left(a\cdot C_a^2+b\cdot N_a+d\cdot N_m\right)\sin\psi d\psi d\varphi}\le f_{-1}$	(132)	$f_0\left[6\left(\frac{f_{-1}}{f_0}\right)^2-\frac{\kappa^2}{2}-\frac{b}{f_0}\right]$	PZ4
PCb	$\sqrt{a\cdot C_a^2+b\cdot N_a+d\cdot N_m}\le f_{-1}$	(133)	$f_{-1}\left[2\frac{f_{-1}}{f_0}-1\right]$	PC4
PPb	$\sqrt{\frac{1}{8\pi^2}\int_\varphi\int_\psi\int_\chi\left(a\cdot T_a^2+b\cdot N_a+d\cdot N_m\right)d\chi\sin\psi d\psi d\varphi}\le f_{-1}$	(134)	$f_0\left[6\left(\frac{f_{-1}}{f_0}\right)^2-\frac{\kappa^2}{2}-\frac{b}{f_0}\right]$	PP3

Tab. 19 List of the three-parameter formulas tested together with their material variables. The *a* and *b* parameters convene with definitions given in Tab. 17.

Except for the PCa2 method, the other "a" variants show that the mean stress effect is too weak – mean values of the {MS} group are significantly lower than that of the {nMS} group. Though the "b" variants could suppress this phenomenon, the computed values of d parameter are obviously too strongly dependent on the f_0 fatigue limit. During analysis, a fact was found that PZa and PPa methods tend to reach better results over all test data if N_{max} is replaced with the values as follows:

$$\begin{aligned} N_m>0 \quad &\Rightarrow \quad N_{\max}=N_a+1.6\cdot N_m,\\ N_m\le 0 \quad &\Rightarrow \quad N_{\max}=N_a. \end{aligned} \tag{135}$$

Mark	Formula		a	b	Carrier
PZc	$\sqrt{\frac{1}{4\pi}\int_\varphi\int_\psi\left[a\cdot C_a^2+b\left(N_a+\frac{f_0}{f_{-1}}N_m\right)\right]\sin\psi d\psi d\varphi}\le f_{-1}$	(136)	$\frac{5}{2}\kappa^2$	$f_{-1}\left(3-\kappa^2\right)$	PZ4
PCc	$\sqrt{a\cdot C_a^2+b\left(N_a+\frac{f_{-1}}{f_0}\cdot N_m\right)}\le f_{-1}$	(137)	$\frac{\kappa^2}{2}+\frac{\sqrt{\kappa^4-\kappa^2}}{2}$	f_{-1}	PC4
PPc	$\sqrt{\frac{1}{8\pi^2}\int_\varphi\int_\psi\int_\chi\left[a\cdot T_a^2+b\left(N_a+\frac{f_0}{f_{-1}}\cdot N_m\right)\right]d\chi\sin\psi d\psi d\varphi}\le f_{-1}$	(138)	$5\kappa^2$	$f_{-1}\left(3-\kappa^2\right)$	PP3
PZd	$\sqrt{\frac{1}{4\pi}\int_\varphi\int_\psi\left[a\cdot C_a^2+b\left(N_a+\frac{f_{-1}}{t_{-1}}N_m\right)\right]\sin\psi d\psi d\varphi}\le f_{-1}$	(139)	$\frac{5}{2}\kappa^2$	$f_{-1}\left(3-\kappa^2\right)$	PZ4
PCd	$\sqrt{a\cdot C_a^2+b\left(N_a+\frac{t_{-1}}{f_{-1}}\cdot N_m\right)}\le f_{-1}$	(140)	$\frac{\kappa^2}{2}+\frac{\sqrt{\kappa^4-\kappa^2}}{2}$	f_{-1}	PC4
PPd	$\sqrt{\frac{1}{8\pi^2}\int_\varphi\int_\psi\int_\chi\left[a\cdot T_a^2+b\left(N_a+\frac{f_{-1}}{t_{-1}}\cdot N_m\right)\right]d\chi\sin\psi d\psi d\varphi}\le f_{-1}$	(141)	$5\kappa^2$	$f_{-1}\left(3-\kappa^2\right)$	PP3
PCe	$\sqrt{a\cdot C_a^2+b\left(N_a+\frac{t_{-1}}{f_0}\cdot N_m\right)}\le f_{-1}$	(142)	$\frac{\kappa^2}{2}+\frac{\sqrt{\kappa^4-\kappa^2}}{2}$	f_{-1}	PC4

Tab. 20 List of two- and three-parameter formulas tested and their material variables.

This trend was observed not only in the summarisation by the partial effects but in the summarisation by tested materials as well. Since the value of the constant 1.6 has its meaning when the hard steels (which are here above all) are discussed, another forms of criteria were proposed (see Tab. 20)

The differences between summarized results of "c" and "d" variants are very slight in the case of PZ and PP families, which both reach their best representatives in these two variants. As regards the PC family, the difference is much more pronounced. Both "c" and "d" variants are more scattered than the PCa2 variant with the MSE according to SWT method. The carrier itself is much better, than any variant with mean stresses. This is the reason, why one more formula is proposed – PCe. This solution shows scatter comparable with the PZ family.

It should be emphasized that although there are again three parameters necessary in the "c" or "e" methods, the influence of the f_0 fatigue limit in repeated axial loading is much lesser here than in "b" versions – see Fig. 36. Thus application of data derived from appropriate formulas described in Sec. 5.2.1 does not encumber the fatigue life estimation so much, as it is observable with the "b" methods or any other criterion presented here.

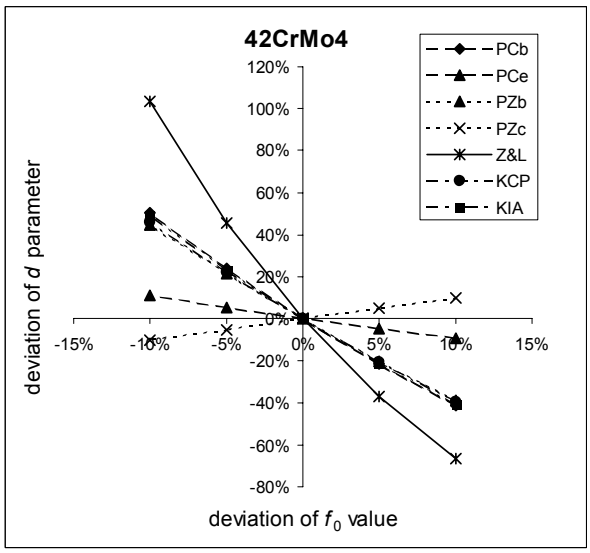

Fig. 36 Sensitivity of the $d \cdot N_m$ parameter on the f_0 fatigue limit in repeated axial loading. Where the d parameter is not defined directly in the appropriate formula, the complete set of coefficients appertaining to the N_m summand is expected.

7.3 ANALYSIS OF FINAL FORMULAS

The best obtained results are derived from the PZ family. The final form of criteria corresponds to the PZd variant:

Mark	Formula	a	b
PZ	$\sqrt{\frac{1}{4\pi}\int_{\varphi}\int_{\psi}\left[a\cdot C_a^2+b\cdot\left(N_a+\frac{f_{-1}}{t_{-1}}N_m\right)\right]\sin\psi d\psi d\varphi}\le f_{-1}$ (143)	$\frac{5}{2}\kappa^2$	$f_{-1}\left(3-\kappa^2\right)$

The results presented in Fig. 37 look very good, because 74.4% of all tests results lies in the range ⟨-5; 5⟩%. This variant was preferred over the PZc variant mainly thanks to smaller number of material parameters necessary for computation. If the repeated axial fatigue limit is available, the solution with PZc formula can be used instead:

Mark	Formula		a	b
PZv2	$\sqrt{\frac{1}{4\pi}\int_{\varphi}\int_{\psi}\left[a\cdot C_a^2+b\cdot\left(N_a+\frac{f_0}{f_{-1}}N_m\right)\right]\sin\psi d\psi d\varphi}\le f_{-1}$	(144)	$\frac{5}{2}\kappa^2$	$f_{-1}\left(3-\kappa^2\right)$

The number of tests in the {MS} group is still small, therefore further testing of both variants should continue. More test values of mild steels ($\kappa > 1.7$) and brittle materials ($\kappa < 1.4$) with MSE would be desirable, because both these groups are very badly covered in this evaluation.

The PP family is abandoned at last. Already results of the carrier itself show its limits. Though, its overall behaviour confirms the choice of damage parameter of the other two families. The method of an integration of resolved shear stress is significantly faster over the MCCM method accepted in the PZ family, but this advantage is fully overshadowed by the PC method, which is both faster as well as more precise.

Positive property of the PC critical plane variant implementation is that under general conditions of computation setup (as described in Sec. 6.1) and under non-proportional loading the PC is 14 times faster than the PZ implementation.

Mark	Formula		a	b
PC	$\sqrt{a\cdot C_a^2+b\cdot\left(N_a+\frac{t_{-1}}{f_0}\cdot N_m\right)}\le f_{-1}$	(145)	$\frac{\kappa^2}{2}+\frac{\sqrt{\kappa^4-\kappa^2}}{2}$	f_{-1}

Moreover, the critical plane criteria altogether seem to cover well also the brittle materials, which cannot be said about integral methods. Precisely as shown in Appendix VI, the PC method results of the grey cast iron tested by Nishihara & Kawamoto coincide perfectly with the other results of the test batch. Unfortunately, there is no mean stress induced, so its impact on the prediction of tests on brittle materials could not be evaluated in full.

The use of f_0 fatigue limit in repeated axial loading is acceptable in given solutions even if it has to be derived from the f_{-1} and t_{-1} reversed fatigue limits. The sensitivity to this parameter is much lesser for both the PZv2 and PC methods. At last, it should be reminded that negative N_m values are set to zero during computation in accordance with (127), so that the methods remain conservative.

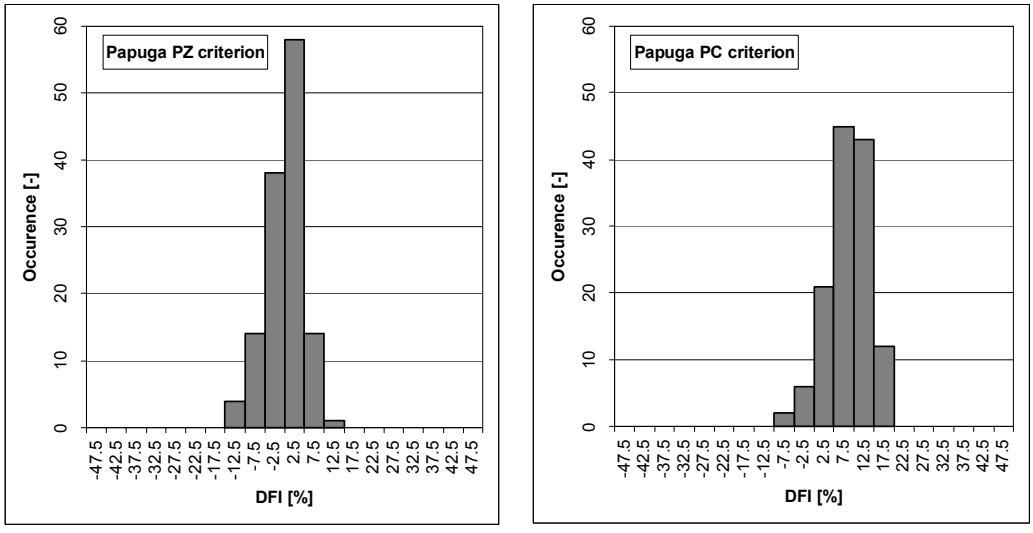

Fig. 37 Histograms of two final proposed methods – the integral criterion on the left and critical plane criterion on the right side.

7.3.1 MAXIMUM DAMAGE CRITERIA FURTHER CHECKED

The high mean value of fatigue index error is interesting in the PC4 family. The results are nearly all on the conservative side of prediction. Since the scatter in the final chosen criterion (PCe) is small, this property does not matter very much and can be regarded as a safety coefficient. The reason for the deviation can be found under closer examination. When the second derivations of the functional of the PC4 formula are done as well (see Appendix IX), the maximum damage is reached when the following conditions is satisfied:

$$\frac{\partial^2 f_{-1}}{\partial \varphi^2} \cdot \frac{\partial^2 f_{-1}}{\partial \psi^2} - \left(\frac{\partial^2 f_{-1}}{\partial \varphi \partial \psi} \right)^2 > 0 , \tag{146}$$

which assures that some extreme is reached, whereas

$$\begin{aligned} &\frac{\partial^2 f_{-1}}{\partial \varphi^2} < 0, \\ &\frac{\partial^2 f_{-1}}{\partial \psi^2} < 0 \end{aligned} \tag{147}$$

guarantees that the extreme is a maximum. The same conditions have to be fulfilled for the reversed torsion loading too. It is specific for the PC4 carrier is that the maximum of the damage is reached only for the torsion loading, whereas the minimum is obtained in the axial loading! In order to fulfil the condition (120) the *a* and *b* parameters derived are thus larger than would correspond to a found maximum of damage. The larger *a* and *b* parameters generate higher fatigue index, which means that the results are shifted towards the conservative side.

Note that a breakpoint $\kappa = 2/\sqrt{3}$ can be derived from the condition (146). Materials with a κ value higher than this breakpoint tend to find minimum damage under the reversed axial loading, whereas those with κ lesser reach correctly maximum damage. The breakpoint is low enough (it is approximately $\kappa = 1.155$), so that vast majority of materials fall into the minimum damage category. This apparently influences the average value of prediction and shifts it to the conservative side. One could expect higher difference in comparison of ΔFI average values of the whole test batch (9.1% for the {nMS} category) and of the grey cast iron (6.3% given in the same category in Appendix VI), but the importance of this comparison is low. There are only 6 experiments done on the grey cast iron. More testing of brittle materials is desirable.

Be aware of a similar problem when the PCb criterion is evaluated as regards the fatigue limit in repeated bending. The inconsistency of the criterion goes here far beyond the point of PC4 carrier. There is no material that fulfils all three conditions for the material set used here. Unluckily the plane found needn't give an extreme at all for some materials (e.g. FGS800-2). If the breakpoint as regards the PC4 carrier was shifted to a sensible value and if it separated more or less brittle material from the rest, the breakpoint here creates much more confusion.

The same examination whether the plane is really the MD one was as well done for the Findley's (46) and Spagnoli's (55) MD approach. The Spagnoli's version of the damage parameter results in a very similar conclusion but the breakpoint appearing in the reversed axial loading is shifted to $\kappa = \sqrt{2}$. Pure reversed torsion loading leads to correct maximum of damage. A majority of steels thus lie in the area of minimum damage, but the breakpoint is shifted to a value which can be reached much more easily (see the tensile loading in the MPA group). That is why the low breakpoint found in the PC4 carrier is more acceptable than the breakpoint found in the Spagnoli criterion if more materials have to be compared.

Now a short flashback has to be done. Remind the results of the CSM v. MD comparison made in Sec. 6.1.7 and commented also further in Sec. 6.3. I wondered over the fact that the CSM method leads to apparently better results, than those the MD approach offers. A question should be raised if its better behaviour should not be predicated to the fact that the CSM method shifts the results to the less conservative side (thus acts contrary to the effect of minimum damage found) and is less sensitive than

the MD, which every time finds the extreme. As stated already in 6.3, the problem is not definitely solved yet and its evaluation should continue.

The Findley criterion shows another interesting behaviour. One can find that when the base 6 equations (two basic equations and four first partial derivations – see similar derivation in Appendix VIII) are formed, two of them are linearly dependent. Therefore the same extreme is reached for infinite number of planes and the only condition here is that a following relation holds true:

$$\kappa \cdot \sin^2 \psi_f \cdot \cos^2 \varphi_f = 1. \tag{148}$$

Any combination of the angles obeying the condition (148) leads to maximum damage for the material tested here. Nevertheless, the result that the maximum damage can be found for infinite number of critical planes under reversed axial loading does not seem to make sense from mathematical point of view. Such a variability of crack locations for one material should have been already observed.

8 CONCLUSION

8.1 FULFILMENT OF GOAL

The goal set was undoubtedly fulfilled. The two criteria proposed in the Chap. 7 show significantly better behaviour under the test batch enlarged to 129 experiments. Three quarters of all results of the PZ variant lies in the range of ΔFI error from –5% to 5%. The criteria were derived on a basis of the analysis of different load effects influencing the final calculation. The analysis was done partly on present criteria but also on a range of different proposals tested in Chap. 7. A commentary to the goal achieved can be read in subsequent sections.

8.2 OVERVIEW

Thanks to the PragTic fatigue solver a broad comparison of existing methods for high-cycle fatigue life calculation could be made. There have been 12 different approaches tested, from which six have been critical plane ones, three were integral ones and three were based on properties of the smallest circumscribed entity over the load path in the Ilyushin five-dimensional space.

The test batch has consisted of 129 test altogether. All of them have been acquired from the references. The scope of tests have contained proportional and non-proportional harmonic iso-frequency two-channel loading above all, but uniaxial tests were used as well if there were non-zero mean stress components active. Loading by a pair of torsion and plane bending has been used in most of the test. Fatigue limit under given loading has been the parameter evaluated here.

All results of individual criteria have been evaluated as one set and in groups separated by subsequent effects from statistical point of view as well. There is some simplification involved, because the data taken from references can differ e.g. in the definition of fatigue limit. It can be defined at various number of cycles by different researchers. Nevertheless, any evaluation of test batches resolutely separated by experimenters' names would not provide an easy analysi. The resulting information would be too discontinuous, moreover it would be hard to find a single test batch sufficiently large. Thus both views have been referred here, but the overall test batch and separation of the effects have been preferred for the final evaluation.

8.2.1 PRESENT CRITERIA

There are two criteria, which have to be directly tucked away. Those are the methods by Sines and McDiarmid, which both lead to highly scattered results. There is no category where they could be evaluated as being of the top rank.

The critical plane approach by Spagnoli leads to poor results in both MD and CSM variants due to the incorrectly induced mean stress effect. It can be easily revised as can be seen in the SpaM and SpaC proposals. Afterwards, the methods lead to results comparable to majority of other already existing methods tested here. It is not a very positive fact, because their scatter is relatively large.

As regards the statistics of the other criteria, it can be concluded that the integral methods seem to be superior to the methods utilizing the CPA. This can be observed above all for non-proportional loading where they show lesser scatter. The fact is interesting that when the PSE and MSE influences are separated, there can be clearly shown that any of the presented contermporary criteria suffers from inadequate inclusion of at least one of them. The unlucky concept of MSE is largerly at fault, but the

increase of scatter, when the proportional and non-proportional loading is compared, is significant as well.

As far as the methods of other authors are concerned, the GAM solution leads to best results unambiguously. Under more detailed inspection, a significant insufficiency in evaluation of the non-proportional loading can be found. This method has been found in references only recently, thus it was not further analyzed in order to improve it. Evaluating the other existing criteria, the second best is the Kenmeugne three-parametric integral criterion.

8.2.2 NUMBER OF PARAMETERS

There is disputation about number of parameters necessary for a criterion, which would suitably cover the mean stress effect too. Although the 3-parameter Kenmeugne integral criterion KIA leads to results more efficient than majority of other methods, remaining more-parameter methods show much worse behaviour. One has to admit that their inadequacy can be induced due to the way, in which the fatigue limits in repeated loading were derived. There is only one material batch (S65A by Gough [29]) where all necessary parameters are experimentally set. Thus, a derivation from experimental data alternatively SWT or Morrow formulas were used for their determination.

Even in the Gough's batch, the results of 3-parameter methods do not show any significant domination over the 2-parameter methods. Thus the use of the third parameter would be questionable. Pursuit of this aspect has to be further followed with more rigorous data.

Let's cite Zenner et al. in their apology for their 4-parameter method. Only changes in notation and in the one referred formula were made here:

> *f_{-1} and t_{-1} are required as initial parameters. f_{-1} can be estimated from the mean stress sensitivity M. Empirical equations for M as a function of the tensile strength are known. t_{-1} is estimated with the use of Eq. (104). Hence, only the first two characteristic parameters are really necessary. The decisive criterion for appraising a hypothesis is not the number of material parameters, but rather the availability of these parameters and the sensitivity with which an error in the assumption of material parameters affects the result.*
>
> *cited from [89], p. 142*

Their commentary is wholly true. It is not necessary to evade the 3- and 4-parameter methods fundamentally. They can work very well – above all if all necessary input parameters are available. If it is not the case, than a dependency of the method on approximate determination of missing parameters should be set. Nevertheless, as shown in Fig. 36, a sensitivity of the appropriate parameter d of the particular methods already published on the error in determination of b_0 fatigue limit is quite high.

8.2.3 NEW CRITERIA

After the results of existing criteria are analyzed and commented, design of new criteria follows. It stems from expectation that determination of the basic fatigue parameter without any mean stress effect (called the carrier here) is necessary. After the scatter of {nMS} data is minimized, the mean stress extensions could be placed onto this carrier and tested. There were 26 new proposals tested. The pursuit of two ways leads to the final criteria – in both cases the damage parameter consist of a hybrid formulation where the shear component is in a quadratic form, whereas the normal component is only linear. At this point the criteria perfectly coincide with the general expectation of the prime effect of the shear parameter and the secondary influence of the normal component.

The best results are achieved by the PZ (143) or PZv2 (144) criteria. The two variants differ in the constant, which amplifies the mean stress effect. Although one of them leads to a three parameter criterion, whose group was criticized above, the error connected to an inaccurate fatigue limit in repeated axial loading is much lesser in contrast to any of the criteria mentioned (see Fig. 36). Under

such conditions, the Zenner defence cited above is fully rightful. Results of the PZ criterion are very impressive, because three quarters of all tests lie in a band of ΔFI of ⟨-5; 5⟩%.

The second successful criterion is the critical plane method denoted as PC (145). It is again a three-parameter method, where the same minor effect of the precise f_0 determination as by PZv2 is seen. The results are notably shifted towards the conservative side of prediction with mean value at 8.6%. Nevertheless the band, in which the results are, is very narrow and thus this property can be taken as another safety coefficient. The PC method shows very good behaviour for the only brittle material tested here too (grey cast iron tested by Nishihara & Kawamoto – it is not covered by the main test batch, but the results are separated into Appendix VI).

There is one important difference between these two methods too. The integral methods require doing the integration discretized over all planes, whereas optimisation techniques can be used in the critical plane methods. There is no great opportunity how to shorten the integration except for increase of the integration step. Nevertheless, such possibility is surely limited. The optimisation of the angular rotation in the integral methods was not studied until now in detail. The PC method is approximately 14 times faster than the PZ under nowadays implementation in PragTic with basic setup of computation parameters defined as given in Sec. 7.1.2. One place value of the computation speed is a convincing moment in the deciding, which method is to be used.

8.2.4 CRITICAL PLANE APPROACHES

By the comparison made in Sec. 6.3, the MD approach is better than the MSSR one. The final statement is based on the {nMS} group, because the methods are too strongly affected by the MSE.

The CSM method gives better results than the MD approach, if the Spagnoli's damage parameter is tested. There is some reasoning written in Sec. 7.3.1, whether this behaviour cannot be affected by the improper mathematical properties of the MD approach applied to the Spagnoli's damage parameter. I hesitate about accepting the fact that the CSM method chooses another critical plane than is the one loaded by the most damaging load combination. Further testing of the CSM approach, which would include also other damage parameter, is thus desirable.

The mentioned mathematical problem of Spagnoli's MD approach concerns the PC damage parameter defined newly as well. When the derivation of material parameters is carefully examined, one finds that the reversed axial loading generates the plane not with maximum but with minimum damage (Appendix IX). The material parameters are thus set higher than they should be, which in consequence lead to higher values of fatigue index. The final effect on the PC method shifts the average value to the conservative side and leaves the result with a scatter better than any other existing and tested criterion could offer. The breakpoint dividing the results of the method to two categories – the first one where the minimum damage was found and results are thus more conservative and the second one where the maximum was reached and results are correct – is low being only $\kappa = 1.155$. Thus the group with more conservative solution comprises vast majority of materials, whereas the second group with κ lesser takes in only very brittle materials.

The Spagnoli's damage parameter in the MD variant leads to similar results, but the breakpoint lies much higher ($\kappa = 1.414$). Research on the Findley method shows that the maximum damage is reached every time. What's suspicious here is the fact that there is infinite number of MD planes under fully reversed axial loading. Their direction is limited only by one condition that relates the values of φ and ψ angles. Such result does not seem to be adequate.

8.3 SIGNIFICANCE FOR RESEARCH AND TECHNICAL PRACTICE

The described project brought three significant benefits:

- The computational evaluation of existing criteria on gathered experimental data given in Chap. 6 brings a good overview of state of the art.
- The two newly defined multiaxial criteria PC and PZ give so good results that no other criterion tested here can be confronted with it. This improvement has to be further checked, because the

load inputs were relatively simple. As will be shown in the following section, there is still room left for further evaluation. All the same, these two new criteria are tested on an experimental data set, which contains more values than many other presented criteria offer.

- The third contribution concerns the PragTic software. It is a strong tool for fast and transparent computation of multiaxial fatigue nowadays. The Sec. 4.4 sums its expected software improvements in the near future, whereas a proposal what to do next with the software package itself is sketched in the next section.

8.4 FURTHER PLANS

8.4.1 ENLARGEMENT OF THE EXPERIMENTAL DATA SET

There were two methods proposed, which lead to very interesting results under conditions given. Now they have to be checked if the conditions were not too limited. The criteria have to be tested under other types of loading (more of tensile tests, biaxial loading, different frequencies of channels etc.). Already a set of triaxial tests done by Mielke was extracted from [39]. New methods behave well even under these conditions, nevertheless more data would be suitable.

What would be very interesting too are the data by Gough [30], which I recently obtained. In addition to the data already cited here in 5.1.5, a much larger set of data can be found there. By the way – these data were used, among others, by McDiarmid for testing his own criterion. All the data refer to in-phase loading composed of plane bending and torsion with or without mean loads. The important fact is that these data are related to notched specimens, whereas here only smooth specimens were used. Thus unlike the results obtained here, this further testing will require FE-models of specimens, so that effects of notches could be enumerated. The ability of the PragTic package to process FE-data will be very advantageous.

There is also room open for search for the fatigue limits in repeated bending, which are missing for the majority of materials tested here. Since there is some reflection open on the strengths and downsides of three- and four-parameter methods, the elaboration of results in this way would be perfect.

8.4.2 FURTHER TESTING AND METHOD DEVELOPMENT

The results of the two criteria are nearly excellent in comparison to the existing methods. Nevertheless, I do not expect that the work is definitely done.

1) The CSM v. MD problem is still open.
2) The improvement of the "a" variants by the fatigue limit ratios proposed in the "c", "d" and "e" variants does not seem to be wholly legitimate, although their application reaches better results. In fact, e.g. the following integral criterion reaches nearly the same statistics of results as the PZa variant:

$$\sqrt{\frac{1}{4\pi}\int_{\varphi}\int_{\psi}\left[a\cdot C_a^2+b\cdot\left(N_a+0.5\cdot N_m\right)^2\right]\sin\psi d\psi d\varphi}\le f_{-1}. \tag{149}$$

   Any purist can say that this is not an undefiled proposal, although results are perfect. One can see that the mean stress effect of the quadrate has to be decreased, whereas the mean stress effect in the hybrid criterion had to be increased by the tuning parameter. Does the correct solution lies somewhere in between?
3) The ambiguity of the final form of the damage parameter referred above in 2) can be also ascribed to the fact that none of the versions is correct. The tested variants cover the space of possible combinations of normal and shear components very broadly. A question should be raised if the incorrectness does not lie in some other part of the calculation – above all in the way, how the shear stress is decomposed. The minimum circumscribed ellipse should be implemented and tested as first.
4) The problem of the PC criterion with the minimum damage found in the search for extreme, when the *a* and *b* parameters have to be set is still open. Further reconsideration, whether there

is not any other way to find the maximum damage for the condition of the fully reversed axial loading as well, has to continue.

8.4.3 WORK WITH LARGE DATA SETS

A group of 129 tests was examined here, which personates a complicacy for any further publishing. The more the test batch will broaden, the more this problem will snowball. It is very probable that a will of reviewers to publish such data e.g. in International Journal of Fatigue would be very limited. Anyway, I believe that presentation of all these data is necessary. When one looks back on data gathered and criteria presented elsewhere, the presented texts are too often erroneous, while any errata too scarce. The fact that e.g. Zenner et al. [89] produce a histogram with a nice prediction values without any description of used material constants necessary for its obtaining is then even more unfortunate, because their criterion is very sensitive as regards the material parameters. One cannot be sure if the authors have substantially better material parameters (then why they are not presented), or if the computation was burdened by some error.

The only way not to get stuck in the problem is to display a detailed presentation of experimental and result data on some web site and then reference it in any report where the data are processed. Thus any further work would become substantially more transparent. The web presentation would be much better accessible, would in fact enable and enhance any suggestions from users and would simplify also corrections of potential errors. One has to bear in mind as well, how many tests were published but I did not find them. This is the way how they could be made much better accessible. The gap between the possibilities given by global network and the community of fatigue researchers is objectively needlessly too wide here. We have an internet, but for what?

8.4.4 THE PRAGTIC PROJECT

The PragTic software is a perfect tool for any further research in the area covered here. Its extension towards the LCF region, or more specifically an integration of the complete stress – strain description together with methods of their linkage, would enhance its strength even more. Nevertheless, until now the development was a one man's work. Such a way is no longer acceptable.

There is open room for a new low-based scientific-oriented fatigue postprocessor. The majority of existing fatigue postprocessors are sophisticated and expensive tools, which do not offer many options to vary the calculation for any scientific purpose. They are aimed at common engineers who need fast answers to their tasks. When a researcher is interested, he can program his own procedures in e.g. Matlab or even in some more low-based programming tool. But the number of processed data is very large to be covered with such a method. If he wants to process them more quickly, the extent of the necessary work will magnify.

I consider a chance to continue this effort with the aim to create a fatigue solver that would allow the user to make the fatigue calculation with much bigger control over the subsequent steps, or even give the user an option to built his own damage parameters. The main targets of such project are the universities and research companies. Moreover, in my opinion, there are more engineering companies, which would be interested in the fatigue calculation, but the purchase price of common fatigue postprocessors, together with the maintenance costs is a mighty challenge to reflect it all over. The price of common fatigue postprocessors seems to be unnecessarily high – the software companies usually have to make profit. The purchase price is further increased by distributors to cover their expenses (and their profit). Big automotive companies need to use the final software on large and complicated structures. Since they are the main costumers buying this type of software, there is a substantial force applied by software producers into the speed up of computation procedures and FE-data upload. It is necessary, so that large computations could be run.

I have a vision of a small group of software workers (3-5) associated in a non-profit organisation with a basis at some university which provides for some necessary services. The university or better a science park is a natural environment for such an effort. The university concentrates students, which are perfect further potential part-time co-workers with not so high financial demands. As regards the university, the project could enlarge knowledge of fatigue and bring increase of university's prestige.

Opening of new and broad room for themes of diploma and dissertation theses and other projects would be interesting as well. The university often disposes of conference and teaching rooms and of qualified personnel as well that is able to teach courses or lead workshops. This part of the project can be even well profitable.

Funding of the project is questionable. The conception of free software is very convincing. There is no need to take care of the code's security. On the contrary, it often allows interacting with possible users and allows them to make comments, corrections or adaptation. In addition, it opens an option to utilize the software even in countries where the financing of a common fatigue solver could be problematic. Although there are many benefits, I remain a bit sceptical. The programmers have to earn their living. Unless there is prospect of a fund source for at least two years, the work is too nerve-wracking.

All the points given above forced me to take some steps. The project will be presented on the domain www.pragtic.com. At first, this PhD thesis, gathered experimental data, results of applied criteria and some main points concerning the project itself will be there. The second step is provision of further funding, which is not easy and leads beyond the framework of this thesis.

REFERENCES

[1] BENNEBACH, M.: Fatigue d'une fonte GS. Influence de l'entaille et d'un traitement de surface. [PhD thesis]. ENSAM CER Bordeaux 1993, p. 157.

[2] BANVILLET, A.; LAGODA, T.; MACHA, E.; NIESLONY, A.; PALIN-LUC, T.; VITTORI, J.-F.: Fatigue life under non-Gaussian random loading from various models. Int. J. Fatigue 26, 2004, pp. 349-363.

[3] BOLLER, C.: Der Einfluss von Probengrösse und Oberflächenrauhigkeit auf Lebensdaruerabschätzungen bei Betrachtung der örtlichen Beanspruchungen. Veröffentlichungen des Instituts für Stahlbau and Werkstoffmechanik der Technischen Hochschule Darmstadt, Heft 46. Darmstadt 1988, p. 160.

[4] BROWN, M. W.; MILLER, K. J.: A theory for fatigue under multiaxial stress-strain conditions. Proc. Inst. Mech. Engrs 187, 1973, pp. 745-755.

[5] BANVILLET, A.; PALIN-LUC, T.; LASSERRE, S.: A volumetric energy based high cycle multiaxial fatigue criterion. Int. J. Fatigue 25, 2003, pp. 755-769.

[6] BALDA, M.; RŮŽIČKA, M.; SVOBODA, J.; PAPUGA, J.; FRÖHLICH, V.: Vliv náhodného víceosého neproporcionálního namáhání na únavovou životnost strojních konstrukcí. [Research Report Z-1353/04]. Czech Academy of Science, Institute of Thermomechanics 2004.

[7] BANNANTINE, J. A.; SOCIE, D. F.: A multiaxial fatigue life estimation technique. In: Advances in Fatigue Lifetime Predictive Techniques, ASTM STP 1122. Eds: M. R. Mitchell a R. W. Landgraf. Philadelphia, American Society for Testing and Materials 1992, pp. 249-275.

[8] BERNASCONI, A.: Efficient algorithms for calculation of shear stress amplitude and amplitude of the second invariant of the stress deviator in fatigue criteria applications. Int. J. Fatigue 24, 2002, pp. 649-657.

[9] BROWN, M. W.; SUKER, D. K.; WANG, C. H.: An analysis of mean stress in multiaxial random fatigue. Fatigue Fract. Engng. Mater. Struct. 19, 1996, No. 2/3, pp. 323-333.

[10] CARPINTERI, A.; BRIGHENTI, R.; MACHA, E.; SPAGNOLI, A.: Expected principal stress directions under multiaxial random loading. Part II: numerical simulation and experimental assessment through the weight function method. Int. J. Fatigue 21, 1999, pp. 89-96.

[11] CARPINTERI, A.; MACHA, E.; BRIGHENTI, R.; SPAGNOLI, A.: Expected principal stress directions under multiaxial random loading. Part I: theoretical aspects of the weight function method. Int. J. Fatigue 21, 1999, pp. 83-88.

[12] CROSSLAND, B.: Effect of large hydrostatic pressure on the torsional fatigue strength of an alloy steel. In: Proc. Int. Conf. on Fatigue of Metals, Institution of Mechanical Engineers, London, 1956, pp. 138-149.

[13] CARPINTERI, A.; SPAGNOLI, A.: Multiaxial high-cycle fatigue criterion for hard metals. Int. J. Fatigue 23, 2001, pp. 135-145.

[14] DAVOLI, P.; BERNASCONI, A.; FILIPPINI, M.; FOLETTI, S.; PAPADOPOULOS, I. V.: Independance of the torsional fatigue limit upon a mean shear stress. Int. J. Fatigue 23, 2003, pp. 471-480.

[15] DELAHAY, T.: Développemenent d'une méthode probabiliste de calcul en fatigue multiaxiale prenant en compte la répartition volumique des contraintes. [PhD thesis], ENSAM CER de Bordeaux 2004.

[16] DOWLING, N. E.: Mean Stress Effects in Stress-Life and Strain-Life Fatigue. SAE Paper No. 2004-01-2227, Fatigue 2004: Second SAE Brasil International Conference on Fatigue, São Paulo, Brasil, June 2004, 14 pages.

[17] DANG VAN, K.: Sur la résistance a la fatigue des métaux. These de Doctorat es Sciences, Sci. Techniq. l´Armement, 47, 1973, p. 647.

[18] DANG VAN, K., CAILLETAUD, G.; FLAVENOT, J. F.; DOUARON, L.; LIEURADE, H. P.: Criterion for high-cycle failure under multiaxial loading. In: Biaxial and Multiaxial Fatigue. Eds: M. Brown and K. Miller, Sheffield, 1989, pp. 459-478.

[19] ELLYIN, F.; XIA, Z.: A general fatigue theory and its applications to out-of-phase cyclic loading. Journal of Engng. Mater. Technol., Transactions of the ASME, 115, 1993, pp. 411-416.

[20] ELLYIN, F.: Fatigue Damage, Crack Growth and Life Prediction. Chapman & Hall 1997.

[21] FINDLEY, W. N.: Fatigue of Metals Under Combinations of Stresses, Transactions of ASME (vol. 79), 1957.

[22] FROUSTEY, C.; LASSERRE, S.: Multiaxial fatigue endurance of 30NCD16 steel. Int. J. Fatigue 11, 1989, No. 3, pp.169-175.

[23] FROUSTEY, C.; LASSERRE, S.; DUBAR, L.: Validité des critéres de fatigue multiaxiale a l'endurance en flexion-torsion. In: Fatigue des structures industrielles. 40 promenade Marx-Dormoy, F-93460 Gournay-sur-Marne, France, IITT International 1989, pp. 126-138.

[24] FROUSTEY, C.: Fatigue multiaxiale en endurance de l'acier 30NCD16. [PhD thesis]. ENSAM CER de Bordeaux 1987.

[25] FATEMI, A.; SOCIE, D. F.: A critical plane approach to multiaxial fatigue damage including out-of-phase loading. Fatigue Fract. Engng. Mater. Struct., 11, 1988, No. 3, pp. 149-165.

[26] GALTIER, A.: Contribution a l'étude de l'endommagement des aciers sous solicitations uni ou multiaxials. [PhD thesis]. ENSAM CER de Bordeaux 1993, p. 193.

[27] GONÇALVES, C. A.; ARAÚJO, J. A.; MAMIYA, E. N.: Multiaxial fatigue: a stress based criterion for hard metals. Int. J. Fatigue 27, 2005, pp. 177-187.

[28] GAIER, C.; LUKACS, A.; HOFWIMMER, K.: Investigation on a statistical measure of the non-proportionality of stresses. Int. J. Fatigue 26, 2004, pp. 331-337.

[29] GOUGH, H. J.: Engineering Steels Under Combined Cyclic and Static Stresses. Journal of Applied Mechanics, June 1950, pp. 113-125.

[30] GOUGH, H. J.; POLLARD, H. V.; CLENSHAW, W. J.: Some Experiments on the Resistance of Metals to Fatigue under Combined Stresses. London, His Majesty's Stationery Office 1951.

[31] HAN, C.; CHEN, X.; KIM, K.: Evaluation of multiaxial fatigue criteria under irregular loading. Int. J. Fatigue, Vol. 24, 2002, pp. 913-922.

[32] M. HOFFMANN; T. SEEGER: A Generalized Method for Estimating Multiaxial Elastic-Plastic Notch Stresses and Strains, Part I & II. . J. of Engng. Mater. & Technology, Vol. 107, 1985, pp. 250-260.

[33] ILYUSHIN; A. A.: Plasticity Foundations of General Mathematical Theory, Akad. Nauk, Moscow, 1963, p. 16.

[34] KENMEUGNE, J. L.; VIDAL-SALLE, E.; ROBERT, J. L.; BAHUAUD, R. J.: On a new multiaxial fatigue criterion based on a selective integration approach. In: Fatigue '96, Proc. of the Sixth Int. Fatigue Congress, Vol. II. Red. G. Lütjering, Berlin, Pergamon 1996, pp. 1013-1018.

[35] KIM, K.; PARK, J.: Shear strain based multiaxial fatigue parameters applied to variable amplitude loading. Int. J. of Fatigue, Vol. 21, 1999, pp. 475-483.

[36] KIM, K.; PARK, J.; LEE, J.: Multiaxial fatigue under variable amplitude loads. J. of Engng. Mater. Tech., Transactions of the ASME, 121, 1999, pp. 286-293.

[37] LASSERRE, S.; FROUSTEY, C.: Multiaxial fatigue of steel – testing out of phase and in blocks: validity and applicability of some criteria. Int. J. Fatigue 14, No. 2, 1992. pp. 113-120.

[38] LIU, J.; ZENNER, H.: Berechnung der Dauerschwingfestigkeit bei mehrachsiger Beanspruchung. Mat. Wiss und Werkstofftech 24(S), 1993, pp. 240–249.

[39] MAMIYA, E. N.; ARAÚJO, J. A.: Fatigue limit under multiaxial loadings: on the definition of the equivalent shear stress. Mechanics Research Communications 29, 2002, pp. 141-151.

[40] MOFTAKHAR, A.; BUCZYNSKI, A.; GLINKA, G.: Calculation of elasto-plastic strains and stresses in notches under multiaxial loading. Int. J. of Fracture, Vol. 70, 1995, pp. 357-373.

[41] MCDIARMID, D. L.: Fatigue under out-of-phase bending and torsion. Fatigue Fract. Engng. Mater. Struct., 9, 1987, pp. 457-475.

[42] MCDIARMID, D. L.: A general criterion for high cycle multiaxial fatigue failure. Fatigue Fract. Engng. Mater. Struct., 14, 1991, No. 4, pp. 429-453.

[43] MCDIARMID, D. L.: A shear stress based critical-plane criterion of multiaxial fatigue failure for design and life prediction. Fatigue Fract. Engng. Mater. Struct 17, 1994, No. 12, pp. 1475-1484.

[44] MOREL, F.: A fatigue life prediction method based on a mesoscopic approach in constant amplitude multiaxial loading. Fatigue Fract. Engng. Mater. Struct 21, 1998, No. 3, pp. 241-256.

[45] MOREL, F.: A critical plane approach for life prediction of high cycle fatigue under multiaxial variable amplitude loading. Int. J. Fat., 22, 2000, pp. 101-119.

[46] MOREL, F.; PALIN-LUC, T.: A non-local theory applied to high cycle multiaxial fatigue. Fatigue Fract. Engng. Mater. Struct. 25, 2002, pp. 649-665.

[47] NISHIHARA, T.; KAWAMOTO, M.: The strength of metals under combined alternating bending and torsion with phase difference. Mem. College Engng., Kyoto Imperial University 11, 1945, pp. 85-112.

[48] PALIN-LUC, T.: Fatigue multiaxiale d'une fonte GS sous solicitations combinées d'amplitude variable. [PhD thesis]. ENSAM CER de Bordeaux 1996, p. 261.

[49] PAPADOPOULOS, I. V.: Fatigue polycyclique des métaux: Une nouvelle approche. [PhD thesis], Paris, École Nationale des Ponts et Chaussées 1987.

[50] PAPADOPOULOS, I. V. Fatigue limit of metals under multiaxial stress conditions: the microscopic approach. Technical note no. I.93.101. Commission of the European Communities, Joint Research Centre, ISEI/IE 2495/93, 1993.

[51] PAPADOPOULOS, I. V.: A new criterion of fatigue strength for out-of-phase bending and torsion of hard metals. Int. J. Fatigue 16, 1994, pp. 377-384.

[52] PAPADOPOULOS, I. V.; DAVOLI, P.; GORLA, C.; FILIPPINI, M.; BERNASCONI, A.: A comparative study of multiaxial high-cycle fatigue criteria for metals. Int. J. Fatigue 19, 1997, No. 3, pp. 219-235.

[53] PAPADOPOULOS, I. V.: Critical plane approaches in high-cycle fatigue: On the definition of the amplitude and mean value of the shear stress acting on the critical plane. Fatigue Fract. Engng. Mater. Struct. 21, 1998, No. 3, pp. 269-285.

[54] PARK, J.; NELSON, D.: Evaluation of energy-based approach and a critical plane approach for predicting constant amplitude multiaxial fatigue life. Int. J. Fatigue 22, 2000, pp. 23-39.

[55] PAPUGA, J.: Program module for fatigue damage calculation. [Diploma thesis], Prague, CTU in Prague 1998. *(in Czech).*

[56] PAPUGA, J.; RŮŽIČKA, M.: Constitutive Equations in Elasto-Plastic Solution. [Research Report 2051/00/26]. CTU in Prague 2000. *(in Czech)*

[57] PAPUGA, J.; RŮŽIČKA, M.; ŠPANIEL, M.: Software solution of fatigue damaging based on the FE-analysis results utilization. In: Abstracts of Conf. Numerical Methods in Continuum Mechanics, University of Žilina 2000, pp. 138-140.

[58] PAPUGA, J.; RŮŽIČKA, M.: Software development aimed to fatigue damage computing in cases of complicated loading combinations and its experimental verification. In: CTU Reports – Proc. of Workshop 2001, Part A. Prague, CTU in Prague 2001, pp. 508-509.

[59] PAPUGA, J.; RŮŽIČKA, M.: Uniaxial and Multiaxial Methods of Fatigue Life Solution with Respect to Its Algorithmization Process. In: Proc. of Computational Mechanics 2001 – Part II. Plzeň, ZČU v Plzni 2001. *(in Czech)*

[60] PAPUGA, J.; RŮŽIČKA, M.; BALDA, M.: Metody multiaxiální analýzy únavové životnosti. In: Proc. of Únava a lomová mechanika 2002 - Metodické a aplikační problémy, Part I. Plzeň: Škoda Výzkum, 2002, pp. 1-26. *(in Czech)*

[61] PAPUGA, J.; RŮŽIČKA, M.; ŠIMEK, D.: Analýza únavového poškození na virtuálním prototypu - přechod k multiaxiálnímu řešení. In: Proc. of Applied Mechanics 2002. Ostrava, VŠB-TUO 2002, pp. 273-280. *(in Czech)*

[62] PAPUGA, J.; ŠIMEK, D.; ŠPANIEL, M.; RŮŽIČKA, M.: Software MAXA - rozvaha projektu. In: Summer Workshop of Applied Mechanics. Prague, CTU in Prague 2002, pp. 175-193. *(in Czech)*

[63] PAPUGA, J.; MICHALEC, J.; RŮŽIČKA, M.: Software Development for Fatigue Damage Analysis and Visualisation of Results. [Research Report 2051/02/1]. Prague, CTU in Prague 2002. *(in Czech)*

[64] PAPUGA, J.; ŠPANIEL, M.; RŮŽIČKA, M.: Datová struktura pro následnou analýzu MKP řešení. In: Proc. of Computational Mechanics 2002, Part 1. Plzeň, ZČU 2002, pp. 333-340. *(in Czech)*

[65] PAPUGA, J.; RŮŽIČKA, M.: In Time Loading History Processing Performed by RainIT Program. [Research Report 2051/02/33]. Prague, CTU in Prague 2002. *(in Czech)*

[66] PAPUGA, J.; RŮŽIČKA, M.: Použití MKP modelů pro únavovou analýzu poškozování. In: Proc. of Degradation of Structural Materials. Žilina, EDIS 2003, pp. 7-12. *(in Czech)*

[67] RŮŽIČKA, M.; CABRNOCH, B.; PAPUGA, J.: Metody a programy pro hodnocení únavové životnosti. [Research Report 211–98–10]. Prague, CTU in Prague 1998. *(in Czech)*

[68] REIS, L; LI, B.; DE FREITAS, M.: Biaxial fatigue for proportional and non-proportional loading paths. Fatigue Fract Engng Mater Struct 27, 2004, pp. 775-784.

[69] RŮŽIČKA, M.; PAPUGA, J.: Postupy predikce životnosti při uniaxiální a multiaxiální únavě materiálu. [Research Report 211–98–12]. Prague, CTU in Prague, 1998. *(in Czech)*

[70] RŮŽIČKA, M.; PAPUGA, J.: Fatigue Life Evaluation of Components under Multiaxial Loading. [Research Report 205/99/25] Prague, CTU in Prague 1999. *(in Czech)*.

[71] RŮŽIČKA, M.; PAPUGA, J.: Metody pro hodnocení únavové životnosti. [Research Report 2051/99/32]. In: CD ROM z 16.setkání uživatelů COSMOS/M. Tech Soft Eng., CTU in Prague 1999. *(in Czech)*

[72] RŮŽIČKA, M.; PAPUGA, J.: Posouzení uniaxiálních a multiaxiálních metod predikce životnosti. In: Proc. of Applied Mechanics 2000. Liberec, TU Liberec 2000. pp. 331-336. *(in Czech)*

[73] RŮŽIČKA, M.; PAPUGA, J.: Diskuse problematiky poškozování při multiaxiálním zatěžování. In: Proc. of Conf. Únava materiálů a konstrukcí 2000, Žinkovy 16. - 18. květen 2000. Mechanická zkušebna a pobočka ČVTS & Škoda Výzkum s.r.o., Plzeň 2000. *(in Czech)*

[74] RŮŽIČKA, M.; PAPUGA, J.; KULIŠ, Z.: Predikce únavové životnosti lokálními přístupy. In: Proc. of Workshop 2000, Prague, CTU in Prague 2000, p. 433.

[75] RŮŽIČKA, M.; PAPUGA, J.: Algorithmization of Approaches for Fatigue Damage Calculation. [Research Report 2051/00/27]. CTU in Prague 2000. *(in Czech)*

[76] PAPUGA, J.; RŮŽIČKA, M.; BALDA, M.; SVOBODA, J.: Several high-cycle fatigue multiaxial criteria compared with experimental results. Proc. of 21st Danubia-Adria Symposium on Experimental Methods in Solid Mechanics. Zagreb, Croatian Society of Mechanics 2004, pp. 286-287.

[77] RŮŽIČKA, M.; PAPUGA, J.; BALDA, M.; SVOBODA, J.: Data Processing Line for Multiaxial Fatigue Computation and its Experimental Verification. In: Proc. of AED 2004 [CD-ROM]. Prague, Orgit 2004.

[78] M. N. K. SINGH; G. GLINKA; R. N. DUBEY: Elastic-plastic stress-strain calculation in notched bodies subjected to non-proportional loading. Vol. 76, 1996, pp. 39-60.

[79] SINES, G.: Failure of materials under combined repeated stresses with superimposed static stresses. [NACA-TN-3495]. Washington, NACA 1955.

[80] SINES, G.: Behavior of metals under complex static and alternating stresses. In: Metal Fatigue. Red. G. Sines a J.L. Waisman, New York, McGraw Hill 1959, pp. 145-469.

[81] SOCIE, D. F.: Critical plane approaches for multiaxial fatigue damage assessment. In: Advances in Multiaxial Fatigue, ASTM STP 1191. Red. D. L. Dowell a R. Ellis, Philadelphia, American Society for Testing and Materials 1993, pp. 7-36.

[82] SPAGNOLI, A.: A new high-cycle fatigue criterion applied to out-of-phase biaxial stress state. International Journal of Mechanical Sciences 43, 2001, pp. 2581-2595.

[83] STEFANOV, S. H.: The curvilinear integral method: Testing 2 (under non-proportional pulsating axial force and internal pressure). Int. Journal of Fatigue, 18, 1996, No. 1, pp. 41-48.

[84] VIDAL-SALLÉ, E.; KENMEUGNE, B.; ROBERT, J. L.; BAHUAUD, J.: On a new multiaxial fatigue criterion based on a selective integration approach. In: Fatigue '96, Proc. of the Sixth Int. Fatigue Congress, Vol. II. Red. G. Lütjering, Berlin, Pergamon 1996, pp. 983-988.

[85] WANG, C. H.; BROWN, M. W.: A path-independent parametr for fatigue under proportional and nonproportional loading. Fatigue Fract. Engng. Mater. Struct., 16, 1993, No. 12, pp. 1285-1298.

[86] WANG, C. H.; BROWN, M. W.: Life prediction techniques for variable amplitude multiaxial fatigue-Part 1: Theories, Part 2: Comparison with experimental results. J. of Engng. Mater. Tech., Transactions of the ASME, 118, 1996, pp. 367-374.

[87] XIA, Z.; KUJAWSKI, D.; ELLYIN, F.: Effect of mean stress and ratchetting strain on fatigue life of steel. Int. Journal of Fatigue, 18, 1996, No. 5, pp. 335-341.

[88] ZENNER, H.; HEIDENREICH, R.; RICHTER, I. Z.: Fatigue strength under nonsynchronous multiaxial stresses, Mat. Wiss und Werkstofftech 16, 1985, p. 101-112.

[89] ZENNER, H.; SIMBÜRGER, A.; LIU, J.: On the fatigue limit of ductile metals under complex multiaxial loading. Int. Journal of Fatigue 22, 2000, pp. 137-145.

LIST OF CANDIDATE'S WORK RELATING TO THE DISSERTATION

- PAPUGA, J.: Program module for fatigue damage calculation. [Diploma thesis], Prague, CTU in Prague 1998. *(in Czech)*
- RŮŽIČKA, M.; CABRNOCH, B.; PAPUGA, J.: Metody a programy pro hodnocení únavové životnosti. [Research Report 211–98–10]. Prague, CTU in Prague 1998. *(in Czech)*
- RŮŽIČKA, M.; PAPUGA, J.: Postupy predikce životnosti při uniaxiální a multiaxiální únavě materiálu. [Research Report 211–98–12]. Prague, CTU in Prague, 1998. *(in Czech)*
- RŮŽIČKA, M.; PAPUGA, J.: Fatigue Life Evaluation of Components under Multiaxial Loading. [Research Report 205/99/25] Prague, CTU in Prague 1999. *(in Czech)*
- RŮŽIČKA, M.; PAPUGA, J.: Metody pro hodnocení únavové životnosti. [Research Report 2051/99/32]. In: CD ROM z 16.setkání uživatelů COSMOS/M. Tech Soft Eng., CTU in Prague 1999. *(in Czech)*
- RŮŽIČKA, M.; PAPUGA, J.: Posouzení uniaxiálních a multiaxiálních metod predikce životnosti. In: Proc. of Applied Mechanics 2000. Liberec, TU Liberec 2000. pp. 331-336. *(in Czech)*
- PAPUGA, J.; RŮŽIČKA, M.; ŠPANIEL, M.: Software solution of fatigue damaging based on the FE-analysis results utilization. In: Abstracts of Conf. Numerical Methods in Continuum Mechanics, University of Žilina 2000, pp. 138-140.
- RŮŽIČKA, M.; PAPUGA, J.: Diskuse problematiky poškozování při multiaxiálním zatěžování. In: Proc. of Conf. Únava materiálů a konstrukcí 2000, Žinkovy 16. - 18. květen 2000. Mechanická zkušebna a pobočka ČVTS & Škoda Výzkum s.r.o., Plzeň 2000. *(in Czech)*
- RŮŽIČKA, M.; PAPUGA, J.: Přístupy a kritéria pro predikci únavové pevnosti při kombinovaném víceosém namáhání. In: Proc. of Conf. Únava materiálů a konstrukcí 2000, Plzeň, Mechanická zkušebna & Škoda Výzkum s.r.o. 2000, pp. 1-15. *(in Czech)*
- RŮŽIČKA, M.; PAPUGA, J.; KULIŠ, Z.: Predikce únavové životnosti lokálními přístupy. In: Proc. of Workshop 2000, Prague, CTU in Prague 2000, p. 433.
- PAPUGA, J.; RŮŽIČKA, M.: Constitutive Equations in Elasto-Plastic Solution. [Research Report 2051/00/26]. CTU in Prague 2000. *(in Czech)*
- RŮŽIČKA, M.; PAPUGA, J.: Algorithmization of Approaches for Fatigue Damage Calculation. [Research Report 2051/00/27]. CTU in Prague 2000. *(in Czech)*
- PAPUGA, J.; RŮŽIČKA, M.: Software development aimed to fatigue damage computing in cases of complicated loading combinations and its experimental verification. In: CTU Reports – Proc. of Workshop 2001, Part A. Prague, CTU in Prague 2001, pp. 508-509.
- PAPUGA, J.; RŮŽIČKA, M.: Uniaxial and Multiaxial Methods of Fatigue Life Solution with Respect to Its Algorithmization Process. In: Proc. of Computational Mechanics 2001 – Part II. Plzeň, ZČU v Plzni 2001. *(in Czech)*
- PAPUGA, J.; RŮŽIČKA, M.; ŠIMEK, D.: Analýza únavového poškození na virtuálním prototypu - přechod k multiaxiálnímu řešení. In: Proc. of Applied Mechanics 2002. Ostrava, VŠB-TUO 2002, pp. 273-280. *(in Czech)*
- PAPUGA, J.; RŮŽIČKA, M.; BALDA, M.: Metody multiaxiální analýzy únavové životnosti. In: Proc. of Únava a lomová mechanika 2002 - Metodické a aplikační problémy, Part I. Plzeň: Škoda Výzkum, 2002, pp. 1-26. *(in Czech)*
- PAPUGA, J.; ŠIMEK, D.; ŠPANIEL, M.; RŮŽIČKA, M.: Software MAXA - rozvaha projektu. In: Summer Workshop of Applied Mechanics. Prague, CTU in Prague 2002, pp. 175-193. *(in Czech)*
- PAPUGA, J.; ŠPANIEL, M.; RŮŽIČKA, M.: Datová struktura pro následnou analýzu MKP řešení. In: Proc. of Computational Mechanics 2002, Part 1. Plzeň, ZČU 2002, pp. 333-340. *(in Czech)*

- PAPUGA, J.; MICHALEC, J.; RŮŽIČKA, M.: Software Development for Fatigue Damage Analysis and Visualisation of Results. [Research Report 2051/02/1]. Prague, CTU in Prague 2002. *(in Czech)*
- PAPUGA, J.; RŮŽIČKA, M.: In Time Loading History Processing Performed by RainIT Program. [Research Report 2051/02/33]. Prague, CTU in Prague 2002. *(in Czech)*
- PAPUGA, J.; RŮŽIČKA, M.: Použití MKP modelů pro únavovou analýzu poškozování. In: Proc. of Degradation of Structural Materials. Žilina, EDIS 2003, pp. 7-12. *(in Czech)*
- RŮŽIČKA, M.; PAPUGA, J.; BALDA, M.; SVOBODA, J.: Data Processing Line for Multiaxial Fatigue Computation and its Experimental Verification. In: Proc. of AED 2004 [CD-ROM]. Prague, Orgit 2004.
- PAPUGA, J.; RŮŽIČKA, M.; BALDA, M.; SVOBODA, J.: Several high-cycle fatigue multiaxial criteria compared with experimental results. In: Proc. of 21st Danubia-Adria Symposium on Experimental Methods in Solid Mechanics. Zagreb, Croatian Society of Mechanics 2004, pp. 286-287.
- BALDA, M.; RŮŽIČKA, M.; SVOBODA, J.; PAPUGA, J.; FRÖHLICH, V.: Vliv náhodného víceosého neproporcionálního namáhání na únavovou životnost strojních konstrukcí. [Research Report Z-1353/04]. Czech Academy of Science, Institute of Thermomechanics 2004.

APPENDIX I ΔFI RESULTS OF EXISTING CRITERIA

The numerical values in the following tables represent directly ΔFI results or their statistical evaluation. All are expressed in %.

HARD STEEL

case	loaded	Sines	Cross	Ppd	FCS	KCP	KIA	McD	DV	Matake	Z&L	SpaM	SpaC	GAM
CS2	PB+To	-3.7	3.8	3.8	4.6	4.6	3.4	-3.4	4.6	4.8	3.4	5.7	1.2	3.9
CS3	PB+To	-0.7	5.5	5.5	8.2	8.2	4.1	0.2	8.2	8.6	4.1	5.6	3.1	5.8
CS4	PB+To	-3.2	0.2	0.2	3.5	3.5	-1.7	0.4	3.5	3.5	-1.7	-1.2	-1.5	0.6
CS6	PB+To	-4.0	2.2	5.5	6.9	6.9	3.2	-0.2	4.9	7.6	2.7	5.1	2.1	5.2
CS7	PB+To	-5.2	-1.7	0.2	3.3	3.3	-2.2	-0.1	2.0	4.5	-2.8	-1.4	-1.8	0.0
CS8	PB+To	-13.6	-7.4	5.5	2.5	2.5	1.2	-6.6	-4.2	3.4	-0.1	4.5	-0.6	3.9
CS9	PB+To	-6.4	-2.9	3.9	6.6	6.6	0.0	1.9	2.1	9.2	-1.3	1.9	1.3	2.3
CS10	PB+To	-9.4	-1.9	3.8	1.7	1.7	6.6	-9.0	-1.9	1.4	5.7	9.2	6.4	8.6
CS11	PB+To	-22.0	-15.6	9.5	-0.9	-0.9	3.5	-13.7	-15.6	1.2	2.0	8.1	3.1	6.7
CS12	PB+To	-6.1	-2.4	7.8	10.3	10.3	2.8	4.7	3.6	13.3	1.1	5.7	4.9	4.0
average		-7.4	-2.0	4.6	4.7	4.7	2.1	-2.6	0.7	5.7	1.3	4.3	1.8	4.1
range		21.3	21.1	9.3	11.2	11.2	8.8	18.4	23.8	12.1	8.5	10.5	8.2	8.6
st. deviation		5.9	5.7	2.8	3.2	3.2	2.6	5.3	6.4	3.6	2.6	3.3	2.5	2.5

MILD STEEL

case	loaded	Sines	Cross	Ppd	FCS	KCP	KIA	McD	DV	Matake	Z&L	SpaM	SpaC	GAM
CS14	PB+To	5.3	6.3	6.3	7.2	7.2	6.2	5.1	7.2	7.2	6.2	11.5	5.9	6.3
CS15	PB+To	4.2	5.0	5.0	7.8	7.8	4.8	5.9	7.8	8.1	4.8	8.2	4.7	5.0
CS16	PB+To	-1.3	-0.8	-0.8	2.6	2.6	-1.1	-0.7	2.6	2.6	-1.1	0.0	-1.0	-0.8
CS18	PB+To	-6.0	-5.1	8.9	3.5	3.5	3.5	0.9	-1.7	3.8	3.3	9.9	3.2	8.6
CS19	PB+To	-1.0	-0.5	6.6	8.4	8.4	2.6	7.4	4.7	9.7	2.4	6.5	4.6	6.3
CS20	PB+To	-0.9	0.1	6.3	1.1	1.1	3.9	-1.3	0.1	1.1	3.8	8.8	7.1	6.2
CS21	PB+To	-12.5	-11.6	16.7	0.0	0.0	8.6	-4.1	-11.6	1.1	8.4	16.5	11.0	16.3
CS22	PB+To	-0.9	-0.5	10.3	11.3	11.3	4.6	9.9	5.9	12.7	4.4	10.0	7.8	9.8
average		-1.6	-0.9	7.4	5.2	5.2	4.2	2.9	1.9	5.8	4.0	8.9	5.4	7.2
range		17.8	17.9	17.5	11.3	11.3	9.7	14.0	19.4	11.7	9.5	16.5	12.0	17.1
st. deviation		5.2	5.2	4.7	3.7	3.8	2.6	4.6	6.0	4.0	2.6	4.4	3.3	4.5

HARD STEEL

case	loaded	Sines	Cross	Ppd	FCS	KCP	KIA	McD	DV	Matake	Z&L	SpaM	SpaC	GAM
PNK01	PB+To	-5.6	-2.3	-2.3	1.0	1.0	-4.1	-1.9	1.0	1.0	-4.1	-3.6	-4.0	-1.9
PNK02	PB+To	-6.0	-2.5	-0.6	2.5	2.5	-3.0	-1.9	1.1	3.6	-3.6	-2.2	-2.6	-0.8
PNK03	PB+To	-7.1	-3.6	3.1	5.8	5.8	-0.7	1.5	1.3	8.3	-2.1	1.1	0.5	1.5
PNK04	PB+To	-7.4	-3.7	6.3	8.8	8.8	1.3	3.7	2.2	11.8	-0.3	4.2	3.4	2.5
PNK05	PB+To	-4.5	1.5	1.5	4.0	4.0	0.1	-1.8	4.0	4.0	0.1	1.6	-0.8	1.7
PNK06	PB+To	-6.0	0.0	3.3	4.7	4.7	1.1	-1.9	2.7	5.4	0.5	2.9	-0.1	3.0
PNK07	PB+To	-14.5	-8.3	4.4	1.5	1.5	0.1	-7.0	-5.2	2.3	-1.1	3.4	-1.6	2.8
PNK08	PB+To	-24.1	-17.8	6.7	-3.5	-3.5	0.9	-15.3	-17.8	-1.4	-0.6	5.3	0.5	3.9
PNK09	PB+To	-6.3	0.9	0.9	1.7	1.7	0.5	-5.5	1.7	1.7	0.5	2.8	-1.6	1.0
PNK10	PB+To	-10.4	-3.0	2.7	-1.3	-1.3	1.0	-9.6	-3.0	-1.6	0.5	3.0	1.1	2.1
average		-9.2	-3.9	2.6	2.5	2.5	-0.3	-4.0	-1.2	3.5	-1.0	1.8	-0.5	1.6
range		19.6	19.3	9.0	12.3	12.3	5.5	18.9	21.8	13.3	4.7	8.9	7.4	5.9
st. deviation		5.7	5.3	2.7	3.3	3.3	1.8	5.3	6.1	3.9	1.6	2.6	2.0	1.7

42CRMO4

case	loaded	Sines	Cross	Ppd	FCS	KCP	KIA	McD	DV	Matake	Z&L	SpaM	SpaC	GAM
PL01	PB+To	-5.4	4.2	4.2	6.7	6.7	2.2	-4.0	6.7	6.7	2.2	2.9	0.7	4.6
PL02	PB+To	-36.5	-28.1	-9.1	-16.1	-16.1	-13.3	-33.3	-28.1	-13.6	-15.0	-10.9	-14.9	-12.5
PL03	PB+To	0.5	7.3	7.3	10.8	10.8	4.2	2.9	10.8	11.1	4.2	4.5	4.1	7.9
PL04	PB+To	-21.2	-14.9	-1.8	0.2	0.2	-7.2	-10.8	-8.6	4.0	-9.4	-4.7	-6.4	-8.0
PL05	PB+To	-23.1	-15.3	-15.3	0.5	-1.6	-11.1	-16.8	-13.3	-2.4	-9.8	-4.9	-16.4	-7.8
PL06	PB+To	-37.2	-28.9	-10.0	-6.2	-8.3	-8.6	-28.4	-28.9	-6.9	-10.0	-6.7	-12.2	-8.0
PL07	PB+To	-3.8	5.9	5.9	18.8	17.1	8.6	2.6	8.4	22.0	9.7	8.9	1.2	1.9
PL08	PB+To	8.8	-2.9	-2.9	22.4	17.7	6.2	-5.8	7.5	18.8	5.2	12.8	1.9	7.0
PL09	PB+To	-12.7	-24.0	-5.9	11.5	6.8	0.8	-23.6	-15.9	13.9	-2.6	8.5	-0.2	1.6
average		-14.5	-10.8	-3.1	5.4	3.7	-2.0	-13.0	-6.8	5.9	-2.8	1.2	-4.7	-1.5
range		46.0	36.2	22.6	38.5	33.9	22.0	36.3	39.7	35.6	24.7	23.7	20.5	20.5
st. deviation		15.2	13.9	7.3	11.5	10.7	7.6	12.5	14.9	11.2	8.1	7.8	7.5	7.2

34CR4

case	loaded	Sines	Cross	Ppd	FCS	KCP	KIA	McD	DV	Matake	Z&L	SpaM	SpaC	GAM
PZ01	PB+To	-6.3	-0.5	-0.5	2.0	2.0	-1.9	-3.2	2.0	2.0	-1.9	-0.4	-2.7	-0.3
PZ02	PB+To	-18.1	-12.3	-0.1	-2.9	-2.9	-4.2	-9.3	-9.3	-2.2	-5.4	-1.1	-5.9	-1.6
PZ03	PB+To	-28.7	-22.9	0.1	-9.5	-9.5	-5.4	-18.4	-22.9	-7.6	-6.8	-1.3	-5.8	-2.5
PZ04	PB+To	-18.1	-12.3	-0.1	-2.9	-2.9	-4.2	-9.3	-9.3	-2.2	-5.4	-1.1	-6.8	-1.6
PZ05	PB+To	-12.5	-8.4	5.2	6.5	6.5	-0.7	1.6	-1.6	9.3	-2.5	3.2	0.0	1.0
PZ06	PB+To	-14.3	-7.3	0.4	-5.0	-5.0	-1.9	-11.5	-7.3	-5.1	-2.5	0.1	-1.8	-0.5
PZ07	PB+To	-5.7	0.1	0.1	16.2	20.7	7.9	6.6	2.6	13.5	14.2	12.8	0.3	6.0
PZ08	PB+To	-18.5	-12.7	-0.5	3.7	8.5	4.1	-6.1	-9.7	0.2	7.5	5.1	-1.6	3.3
PZ09	PB+To	-29.0	-23.2	-0.1	-0.6	3.8	2.8	-12.7	-23.0	-1.7	4.5	3.9	-2.1	1.4
PZ10	PB+To	13.4	-6.4	-6.4	16.3	24.7	11.1	3.0	4.3	13.9	10.6	11.0	-0.1	-0.2
PZ11	PB+To	-5.3	-25.5	-4.8	8.9	17.9	9.7	-8.8	-16.9	10.7	8.0	12.6	2.3	0.0
PZ12	PB+To	-12.7	-6.2	-6.2	11.8	17.3	3.6	0.5	-5.2	10.2	8.3	10.6	-4.7	-0.8
PZ13	PB+To	5.7	-9.4	3.4	21.4	28.1	11.5	9.5	3.4	24.0	6.6	10.5	4.3	3.4
PZ14	PB+To	0.8	3.2	7.3	10.1	10.1	4.5	8.9	7.0	13.3	3.4	5.6	5.5	4.8
average		-10.7	-10.3	-0.2	5.4	8.5	2.6	-3.5	-6.1	5.6	2.8	5.1	-1.4	0.9
range		42.4	28.7	13.6	30.9	37.6	17.0	27.9	30.0	31.6	21.0	14.1	12.3	8.5
st. deviation		11.7	8.5	3.7	8.8	11.3	5.6	8.4	9.5	8.9	6.5	5.2	3.6	2.5

30NCD16 – [52], [22]

case	loaded	Sines	Cross	Ppd	FCS	KCP	KIA	McD	DV	Matake	Z&L	SpaM	SpaC	GAM
PF01	PB+To	-3.4	1.8	1.8	4.7	4.7	0.3	2.2	4.7	4.7	0.3	1.8	-0.3	2.1
PF02	PB+To	-32.4	-27.3	0.7	-6.1	-6.1	-5.5	-11.7	-18.2	-4.1	-7.0	-0.7	-5.9	-2.2
PF03	PB+To	14.2	3.9	3.9	20.4	24.9	13.7	13.2	12.5	19.2	13.5	14.7	3.9	7.6
PF04	PB+To	6.9	-3.4	3.9	17.7	22.2	11.9	9.4	5.8	17.8	10.7	14.7	1.9	6.8
PF05	PB+To	-0.5	-10.9	1.6	13.6	17.9	8.6	4.4	-1.1	13.5	6.8	12.4	2.0	3.9
PF06	PB+To	-14.8	-25.1	2.5	10.3	15.0	7.8	-0.1	-10.6	12.3	5.9	13.3	5.8	4.0
PF07	PB+To	9.2	0.1	0.1	12.9	16.9	11.3	4.9	6.8	10.8	13.8	15.6	2.2	4.3
PF08	PB+To	2.1	-7.2	-4.1	5.6	9.8	6.4	-2.1	-1.2	4.1	7.9	11.4	-3.1	-0.1
PF09	PB+To	-5.3	-15.0	-8.1	-4.2	-0.7	1.6	-11.9	-9.3	-7.6	2.1	7.2	-2.3	-4.5
PF10	PB+To	12.5	-0.7	-0.7	16.6	21.3	8.4	11.5	7.8	16.3	3.3	2.5	-1.4	1.9
FL01	PB+To	7.3	-1.3	-1.3	6.9	10.1	10.6	-0.6	4.3	4.4	14.2	16.0	0.3	3.0
FL02	PB+To	8.9	-6.5	-6.5	7.7	12.4	3.9	4.5	-0.9	8.0	-2.7	-8.0	-8.0	-5.2
FL04	PB+To	12.5	-0.5	4.4	21.8	26.5	12.1	16.3	9.3	24.6	6.2	7.0	2.7	3.7
average		1.3	-7.1	-0.1	9.9	13.5	7.0	3.1	0.8	9.5	5.8	8.3	-0.2	1.9
range		46.6	31.2	12.6	27.9	32.6	19.2	28.2	30.7	32.3	21.2	24.0	13.8	12.8
st. deviation		12.6	9.6	3.8	8.3	9.4	5.3	8.3	8.5	8.9	6.3	7.2	3.8	3.8

30NCD16 – [5] – RB+TO

case	loaded	Sines	Cross	Ppd	FCS	KCP	KIA	McD	DV	Matake	Z&L	SpaM	SpaC	GAM
MPA01	RB+To	-10.9	-5.1	-5.1	-2.0	-2.0	-7.8	-5.5	-2.0	-2.0	-7.8	-7.5	-7.8	-4.6%
MPA02	RB+To	-15.0	-6.8	-6.8	-4.6	-4.6	-8.6	-10.4	-4.6	-4.5	-8.6	-7.9	-9.8	-6.4%
average		-13.0%	-6.0	-6.0	-3.3	-3.3	-8.2	-7.9	-3.3	-3.3	-8.2	-7.7	-8.8	-5.5
range		4.2%	1.7	1.7	2.6	2.6	0.8	4.9	2.6	2.5	0.8	0.4	2.0	1.8
st. deviation		2.1%	0.8	0.8	1.3	1.3	0.4	2.5	1.3	1.3	0.4	0.2	1.0	0.9

30NCD16 – [5] BPL03– TEN

case	loaded	Sines	Cross	Ppd	FCS	KCP	KIA	McD	DV	Matake	Z&L	SpaM	SpaC	GAM
MPA03	Ten	9.9	-25.5	-25.5	25.4	-8.8	-12.1	-45.5	-12.0	-11.4	-32.7	-14.3	-29.5	19.0
MPA04	Ten	7.8	-24.4	-24.4	23.0	-9.1	-11.8	-44.9	-11.7	-11.1	-29.6	-12.6	-27.7	17.6
MPA05	Ten	-5.6	3.8	3.8	16.0	7.3	7.7	-21.0	7.8	8.3	11.6	12.2	1.2	17.0
average		4.1	-15.4	-15.4	21.5	-3.5	-5.4	-37.1	-5.3	-4.8	-16.9	-4.9	-18.7	17.9
range		15.5	29.3	29.3	9.3	16.4	19.8	24.5	19.8	19.7	44.3	26.5	30.7	1.9
st. deviation		6.9	13.6	13.6	4.0	7.7	9.2	11.4	9.3	9.2	20.2	12.1	14.1	0.8

30NCD16 – [5] – PB+TO

case	loaded	Sines	Cross	Ppd	FCS	KCP	KIA	McD	DV	Matake	Z&L	SpaM	SpaC	GAM
MPA06	PB	-0.2	-12.9	-12.9	-2.8	1.2	1.6	-11.1	-6.1	-6.0	3.3	7.1	-10.3	-7.8
MPA06X	PB	0.6	-14.8	-14.8	-3.2	1.5	1.8	-13.6	-7.1	-6.8	3.2	7.5	-11.6	-9.0
MPA07	PB	0.7	-6.4	-6.4	0.8	3.6	4.1	-5.8	-1.5	-1.4	6.3	8.9	-5.1	-2.7
MPA08	PB	0.8	0.0	0.0	4.0	5.5	5.9	-1.4	2.8	2.9	7.6	9.3	-0.3	2.1
MPA09	PB+To	-2.4	2.8	2.8	5.7	5.7	1.4	3.3	5.7	5.8	1.4	2.9	0.8	3.1
MPA10	PB+To	-30.7	-25.5	1.8	-5.8	-5.8	-4.4	-11.3	-18.3	-3.8	-5.8	0.4	-4.9	-1.0
MPA11	PB+To	1.7	-8.2	-8.2	4.9	8.9	4.1	-3.0	-0.4	0.7	7.5	6.0	-6.4	-1.7
MPA12	PB+To	-20.3	-30.1	-5.7	3.2	8.8	1.5	-6.8	-18.5	2.8	-0.2	6.2	-6.5	-2.6
MPA13	PB+To	-0.4	-10.1	-3.3	9.3	13.7	4.4	2.1	-1.6	9.5	2.4	7.1	-5.8	-0.6
MPA14	PB+To	-7.2	-17.0	-5.3	5.3	9.7	1.4	-2.6	-8.1	5.6	-1.1	5.1	-5.9	-3.2
MPA15	PB+To	-4.7	-13.3	-10.4	-1.5	2.2	-0.8	-8.7	-7.5	-3.0	-0.5	3.8	-10.7	-6.9
MPA16	PB+To	-36.1	-31.3	-6.2	-13.3	-13.3	-12.0	-18.3	-24.8	-11.4	-13.3	-7.5	-13.2	-8.8
MPA17	PB+To	-2.2	-9.8	-4.8	7.0	10.1	-1.0	3.4	-2.2	9.5	-5.9	-3.4	-7.0	-6.2
MPA18	PB+To	-18.9	-28.9	-4.3	2.4	7.0	1.1	-7.0	-17.4	4.2	-1.4	6.3	-1.6	-2.7
MPA19	PB+To	-11.9	-20.7	-14.6	-11.0	-7.8	-5.6	-17.6	-15.6	-13.9	-6.2	-0.4	-10.2	-11.3
MPA20	PB+To	-13.6	-32.5	-10.0	5.3	12.6	2.6	-6.2	-18.5	6.9	-1.4	6.7	-3.6	-5.8
MPA21	PB+To	-6.8	-33.2	-11.0	11.5	21.1	7.6	-2.0	-16.1	13.1	2.4	10.1	-2.5	-4.8
MPA22	PB+To	10.2	-4.5	-4.5	9.1	13.7	5.6	6.3	0.9	9.3	-0.7	-5.9	-5.9	-3.3
MPA23	PB+To	24.8	0.9	0.9	23.0	30.4	17.6	17.6	9.7	23.3	9.3	-0.3	-12.0	3.4
MPA24	PB+To	23.8	-8.4	-8.4	21.4	31.4	14.8	13.0	3.5	21.9	2.7	-8.0	-17.0	-4.2
MPA25	PB+To	-9.7	-4.9	-4.9	-2.2	-2.2	-6.2	-4.8	-2.2	-2.2	-6.2	-4.7	-6.8	-4.6
MPA26	PB+To	4.1	-8.5	-8.5	7.9	12.5	0.3	3.4	-0.5	7.5	-5.3	-5.2	-9.2	-6.1
MPA27	PB+To	6.4	-3.3	-3.3	12.0	16.4	6.0	5.6	4.6	10.8	5.0	7.1	-3.1	0.2
MPA28	PB+To	2.1	-5.8	-5.8	5.5	9.2	4.3	-1.5	0.2	3.6	5.6	8.3	-4.0	-2.1
MPA29	PB+To	12.3	-6.5	-6.5	16.5	23.5	9.7	7.5	4.6	14.5	7.9	10.4	-0.9	-0.9
MPA30	PB+To	15.1	-11.9	-11.9	17.7	27.1	10.9	5.4	1.8	14.7	7.9	11.3	-6.3	-4.2
average		-2.4	-13.3	-6.4	5.1	9.5	2.9	-2.1	-5.1	4.5	0.9	3.4	-6.5	-3.5
range		60.9	36.0	17.6	36.3	44.7	29.6	36.0	34.4	37.2	22.5	19.3	17.8	14.7
st. deviation		14.1	10.7	4.6	8.7	10.9	6.2	8.6	9.1	9.0	5.5	5.9	4.2	3.6

XC18

case	loaded	Sines	Cross	Ppd	FCS	KCP	KIA	McD	DV	Matake	Z&L	SpaM	SpaC	GAM
MPB01	PB+To	6.5	4.2	4.2	7.4	7.4	17.1	12.7	7.4	7.4	4.9	9.0	5.1	4.1
MPB02	PB+To	-1.6	-3.9	4.2	2.4	2.4	13.8	8.7	-0.1	2.7	0.9	7.3	0.6	4.5
MPB03	PB+To	-18.1	-20.5	11.8	-3.9	-3.9	17.5	5.0	-11.9	-3.3	3.2	12.5	5.5	13.1
average		-4.4	-6.7	6.7	1.9	1.9	16.1	8.8	-1.5	2.3	3.0	9.6	3.7	7.2
range		24.5	24.7	7.6	11.3	11.3	3.7	7.7	19.2	10.7	3.9	5.2	4.8	9.0
st. deviation		10.2	10.3	3.6	4.6	4.6	1.7	3.2	7.9	4.4	1.6	2.2	2.2	4.1

FGS 800-2

case	loaded	Sines	Cross	Ppd	FCS	KCP	KIA	McD	DV	Matake	Z&L	SpaM	SpaC	GAM
MPC01	PB+To	-15.3	2.5	2.5	5.0	5.0	-2.0	-12.9	5.0	5.1	-2.0	-1.5	-3.0	3.5
MPC02	PB+To	-35.5	-16.4	10.1	11.3	11.3	5.3	-20.0	-7.8	19.8	2.6	5.4	4.7	-0.7
MPC03	PB+To	-15.2	0.3	0.3	3.1	3.1	-4.9	-12.3	3.1	3.2	-4.9	-4.5	-5.2	1.4
MPC04	PB	3.2	-19.9	-19.9	4.9	0.5	0.1	-43.4	-12.0	-11.6	-2.9	-6.7	-20.9	4.0
average		-15.7	-8.4	-1.8	6.1	5.0	-0.4	-22.2	-2.9	4.1	-1.8	-1.8	-6.1	2.0
range		38.6	22.4	30.1	8.2	10.8	10.2	31.2	17.0	31.4	7.5	12.1	25.7	4.7
st. deviation		13.7	9.9	11.1	3.1	4.0	3.7	12.7	7.2	11.1	2.7	4.6	9.3	1.8

S65A

case	loaded	Sines	Cross	Ppd	FCS	KCP	KIA	McD	DV	Matake	Z&L	SpaM	SpaC	GAM
G02	PB	-5.4	-1.2	-1.2	7.6	-1.0	-1.0	-2.2	4.4	4.5	-1.9	15.3	-0.4	4.5
G03	PB	0.0	-0.5	-0.5	18.1	0.0	0.0	3.3	10.7	10.8	0.0	29.1	3.3	10.9
G05	To	-8.5	-8.5	-8.5	-4.5	-7.3	-7.1	-5.1	-8.5	-8.5	-6.4	-8.5	-9.0	-2.3
G06	To	-7.3	-7.3	-7.3	2.3	-4.6	-4.3	-1.1	-7.3	-7.3	0.7	-7.3	-7.5	5.3
G07	PB+To	-14.4	-5.8	-5.8	6.2	-1.7	-4.2	-2.5	-5.8	6.0	-4.5	4.6	-4.0	-4.0
G08	PB+To	-15.8	-7.4	-7.4	16.9	0.9	-4.1	4.6	-7.4	16.6	-2.9	11.3	-0.4	-1.3
G09	PB+To	-4.9	-0.6	-0.6	19.7	3.6	0.0	6.5	4.9	16.8	-0.4	20.0	7.4	6.3
G10	PB+To	-4.9	-0.6	-0.6	31.7	7.7	1.2	15.0	4.9	28.9	2.5	26.4	10.0	9.6
G11	PB+To	-9.9	-11.3	-11.3	18.4	-6.8	-10.7	1.1	-0.2	11.6	-11.2	19.3	0.3	1.0
G12	PB+To	-9.4	-10.8	-10.8	30.4	-2.2	-9.4	9.8	0.3	24.3	-8.4	24.0	6.9	4.4
G13	PB+To	-7.3	-11.7	-11.7	3.2	-9.3	-12.0	-1.2	-6.1	3.6	-14.4	-13.8	-13.9	-9.9
G14	PB+To	-6.3	-15.1	-15.1	14.9	-10.2	-15.5	4.4	-3.9	15.5	-19.4	-15.9	-22.3	-9.7
G15	PB+To	-9.4	-13.8	-13.8	4.9	-10.2	-13.6	-1.5	-8.2	1.5	-14.9	-14.9	-18.2	-6.1
G16	PB+To	-7.2	-15.9	-15.9	17.5	-9.9	-16.1	5.3	-4.8	14.6	-18.8	-13.9	-22.5	-5.5
G17	PB+To	-8.2	-12.5	-12.5	11.4	-7.5	-11.2	2.4	-7.0	2.7	-8.5	-11.2	-15.5	1.4
G18	PB+To	-3.8	-12.6	-12.6	25.7	-5.2	-12.0	11.1	-1.4	18.0	-10.7	-6.7	-19.1	3.5
G19	PB+To	-4.9	3.6	3.6	4.9	4.9	2.8	0.1	4.9	5.0	2.8	4.4	0.7	3.8
G20	PB+To	-7.4	-1.4	-1.4	1.7	1.7	-3.3	-2.3	1.7	1.7	-3.3	-2.4	-3.8	-0.9
G21	PB+To	-5.7	-3.0	-3.0	-0.4	-0.4	-4.9	-1.0	-0.4	-0.4	-4.9	-4.7	-4.7	-2.7
G22	PB+To	-5.3	-1.9	-1.9	15.4	1.9	-1.8	3.8	4.8	10.7	-1.8	17.6	3.4	6.6
G23	PB+To	-2.4	-1.0	-1.0	13.3	2.8	-2.1	4.4	7.5	7.8	-2.0	11.5	-1.0	8.1
G24	PB+To	-1.1	-2.9	-2.9	15.9	2.3	-4.2	8.3	5.1	11.5	-4.7	0.4	-5.5	5.7
G25	PB+To	-8.7	-10.7	-10.7	24.6	-4.1	-9.6	5.5	1.4	13.6	-6.9	24.7	-0.8	6.5
G26	PB+To	-8.0	-11.9	-11.9	16.3	-7.2	-11.7	0.4	1.7	2.3	-8.7	17.6	-10.0	6.0
G27	PB+To	-12.3	-19.0	-19.0	17.4	-11.4	-19.3	1.8	-6.0	6.7	-18.0	-1.7	-16.9	-1.8
G28	PB+To	0.3	1.9	1.9	19.6	7.2	-0.1	10.5	10.5	18.3	-1.7	10.6	0.1	6.6
G29	PB+To	-8.7	-2.8	-2.8	10.3	3.6	-3.0	3.7	0.2	7.6	-2.5	4.5	-3.9	3.0
average		-6.9	-6.8	-6.8	13.5	-2.3	-6.6	3.2	-0.1	9.1	-6.3	5.2	-5.5	1.8
range		16.1	22.6	22.6	36.1	19.1	22.1	20.0	19.2	37.5	22.2	45.0	32.5	20.8
st. deviation		3.8	6.0	6.0	9.0	5.6	5.8	4.8	5.7	8.5	6.3	13.9	9.0	5.5

APPENDIX II SUMMARY OF RESULTS OF EXISTING CRITERIA

All numerical values in following tables concern directly ΔFI results of described groups or their statistical evaluation. All are expressed in %.

MATERIAL & LOAD TYPE - AVERAGE

case	ref.	loaded	tests	Sines	Cross	Ppd	FCS	KMC	KMI	McD	DV	Matake	Z&L	SpaM	SpaC	GAM
hard steel	[13]	PB+To	10	-7.4	-2.0	4.6	4.7	4.7	2.1	-2.6	0.7	5.7	1.3	4.3	1.8	4.1
mild steel	[13]	PB+To	8	-1.6	-0.9	7.4	5.2	5.2	4.2	2.9	1.9	5.8	4.0	8.9	5.4	7.2
hard steel	[52]	PB+To	10	-9.2	-3.9	2.6	2.5	2.5	-0.3	-4.0	-1.2	3.5	-1.0	1.8	-0.5	1.6
42CrMo4	[52]	PB+To	9	-14.5	-10.8	-3.1	5.4	3.7	-2.0	-13.0	-6.8	5.9	-2.8	1.2	-4.7	-1.5
34Cr4	[52]	PB+To	14	-10.7	-10.3	-0.2	5.4	8.5	2.6	-3.5	-6.1	5.6	2.8	5.1	-1.4	0.9
30NCD16	[22]	PB+To	13	1.3	-7.1	-0.1	9.9	13.5	7.0	3.1	0.8	9.5	5.8	8.3	-0.2	1.9
30NCD16	[5]	Rb+To	2	-13.0	-6.0	-6.0	-3.3	-3.3	-8.2	-7.9	-3.3	-3.3	-8.2	-7.7	-8.8	-5.5
30NCD16	[5]	Ten	3	4.1	-15.4	-15.4	21.5	-3.5	-5.4	-37.1	-5.3	-4.8	-16.9	-4.9	-18.7	17.9
30NCD16	[5]	PB+To	26	-2.4	-13.3	-6.4	5.1	9.5	2.9	-2.1	-5.1	4.5	0.9	3.4	-6.5	-3.5
XC18	[5]	PB+To	3	-4.4	-6.7	6.7	1.9	1.9	16.1	8.8	-1.5	2.3	3.0	9.6	3.7	7.2
FGS800-2	[5]	PB+To	4	-15.7	-8.4	-1.8	6.1	5.0	-0.4	-22.2	-2.9	4.1	-1.8	-1.8	-6.1	2.0
S65A	[29]	PB+To	27	-6.9	-6.8	-6.8	13.5	-2.3	-6.6	3.2	-0.1	9.1	-6.3	5.2	-5.5	1.8
range				19.7	14.5	22.8	24.7	17.0	24.4	45.9	8.7	14.3	22.7	17.3	24.1	23.4
standard deviation				6.0	4.1	6.3	6.0	5.0	6.3	12.2	2.8	4.1	6.1	5.2	6.2	5.8

MATERIAL & LOAD TYPE - RANGE

case	ref.	loaded	tests	Sines	Cross	Ppd	FCS	KMC	KMI	McD	DV	Matake	Z&L	SpaM	SpaC	GAM
hard steel	[13]	PB+To	10	21.3	21.1	9.3	11.2	11.2	8.8	18.4	23.8	12.1	8.5	10.5	8.2	8.6
mild steel	[13]	PB+To	8	17.8	17.9	17.5	11.3	11.3	9.7	14.0	19.4	11.7	9.5	16.5	12.0	17.1
hard steel	[52]	PB+To	10	19.6	19.3	9.0	12.3	12.3	5.5	18.9	21.8	13.3	4.7	8.9	7.4	5.9
42CrMo4	[52]	PB+To	9	46.0	36.2	22.6	38.5	33.9	22.0	36.3	39.7	35.6	24.7	23.7	20.5	20.5
34Cr4	[52]	PB+To	14	42.4	28.7	13.6	30.9	37.6	17.0	27.9	30.0	31.6	21.0	14.1	12.3	8.5
30NCD16	[22]	PB+To	13	46.6	31.2	12.6	27.9	32.6	19.2	28.2	30.7	32.3	21.2	24.0	13.8	12.8
30NCD16	[5]	Rb+To	2	4.2	1.7	1.7	2.6	2.6	0.8	4.9	2.6	2.6	0.8	0.4	2.0	1.8
30NCD16	[5]	Ten	3	15.5	29.3	29.3	9.3	16.4	19.8	24.5	19.8	19.7	44.3	26.5	30.7	1.9
30NCD16	[5]	PB+To	26	60.9	36.0	17.6	36.3	44.7	29.6	36.0	34.4	37.2	22.5	19.3	17.8	14.7
XC18	[5]	PB+To	3	24.5	24.7	7.6	11.3	11.3	3.7	7.7	19.2	10.7	3.9	5.2	4.8	9.0
FGS800-2	[5]	PB+To	4	38.6	22.4	30.1	8.2	10.8	10.2	31.2	17.0	31.4	7.5	12.1	25.7	4.7
S65A	[29]	PB+To	27	16.1	22.6	22.6	36.1	19.1	22.1	20.0	19.2	37.5	22.2	45.0	32.5	20.8
max				60.9	36.2	30.1	38.5	44.7	29.6	36.3	39.7	37.5	44.3	45.0	32.5	20.8
average				29.5	24.2	16.1	19.7	20.3	14.0	22.3	23.2	23.0	15.9	17.2	15.6	10.5

MATERIAL & LOAD TYPE - STANDARD DEVIATION

case	ref.	loaded	tests	Sines	Cross	Ppd	FCS	KMC	KMI	McD	DV	Matake	Z&L	SpaM	SpaC	GAM
hard steel	[13]	PB+To	10	5.9	5.7	2.8	3.2	3.2	2.6	5.3	6.4	3.6	2.6	3.3	2.5	2.5
mild steel	[13]	PB+To	8	5.2	5.2	4.7	3.7	3.8	2.6	4.6	6.0	4.0	2.6	4.4	3.3	4.5
hard steel	[52]	PB+To	10	5.7	5.3	2.7	3.3	3.3	1.8	5.3	6.1	3.9	1.6	2.6	2.0	1.7
42CrMo4	[52]	PB+To	9	15.2	13.9	7.3	11.5	10.7	7.6	12.5	14.9	11.2	8.1	7.8	7.5	7.2
34Cr4	[52]	PB+To	14	11.7	8.5	3.7	8.8	11.3	5.6	8.4	9.5	8.9	6.5	5.2	3.6	2.5
30NCD16	[22]	PB+To	13	12.6	9.6	3.8	8.3	9.4	5.3	8.3	8.5	8.9	6.3	7.2	3.8	3.8
30NCD16	[5]	Rb+To	2	2.1	0.8	0.8	1.3	1.3	0.4	2.5	1.3	1.3	0.4	0.2	1.0	0.9
30NCD16	[5]	Ten	3	6.9	13.6	13.6	4.0	7.7	9.2	11.4	9.3	9.2	20.2	12.1	14.1	0.8
30NCD16	[5]	PB+To	26	14.1	10.7	4.6	8.7	10.9	6.2	8.6	9.1	9.0	5.5	5.9	4.2	3.6
XC18	[5]	PB+To	3	10.2	10.3	3.6	4.6	4.6	1.7	3.2	7.9	4.4	1.6	2.2	2.2	4.1
FGS800-2	[5]	PB+To	4	13.7	9.9	11.1	3.1	4.0	3.7	12.7	7.2	11.1	2.7	4.6	9.3	1.8
S65A	[29]	PB+To	27	3.8	6.0	6.0	9.0	5.6	5.8	4.8	5.7	8.5	6.3	13.9	9.0	5.5
max				15.2	13.9	13.6	11.5	11.3	9.2	12.7	14.9	11.2	20.2	13.9	14.1	7.2
average				8.9	8.3	5.4	5.8	6.3	4.4	7.3	7.7	7.0	5.4	5.8	5.2	3.3

PARTIAL EFFECTS - AVERAGE

case	tests	Sines	Cross	Ppd	FCS	KCP	KIA	McD	DV	Matake	Z&L	SpaM	SpaC	GAM
All	129	-6.1	-8.1	-2.3	7.4	4.9	0.6	-2.5	-2.3	5.9	-0.7	4.2	-3.2	1.3
P	61	-3.6	-3.8	-3.8	10.2	4.2	-1.4	1.4	1.7	7.8	-1.5	4.6	-3.5	1.4
NP	55	-11.9	-12.5	1.0	3.5	5.1	2.0	-4.9	-7.0	4.6	0.2	4.7	-1.0	0.9
nMS	56	-10.3	-5.2	2.9	2.2	2.2	0.4	-3.7	-1.9	3.2	-0.9	2.4	-0.5	2.0
MS	73	-2.8	-10.3	-6.3	11.4	7.0	0.7	-1.6	-2.7	8.0	-0.5	5.6	-5.3	0.8
P, nMS	23	-4.8	1.1	1.1	3.6	3.6	0.0	-1.6	3.6	3.7	-0.5	1.0	-1.2	1.4
NP, nMS	33	-14.1	-9.5	4.1	1.2	1.2	0.6	-5.2	-5.8	2.8	-1.2	3.3	0.0	2.3
MS - torsion	12	-15.4	-9.3	-4.8	6.3	4.0	-1.3	-4.6	-8.2	4.1	0.7	2.9	-5.0	-0.3
MS - axial	44	2.1	-10.8	-5.9	10.5	11.0	4.2	-3.2	-2.1	7.7	1.4	5.5	-5.3	0.3
NP - 90 deg	34	-15.3	-16.6	0.6	2.3	4.0	1.6	-7.4	-10.6	3.8	-0.6	4.5	-0.7	0.3
NP - 90 deg, nMS	20	-17.9	-12.8	4.5	-0.2	-0.2	0.5	-7.7	-9.0	1.9	-1.4	3.6	0.4	2.1
NP - not 90 deg	21	-7.0	-7.3	1.8	4.4	5.8	3.1	-0.7	-2.2	4.8	1.2	5.2	-1.2	2.4
NP - not 90 deg, nMS	13	-8.3	-4.5	3.4	3.2	3.2	0.9	-1.2	-0.9	4.3	-0.9	2.8	-0.5	2.6

PARTIAL EFFECTS - RANGE

case	tests	Sines	Cross	Ppd	FCS	KCP	KIA	McD	DV	Matake	Z&L	SpaM	SpaC	GAM
All	129	62.0	40.5	42.2	47.8	47.6	36.9	63.2	41.3	42.8	47.0	45.0	40.5	31.5
P	61	38.2	26.3	26.3	36.2	38.5	36.4	31.8	25.8	37.5	33.6	45.0	32.5	20.8
NP	55	49.7	39.1	31.3	38.0	44.2	30.8	49.6	38.2	38.5	25.7	27.4	25.8	28.8
nMS	56	43.0	38.6	25.8	27.5	27.5	30.8	46.0	39.0	33.4	23.4	27.4	25.8	28.8
MS	73	62.0	39.1	31.4	42.7	42.8	36.9	63.2	41.3	42.8	47.0	45.0	39.5	30.3
P, nMS	23	21.7	14.1	14.1	15.4	15.4	25.7	25.6	15.4	15.6	14.8	19.4	15.8	14.4
NP, nMS	33	37.3	34.5	25.8	27.5	27.5	30.8	43.2	35.2	33.4	23.4	27.4	25.8	28.8
MS - torsion	12	33.4	34.8	21.3	25.0	28.9	19.7	35.0	37.3	30.6	24.1	21.3	17.7	14.0
MS - axial	44	43.7	37.1	29.9	36.4	41.7	33.2	63.2	30.9	38.5	47.0	45.0	35.3	30.3
NP - 90 deg	34	49.7	36.3	31.3	38.0	44.2	30.8	49.6	38.2	38.5	23.4	27.4	25.8	28.8
NP - 90 deg, nMS	20	37.3	34.5	25.8	27.5	27.5	30.8	43.2	35.2	33.4	23.4	27.4	25.8	28.8
NP - not 90 deg	21	25.4	22.7	22.2	21.6	26.2	21.7	18.7	17.7	21.1	16.1	16.9	16.2	20.0
NP - not 90 deg, nMS	13	17.1	14.5	9.5	11.4	11.4	18.0	18.0	14.2	11.9	8.7	12.1	11.4	10.2

PARTIAL EFFECTS - STANDARD DEVIATION

case	tests	Sines	Cross	Ppd	FCS	KCP	KIA	McD	DV	Matake	Z&L	SpaM	SpaC	GAM
All	129	11.4	9.6	7.5	9.0	9.7	7.4	11.1	8.8	8.7	7.8	8.8	7.4	5.8
P	61	8.0	6.3	6.3	8.3	9.4	7.7	6.3	5.5	7.3	7.6	10.5	7.2	4.8
NP	55	11.6	10.6	6.5	8.0	9.3	6.1	10.0	9.8	8.8	5.5	5.7	5.5	5.6
nMS	56	10.4	9.3	4.8	5.8	5.8	5.9	8.5	8.9	6.1	4.8	5.5	5.1	5.0
MS	73	11.1	9.3	6.7	9.0	11.4	8.4	12.6	8.8	9.7	9.5	10.4	8.2	6.2
P, nMS	23	5.8	3.7	3.7	3.6	3.6	5.4	5.7	3.6	3.7	4.2	5.1	4.1	3.7
NP, nMS	33	11.1	9.5	5.0	6.7	6.7	6.1	9.7	9.4	7.3	5.1	5.6	5.7	5.8
MS - torsion	12	9.7	9.2	5.4	8.1	9.5	6.2	9.8	9.8	9.7	7.7	7.4	5.1	4.5
MS - axial	44	9.7	9.8	7.1	8.4	11.3	7.3	14.4	8.6	9.9	9.8	9.5	8.2	7.0
NP - 90 deg	34	12.6	11.0	7.5	9.0	10.5	6.7	11.2	10.3	10.0	5.9	6.2	6.3	6.5
NP - 90 deg, nMS	20	12.1	10.5	6.0	7.9	7.9	7.0	10.9	10.3	8.8	6.2	6.5	6.8	7.0
NP - not 90 deg	21	7.1	5.8	4.9	5.1	6.4	5.7	5.6	5.3	5.3	4.2	4.8	4.0	4.3
NP - not 90 deg, nMS	13	5.6	4.3	2.8	3.3	3.3	4.5	5.5	4.6	3.7	2.8	3.6	3.1	3.0

APPENDIX III RESULTS OF SPAGNOLI METHOD – CSM V. MD

The numerical values in the following tables represent directly ΔFI results or their statistical evaluation. All are expressed in %.

Case	Spa	SpaM	SpaC1	SpaC2	SpaC3	SpaC2S	SpaC3S
CS2	5.7	5.7	1.2	1.2	1.2	1.2	1.2
CS3	5.6	5.6	3.1	3.1	3.1	3.1	3.1
CS4	-1.2	-1.2	-1.5	-1.5	-1.5	-1.5	-1.5
CS6	5.1	5.1	2.2	2.1	2.1	2.1	2.1
CS7	-1.4	-1.4	-1.7	-1.8	-1.7	-1.8	-1.7
CS8	4.5	4.5	-1.1	-0.6	-0.8	-0.6	-0.8
CS9	1.9	1.9	1.5	1.3	1.4	1.3	1.4
CS10	9.2	9.2	3.5	6.4	6.0	6.4	6.0
CS11	8.1	8.1	-1.0	3.1	2.5	3.1	2.5
CS12	5.7	5.7	5.3	4.9	5.0	4.9	5.0
CS14	11.5	11.5	5.9	5.9	5.9	5.9	5.9
CS15	8.2	8.2	4.7	4.7	4.7	4.7	4.7
CS16	0.0	0.0	-1.0	-1.0	-1.0	-1.0	-1.0
CS18	9.9	9.9	2.6	3.2	2.9	3.2	2.9
CS19	6.5	6.5	5.3	4.6	4.7	4.6	4.7
CS20	8.8	8.8	3.5	7.1	6.6	7.1	6.6
CS21	16.5	16.5	3.4	11.0	10.1	11.0	10.1
CS22	10.0	10.0	8.5	7.8	7.9	7.8	7.9
PNK01	-3.6	-3.6	-4.0	-4.0	-4.0	-4.0	-4.0
PNK02	-2.2	-2.2	-2.5	-2.6	-2.6	-2.6	-2.6
PNK03	1.1	1.1	0.7	0.5	0.6	0.5	0.6
PNK04	4.2	4.2	3.8	3.4	3.5	3.4	3.5
PNK05	1.6	1.6	-0.8	-0.8	-0.8	-0.8	-0.8
PNK06	2.9	2.9	0.0	-0.1	-0.1	-0.1	-0.1
PNK07	3.4	3.4	-2.2	-1.6	-1.8	-1.6	-1.8
PNK08	5.3	5.3	-3.6	0.5	-0.1	0.5	-0.1
PNK09	2.8	2.8	-1.6	-1.6	-1.6	-1.6	-1.6
PNK10	3.0	3.0	-1.1	1.1	0.8	1.1	0.8
PZ01	-0.4	-0.4	-2.7	-2.7	-2.7	-2.7	-2.7
PZ02	-1.1	-1.1	-6.2	-5.9	-6.0	-5.9	-6.0
PZ03	-1.3	-1.3	-11.4	-5.8	-6.3	-5.8	-6.3
PZ04	-1.1	-1.1	-6.8	-6.8	-6.8	-6.8	-6.8
PZ05	3.2	3.2	1.6	0.0	0.2	0.0	0.2
PZ06	0.1	0.1	-5.1	-1.8	-2.3	-1.8	-2.3
PZ07	31.3	12.8	3.5	3.5	3.5	0.3	0.3
PZ08	23.0	5.1	-1.6	-1.6	-1.5	-1.6	-1.5
PZ09	17.3	3.9	-2.7	-2.1	-2.1	-2.1	-2.1
PZ10	47.8	11.0	8.9	16.4	13.8	-0.1	-1.0
PZ11	49.2	12.6	13.5	30.9	27.8	2.3	0.6
PZ12	30.9	10.6	1.0	1.0	1.0	-4.7	-4.7
PZ13	32.5	10.5	14.2	25.3	24.0	4.3	3.2
PZ14	5.6	5.6	5.4	5.5	5.5	5.5	5.5

Case	Spa	SpaM	SpaC1	SpaC2	SpaC3	SpaC2S	SpaC3S
PF01	1.8	1.8	-0.3	-0.3	-0.3	-0.3	-0.3
PF02	-0.7	-0.7	-10.7	-5.9	-6.5	-5.9	-6.5
PF03	36.7	14.7	11.9	11.9	11.9	3.9	3.9
PF04	36.3	14.7	12.0	16.3	14.2	1.9	0.3
PF05	34.1	12.4	9.0	17.9	15.5	2.0	0.2
PF06	34.7	13.3	10.1	24.1	21.8	5.8	4.2
PF07	39.7	15.6	10.8	10.8	10.8	2.2	2.2
PF08	35.6	11.4	5.9	9.7	8.1	-3.1	-4.2
PF09	31.5	7.2	3.6	12.6	10.6	-2.3	-3.4
PF10	20.3	2.5	2.2	12.0	9.8	-1.4	-2.8
FL01	40.9	16.0	9.9	9.9	9.9	0.3	0.3
FL02	5.8	-8.0	5.4	5.4	5.4	-8.0	-8.0
FL04	22.6	7.0	19.0	19.0	18.8	2.7	2.5
MPA01	-7.5	-7.5	-7.8	-7.8	-7.8	-7.8	-7.8
MPA02	-7.9	-7.9	-9.8	-9.8	-9.8	-9.8	-9.8
MPA03	75.0	-14.3	38.1	38.1	38.1	-29.5	-29.5
MPA04	70.5	-12.6	35.0	35.0	35.0	-27.7	-27.7
MPA05	33.8	12.2	16.0	16.0	16.0	1.2	1.2
MPA06	37.7	7.1	2.0	2.0	2.0	-10.3	-10.3
MPA06X	42.9	7.5	3.0	3.0	3.0	-11.6	-11.6
MPA07	30.4	8.9	3.1	3.1	3.1	-5.1	-5.1
MPA08	21.0	9.3	3.9	3.9	3.9	-0.3	-0.3
MPA09	2.9	2.9	0.8	0.8	0.8	0.8	0.8
MPA10	0.4	0.4	-9.7	-4.9	-5.3	-4.9	-5.3
MPA11	37.7	6.0	1.2	2.2	1.8	-6.4	-6.6
MPA12	32.6	6.2	-1.9	2.3	1.0	-6.5	-7.3
MPA13	27.5	7.1	4.4	7.4	5.9	-5.8	-6.9
MPA14	25.5	5.1	1.6	8.6	6.8	-5.9	-7.2
MPA15	26.0	3.8	-1.4	0.4	-0.3	-10.7	-10.8
MPA16	-7.5	-7.5	-16.9	-13.2	-13.5	-13.2	-13.5
MPA17	5.3	-3.4	3.2	2.2	2.3	-7.0	-6.9
MPA18	27.0	6.3	3.3	15.4	13.4	-1.6	-3.0
MPA19	21.8	-0.4	-3.9	2.5	1.3	-10.2	-10.9
MPA20	42.6	6.7	10.0	24.7	22.0	-3.6	-5.1
MPA21	60.3	10.1	19.5	35.8	32.7	-2.5	-4.0
MPA22	6.6	-5.9	6.1	6.1	6.1	-5.9	-5.9
MPA23	26.9	-0.3	26.8	15.4	18.7	-12.0	-9.2
MPA24	36.6	-8.0	35.0	21.7	23.5	-17.0	-16.0
MPA25	-4.7	-4.7	-6.8	-6.8	-6.8	-6.8	-6.8
MPA26	12.0	-5.2	-5.7	3.8	1.6	-9.2	-10.6
MPA27	27.9	7.1	4.3	4.3	4.3	-3.1	-3.1
MPA28	29.8	8.3	3.7	3.7	3.7	-4.0	-4.0
MPA29	47.1	10.4	7.9	15.5	12.9	-0.9	-1.6
MPA30	63.8	11.3	11.0	11.1	13.7	-6.3	-5.3

Case	Spa	SpaM	SpaC1	SpaC2	SpaC3	SpaC2S	SpaC3S
average	18.1	4.3	3.6	5.8	5.4	-2.4	-2.7
range	82.9	30.8	55.0	51.3	51.6	40.5	39.5
standard deviation	19.1	6.6	9.4	10.1	9.8	6.6	6.5

APPENDIX IV ΔFI RESULTS OF THE NEW PROPOSALS

The final criteria selected are PZc (reported as PZv2 as well), PZd (PZ) and PCe (PC). Their columns are further darkened in order to enable their fast localisation. All numerical values in the following tables concern directly ΔFI results or their statistical evaluation; they are expressed in %.

HARD STEEL – [13]

case	loaded	PZa	PZb	PZc	PZd	PCa	PCa2	PCb	PCc	PCd	PCe	PPa	PPb	PPc	PPd
CS2	PB+To	3.6	3.6	3.6	3.6	11.5	11.5	11.5	11.5	11.5	11.5	3.6	3.6	3.6	3.6
CS3	PB+To	5.9	5.9	5.9	5.9	12.6	12.6	12.6	12.6	12.6	12.6	5.9	5.9	5.9	5.9
CS4	PB+To	2.7	2.7	2.7	2.7	6.3	6.3	6.3	6.3	6.3	6.3	2.7	2.7	2.7	2.7
CS6	PB+To	4.6	4.6	4.6	4.6	12.1	12.1	12.1	12.1	12.1	12.1	6.1	6.1	6.1	6.1
CS7	PB+To	1.8	1.8	1.8	1.8	6.2	6.2	6.2	6.2	6.2	6.2	2.8	2.8	2.8	2.8
CS8	PB+To	1.9	1.9	1.9	1.9	10.7	10.7	10.7	10.7	10.7	10.7	6.4	6.4	6.4	6.4
CS9	PB+To	3.3	3.3	3.3	3.3	9.4	9.4	9.4	9.4	9.4	9.4	6.7	6.7	6.7	6.7
CS10	PB+To	6.1	6.1	6.1	6.1	11.5	11.5	11.5	11.5	11.5	11.5	10.0	10.0	10.0	10.0
CS11	PB+To	3.6	3.6	3.6	3.6	11.8	11.8	11.8	11.8	11.8	11.8	10.4	10.4	10.4	10.4
CS12	PB+To	5.5	5.5	5.5	5.5	12.7	12.7	12.7	12.7	12.7	12.7	10.5	10.5	10.5	10.5
average		3.9	3.9	3.9	3.9	10.5	10.5	10.5	10.5	10.5	10.5	6.5	6.5	6.5	6.5
range		4.3	4.3	4.3	4.3	6.5	6.5	6.5	6.5	6.5	6.5	7.8	7.8	7.8	7.8
st. deviation		1.5	1.5	1.5	1.5	2.3	2.3	2.3	2.3	2.3	2.3	2.8	2.8	2.8	2.8

MILD STEEL

case	loaded	PZa	PZb	PZc	PZd	PCa	PCa2	PCb	PCc	PCd	PCe	PPa	PPb	PPc	PPd
CS14	PB+To	6.2	6.2	6.2	6.2	17.3	17.3	17.3	17.3	17.3	17.3	6.2	6.2	6.2	6.2
CS15	PB+To	5.0	5.0	5.0	5.0	15.5	15.5	15.5	15.5	15.5	15.5	5.0	5.0	5.0	5.0
CS16	PB+To	-0.5	-0.5	-0.5	-0.5	7.3	7.3	7.3	7.3	7.3	7.3	-0.5	-0.5	-0.5	-0.5
CS18	PB+To	3.6	3.6	3.6	3.6	15.8	15.8	15.8	15.8	15.8	15.8	8.9	8.9	8.9	8.9
CS19	PB+To	3.0	3.0	3.0	3.0	13.6	13.6	13.6	13.6	13.6	13.6	6.9	6.9	6.9	6.9
CS20	PB+To	3.9	3.9	3.9	3.9	14.2	14.2	14.2	14.2	14.2	14.2	6.2	6.2	6.2	6.2
CS21	PB+To	8.6	8.6	8.6	8.6	18.5	18.5	18.5	18.5	18.5	18.5	16.6	16.6	16.6	16.6
CS22	PB+To	5.0	5.0	5.0	5.0	16.9	16.9	16.9	16.9	16.9	16.9	10.5	10.5	10.5	10.5
average		4.4	4.4	4.4	4.4	14.9	14.9	14.9	14.9	14.9	14.9	7.5	7.5	7.5	7.5
range		9.0	9.0	9.0	9.0	11.2	11.2	11.2	11.2	11.2	11.2	17.1	17.1	17.1	17.1
st. deviation		2.5	2.5	2.5	2.5	3.2	3.2	3.2	3.2	3.2	3.2	4.6	4.6	4.6	4.6

HARD STEEL – [52]

case	loaded	PZa	PZb	PZc	PZd	PCa	PCa2	PCb	PCc	PCd	PCe	PPa	PPb	PPc	PPd
PNK01	PB+To	0.3	0.3	0.3	0.3	4.2	4.2	4.2	4.2	4.2	4.2	0.3	0.3	0.3	0.3
PNK02	PB+To	1.0	1.0	1.0	1.0	5.5	5.5	5.5	5.5	5.5	5.5	2.0	2.0	2.0	2.0
PNK03	PB+To	2.5	2.5	2.5	2.5	8.7	8.7	8.7	8.7	8.7	8.7	5.9	5.9	5.9	5.9
PNK04	PB+To	4.2	4.2	4.2	4.2	11.4	11.4	11.4	11.4	11.4	11.4	9.1	9.1	9.1	9.1
PNK05	PB+To	2.1	2.1	2.1	2.1	9.4	9.4	9.4	9.4	9.4	9.4	2.1	2.1	2.1	2.1
PNK06	PB+To	2.6	2.6	2.6	2.6	10.3	10.3	10.3	10.3	10.3	10.3	4.0	4.0	4.0	4.0
PNK07	PB+To	0.9	0.9	0.9	0.9	9.9	9.9	9.9	9.9	9.9	9.9	5.4	5.4	5.4	5.4
PNK08	PB+To	1.2	1.2	1.2	1.2	9.9	9.9	9.9	9.9	9.9	9.9	7.7	7.7	7.7	7.7
PNK09	PB+To	0.9	0.9	0.9	0.9	9.3	9.3	9.3	9.3	9.3	9.3	0.9	0.9	0.9	0.9
PNK10	PB+To	0.9	0.9	0.9	0.9	8.2	8.2	8.2	8.2	8.2	8.2	2.9	2.9	2.9	2.9
average		1.6	1.6	1.6	1.6	8.7	8.7	8.7	8.7	8.7	8.7	4.0	4.0	4.0	4.0
range		3.9	3.9	3.9	3.9	7.2	7.2	7.2	7.2	7.2	7.2	8.8	8.8	8.8	8.8
st. deviation		1.1	1.1	1.1	1.1	2.1	2.1	2.1	2.1	2.1	2.1	2.8	2.8	2.8	2.8

42CRMO4

case	loaded	PZa	PZb	PZc	PZd	PCa	PCa2	PCb	PCc	PCd	PCe	PPa	PPb	PPc	PPd
PL01	PB+To	4.8	4.8	4.8	4.8	9.7	9.7	9.7	9.7	9.7	9.7	4.8	4.8	4.8	4.8
PL02	PB+To	-11.3	-11.3	-11.3	-11.3	-1.9	-1.9	-1.9	-1.9	-1.9	-1.9	-6.4	-6.4	-6.4	-6.4
PL03	PB+To	9.8	9.8	9.8	9.8	11.5	11.5	11.5	11.5	11.5	11.5	9.8	9.8	9.8	9.8
PL04	PB+To	-3.3	-3.3	-3.3	-3.3	4.0	4.0	4.0	4.0	4.0	4.0	2.2	2.2	2.2	2.2
PL05	PB+To	-10.5	-7.9	-9.1	-9.2	10.2	2.0	-0.6	4.9	5.1	1.5	-10.5	-7.9	-9.1	-9.2
PL06	PB+To	-9.3	-6.5	-7.9	-7.9	7.7	0.7	-1.1	2.9	3.1	0.3	-4.6	-1.9	-3.2	-3.3
PL07	PB+To	9.0	11.7	10.4	10.3	19.5	14.6	13.1	16.1	16.2	14.2	9.0	11.7	10.4	10.3
PL08	PB+To	-1.0	7.0	3.2	3.0	28.7	11.5	7.6	18.6	18.9	11.9	-1.0	7.0	3.2	3.0
PL09	PB+To	-6.9	1.4	-2.5	-2.8	25.8	8.7	4.6	15.6	16.0	8.9	-2.7	5.2	1.5	1.3
average		-2.1	0.6	-0.7	-0.7	12.8	6.8	5.2	9.1	9.2	6.7	0.1	2.7	1.5	1.4
range		21.1	23.0	21.7	21.6	30.6	16.5	15.0	20.5	20.8	16.1	20.3	19.6	19.5	19.5
st. deviation		7.8	7.8	7.6	7.6	9.4	5.4	5.3	6.6	6.7	5.5	6.5	6.5	6.3	6.3

34CR4

case	loaded	PZa	PZb	PZc	PZd	PCa	PCa2	PCb	PCc	PCd	PCe	PPa	PPb	PPc	PPd
PZ01	PB+To	0.2	0.2	0.2	0.2	7.8	7.8	7.8	7.8	7.8	7.8	0.2	0.2	0.2	0.2
PZ02	PB+To	-3.2	-3.2	-3.2	-3.2	6.6	6.6	6.6	6.6	6.6	6.6	1.1	1.1	1.1	1.1
PZ03	PB+To	-4.7	-4.7	-4.7	-4.7	5.4	5.4	5.4	5.4	5.4	5.4	1.4	1.4	1.4	1.4
PZ04	PB+To	-3.2	-3.2	-3.2	-3.2	6.6	6.6	6.6	6.6	6.6	6.6	1.1	1.1	1.1	1.1
PZ05	PB+To	1.5	1.5	1.5	1.5	10.8	10.8	10.8	10.8	10.8	10.8	7.6	7.6	7.6	7.6
PZ06	PB+To	-1.8	-1.8	-1.8	-1.8	5.9	5.9	5.9	5.9	5.9	5.9	0.8	0.8	0.8	0.8
PZ07	PB+To	2.5	7.8	3.3	3.6	24.1	15.5	14.3	19.2	18.3	15.2	2.5	7.8	3.3	3.6
PZ08	PB+To	-1.8	3.7	-0.9	-0.7	17.5	8.0	6.7	12.2	11.2	7.7	2.5	7.7	3.3	3.5
PZ09	PB+To	-3.0	2.5	-2.2	-1.9	15.6	8.4	7.4	11.2	10.4	8.0	3.0	8.2	3.8	4.0
PZ10	PB+To	-4.8	10.1	-2.4	-1.8	28.4	11.8	10.7	19.9	18.2	12.5	-4.8	10.1	-2.4	-1.8
PZ11	PB+To	-8.0	7.7	-5.5	-4.7	28.8	12.0	10.5	20.0	18.3	12.3	-2.8	12.1	-0.4	0.2
PZ12	PB+To	-3.5	2.7	-2.6	-2.3	23.0	12.6	11.2	17.3	16.2	12.4	-3.5	2.7	-2.6	-2.3
PZ13	PB+To	0.2	11.3	1.9	2.4	28.3	15.8	14.8	21.7	20.4	16.1	5.8	16.3	7.4	7.9
PZ14	PB+To	8.6	8.6	8.6	8.6	10.4	10.4	10.4	10.4	10.4	10.4	10.9	10.9	10.9	10.9
average		-1.5	3.1	-0.8	-0.6	15.7	9.8	9.2	12.5	11.9	9.8	1.8	6.3	2.5	2.7
range		16.6	15.9	14.1	13.4	23.5	10.5	9.4	16.3	15.1	10.8	15.7	16.1	13.5	13.2
st. deviation		3.9	5.1	3.6	3.5	8.9	3.3	2.9	5.7	5.1	3.4	4.1	4.9	3.7	3.7

30NCD16 - [52], [22]

case	loaded	PZa	PZb	PZc	PZd	PCa	PCa2	PCb	PCc	PCd	PCe	PPa	PPb	PPc	PPd
PF01	PB+To	2.6	2.6	2.6	2.6	9.7	9.7	9.7	9.7	9.7	9.7	2.6	2.6	2.6	2.6
PF02	PB+To	-4.6	-4.6	-4.6	-4.6	6.5	6.5	6.5	6.5	6.5	6.5	2.2	2.2	2.2	2.2
PF03	PB+To	4.5	13.3	6.0	6.3	27.7	17.3	15.5	21.7	20.9	17.0	4.5	13.3	6.0	6.3
PF04	PB+To	2.0	10.9	3.4	3.8	27.0	16.7	14.8	21.1	20.2	16.3	4.9	13.7	6.4	6.7
PF05	PB+To	-1.5	7.7	0.0	0.4	25.1	14.5	12.6	19.0	18.1	14.1	2.9	11.8	4.4	4.7
PF06	PB+To	-2.7	6.7	-1.1	-0.8	25.2	14.5	12.5	19.0	18.1	14.1	3.8	12.7	5.3	5.6
PF07	PB+To	0.4	9.5	1.9	2.2	24.5	14.7	12.8	18.7	17.9	14.2	0.4	9.5	1.9	2.2
PF08	PB+To	-4.4	5.1	-2.8	-2.5	21.0	10.9	9.0	15.1	14.2	10.4	-3.3	6.2	-1.7	-1.3
PF09	PB+To	-9.0	0.9	-7.4	-7.0	17.0	6.3	4.2	10.6	9.7	5.7	-6.8	2.9	-5.2	-4.8
PF10	PB+To	2.3	11.3	3.8	4.1	22.0	10.3	9.0	15.6	14.7	10.6	2.3	11.3	3.8	4.1
FL01	PB+To	-1.1	8.2	0.5	0.8	21.1	12.5	10.8	15.9	15.2	12.0	-1.1	8.2	0.5	0.8
FL02	PB+To	-1.3	7.9	0.2	0.6	12.9	-0.2	-0.9	6.2	5.2	0.8	-1.3	7.9	0.2	0.6
FL04	PB+To	4.9	13.6	6.3	6.7	25.5	14.0	12.9	19.3	18.4	14.4	7.5	16.0	8.9	9.2
average		-0.6	7.2	0.7	1.0	20.4	11.4	10.0	15.3	14.5	11.2	1.4	9.1	2.7	3.0
range		13.9	18.3	13.7	13.7	21.2	17.5	16.4	15.5	15.6	16.2	14.3	13.9	14.1	14.0
st. deviation		3.8	5.0	3.8	3.9	6.6	4.7	4.4	5.1	5.0	4.5	3.7	4.4	3.6	3.6

30NCD16 – [5] – RB+TO

case	loaded	PZa	PZb	PZc	PZd	PCa	PCa2	PCb	PCc	PCd	PCe	PPa	PPb	PPc	PPd
MPA01	RB+To	-1.9	-1.9	-1.9	-1.9	1.5	1.5	1.5	1.5	1.5	1.5	-1.9	-1.9	-1.9	-1.9
MPA02	RB+To	-5.3	-5.3	-5.3	-5.3	1.4	1.4	1.4	1.4	1.4	1.4	-5.3	-5.3	-5.3	-5.3
average		-3.6	-3.6	-3.6	-3.6	1.4	1.4	1.4	1.4	1.4	1.4	-3.6	-3.6	-3.6	-3.6
range		3.3	3.3	3.3	3.3	0.0	0.0	0.0	0.0	0.0	0.0	3.3	3.3	3.3	3.3
st. deviation		1.7	1.7	1.7	1.7	0.0	0.0	0.0	0.0	0.0	0.0	1.7	1.7	1.7	1.7

30NCD16 – [5] – TEN

case	loaded	PZa	PZb	PZc	PZd	PCa	PCa2	PCb	PCc	PCd	PCe	PPa	PPb	PPc	PPd
MPA03	Ten	-7.7	-3.5	6.3	1.4	32.3	-7.4	-6.4	14.6	19.9	5.0	-7.7	-3.5	6.3	1.4
MPA04	Ten	-8.0	-4.0	5.4	0.7	30.6	-6.5	-6.2	13.7	18.7	4.6	-8.0	-4.0	5.4	0.7
MPA05	Ten	3.9	5.0	7.8	6.4	15.7	6.1	4.1	9.9	11.5	7.1	3.9	5.0	7.8	6.4
average		-3.9	-0.8	6.5	2.8	26.2	-2.6	-2.8	12.7	16.7	5.6	-3.9	-0.8	6.5	2.8
range		11.9	9.0	2.5	5.7	16.6	13.5	10.4	4.7	8.3	2.5	11.9	9.0	2.5	5.7
st. deviation		5.5	4.1	1.0	2.6	7.5	6.2	4.9	2.0	3.7	1.1	5.5	4.1	1.0	2.6

30NCD16 – [5] – PB+TO

case	loaded	PZa	PZb	PZc	PZd	PCa	PCa2	PCb	PCc	PCd	PCe	PPa	PPb	PPc	PPd
MPA06	PB	-11.4	0.8	-9.4	-8.9	17.7	5.7	3.5	10.6	9.6	5.2	-11.4	0.8	-9.4	-8.9
MPA06X	PB	-13.0	1.1	-10.6	-10.1	19.6	5.2	2.9	11.3	10.0	4.9	-13.0	1.1	-10.6	-10.1
MPA07	PB	-5.7	2.9	-4.3	-4.0	16.3	8.5	6.9	11.6	10.9	8.0	-5.7	2.9	-4.3	-4.0
MPA08	PB	0.0	4.7	0.8	1.0	15.3	11.3	10.3	12.8	12.4	10.9	0.0	4.7	0.8	1.0
MPA09	PB+To	3.5	3.5	3.5	3.5	10.6	10.6	10.6	10.6	10.6	10.6	3.5	3.5	3.5	3.5
MPA10	PB+To	-3.7	-3.7	-3.7	-3.7	7.2	7.2	7.2	7.2	7.2	7.2	3.1	3.1	3.1	3.1
MPA11	PB+To	-6.3	4.0	-4.6	-4.3	19.4	8.0	6.1	12.7	11.7	7.6	-6.3	4.0	-4.6	-4.3
MPA12	PB+To	-9.3	1.3	-7.5	-7.1	22.3	9.4	7.3	14.9	13.7	9.1	-3.4	6.6	-1.8	-1.4
MPA13	PB+To	-4.5	4.5	-3.1	-2.7	21.4	11.2	9.4	15.5	14.6	10.8	-1.8	7.0	-0.4	-0.1
MPA14	PB+To	-7.6	1.7	-6.1	-5.8	19.7	9.3	7.4	13.7	12.8	8.9	-3.6	5.4	-2.1	-1.8
MPA15	PB+To	-10.2	-0.8	-8.6	-8.3	15.8	6.2	4.3	10.2	9.3	5.6	-9.1	0.1	-7.6	-7.3
MPA16	PB+To	-10.7	-10.7	-10.7	-10.7	1.4	1.4	1.4	1.4	1.4	1.4	-4.5	-4.5	-4.5	-4.5
MPA17	PB+To	-4.1	2.1	-3.1	-2.8	12.6	4.9	3.7	8.2	7.6	4.8	-1.5	4.6	-0.5	-0.3
MPA18	PB+To	-8.4	1.1	-6.9	-6.5	20.3	9.7	7.7	14.2	13.2	9.2	-2.5	6.5	-1.1	-0.7
MPA19	PB+To	-14.7	-4.9	-13.2	-12.8	12.3	1.8	-0.2	6.0	5.1	1.3	-12.8	-3.1	-11.2	-10.8
MPA20	PB+To	-12.7	2.6	-10.2	-9.6	26.2	9.0	6.8	16.9	15.4	9.2	-7.5	7.1	-5.1	-4.5
MPA21	PB+To	-13.2	6.6	-9.8	-9.0	33.2	10.6	8.5	21.5	19.7	11.7	-8.2	10.7	-5.0	-4.2
MPA22	PB+To	0.6	9.4	2.0	2.3	13.6	1.3	0.7	7.3	6.4	2.2	0.6	9.4	2.0	2.3
MPA23	PB+To	5.7	19.0	7.9	8.4	27.1	7.6	7.8	17.8	16.4	10.2	5.7	19.0	7.9	8.4
MPA24	PB+To	-3.1	15.9	0.1	0.9	29.3	1.7	3.1	16.9	15.0	6.4	-3.1	15.9	0.1	0.9
MPA25	PB+To	-3.9	-3.9	-3.9	-3.9	4.4	4.4	4.4	4.4	4.4	4.4	-3.9	-3.9	-3.9	-3.9
MPA26	PB+To	-5.2	4.0	-3.7	-3.4	15.7	4.0	2.6	9.3	8.4	4.2	-5.2	4.0	-3.7	-3.4
MPA27	PB+To	-2.2	6.7	-0.7	-0.4	21.9	11.7	9.9	16.0	15.2	11.4	-2.2	6.7	-0.7	-0.4
MPA28	PB+To	-5.1	3.6	-3.7	-3.4	19.1	10.0	8.2	13.7	12.9	9.5	-5.1	3.6	-3.7	-3.4
MPA29	PB+To	-4.9	9.3	-2.6	-2.0	28.9	12.1	10.1	19.9	18.5	12.5	-4.9	9.3	-2.6	-2.0
MPA30	PB+To	-9.6	10.0	-6.3	-5.5	33.8	10.6	8.9	21.9	20.1	12.0	-9.6	10.0	-6.3	-5.5
average		-6.1	3.5	-4.6	-4.2	18.7	7.4	6.1	12.6	11.6	7.7	-4.3	5.2	-2.8	-2.4
range		20.5	29.8	21.0	21.2	32.3	10.8	10.8	20.5	18.6	11.2	18.7	23.5	19.1	19.2
st. deviation		5.1	6.1	4.8	4.8	8.0	3.4	3.1	5.0	4.6	3.3	4.7	5.3	4.3	4.3

XC18

case	loaded	PZa	PZb	PZc	PZd	PCa	PCa2	PCb	PCc	PCd	PCe	PPa	PPb	PPc	PPd
MPB01	PB+To	3.9	3.9	3.9	3.9	16.6	16.6	16.6	16.6	16.6	16.6	3.9	3.9	3.9	3.9
MPB02	PB+To	-0.1	-0.1	-0.1	-0.1	15.0	15.0	15.0	15.0	15.0	15.0	3.6	3.6	3.6	3.6
MPB03	PB+To	2.3	2.3	2.3	2.3	17.2	17.2	17.2	17.2	17.2	17.2	11.2	11.2	11.2	11.2
average		2.0	2.0	2.0	2.0	16.3	16.3	16.3	16.3	16.3	16.3	6.2	6.2	6.2	6.2
range		4.0	4.0	4.0	4.0	2.3	2.3	2.3	2.3	2.3	2.3	7.6	7.6	7.6	7.6
st. deviation		1.7	1.7	1.7	1.7	1.0	1.0	1.0	1.0	1.0	1.0	3.5	3.5	3.5	3.5

FGS 800-2

case	loaded	PZa	PZb	PZc	PZd	PCa	PCa2	PCb	PCc	PCd	PCe	PPa	PPb	PPc	PPd
MPC01	PB+To	4.5	4.5	4.5	4.5	3.9	3.9	3.9	3.9	3.9	3.9	4.5	4.5	4.5	4.5
MPC02	PB+To	7.6	7.6	7.6	7.6	8.6	8.6	8.6	8.6	8.6	8.6	13.2	13.2	13.2	13.2
MPC03	PB+To	3.9	3.9	3.9	3.9	2.4	2.4	2.4	2.4	2.4	2.4	3.9	3.9	3.9	3.9
MPC04	PB	-10.8	0.5	-5.0	-5.1	17.9	-3.4	0.0	9.3	9.5	2.6	-10.8	0.5	-5.0	-5.1
average		1.3	4.1	2.8	2.7	8.2	2.9	3.7	6.1	6.1	4.4	2.7	5.5	4.1	4.1
range		18.4	7.1	12.6	12.7	15.6	12.0	8.6	7.0	7.1	6.2	23.9	12.7	18.2	18.3
st. deviation		7.1	2.5	4.7	4.7	6.1	4.3	3.1	3.0	3.0	2.5	8.6	4.7	6.4	6.5

S65A

case	loaded	PZa	PZb	PZc	PZd	PCa	PCa2	PCb	PCc	PCd	PCe	PPa	PPb	PPc	PPd
G02	PB	-0.8	-0.9	2.5	1.5	20.2	11.3	5.5	12.8	14.3	9.6	-0.8	-0.9	2.5	1.5
G03	PB	0.2	0.0	6.5	4.7	35.1	15.4	4.6	19.9	22.8	13.1	0.2	0.0	6.5	4.7
G05	To	-0.2	-0.2	1.1	0.7	-0.1	-4.5	-6.9	-3.8	-3.1	-5.2	-0.2	-0.2	1.1	0.7
G06	To	2.7	2.6	5.2	4.5	10.3	-0.5	-5.2	1.7	3.2	-1.6	2.7	2.6	5.2	4.5
G07	PB+To	-3.6	-3.7	-2.3	-2.7	15.6	9.1	4.7	10.2	11.3	7.8	-3.6	-3.7	-2.3	-2.7
G08	PB+To	-3.4	-3.5	-0.6	-1.4	26.2	12.8	4.8	15.8	17.8	11.0	-3.4	-3.5	-0.6	-1.4
G09	PB+To	0.2	0.0	3.7	2.7	29.7	15.8	7.0	18.9	21.1	13.8	0.2	0.0	3.7	2.7
G10	PB+To	1.4	1.2	5.9	4.6	39.5	19.7	8.1	24.8	27.7	17.7	1.4	1.2	5.9	4.6
G11	PB+To	-8.6	-8.9	-1.6	-3.6	36.0	11.8	-1.9	18.5	22.0	9.9	-8.6	-8.9	-1.6	-3.6
G12	PB+To	-7.3	-7.6	0.3	-2.0	44.2	15.1	-0.3	23.9	28.1	13.8	-7.3	-7.6	0.3	-2.0
G13	PB+To	-4.9	-5.0	-1.5	-2.5	8.6	-5.0	-11.5	-1.0	1.0	-5.5	-4.9	-5.0	-1.5	-2.5
G14	PB+To	-7.6	-7.9	-0.8	-2.8	23.0	-4.7	-15.3	5.4	9.0	-3.2	-7.6	-7.9	-0.8	-2.8
G15	PB+To	-6.4	-6.5	-2.5	-3.7	13.2	-4.4	-12.6	1.1	3.5	-4.7	-6.4	-6.5	-2.5	-3.7
G16	PB+To	-8.2	-8.5	-1.2	-3.3	27.3	-3.3	-15.2	8.1	12.1	-1.5	-8.2	-8.5	-1.2	-3.3
G17	PB+To	-3.8	-4.0	0.9	-0.5	22.0	-1.0	-10.8	6.3	9.4	-1.1	-3.8	-4.0	0.9	-0.5
G18	PB+To	-4.4	-4.7	3.0	0.8	35.4	1.2	-11.8	14.1	18.4	3.3	-4.4	-4.7	3.0	0.8
G19	PB+To	3.5	3.5	3.5	3.5	10.6	10.6	10.6	10.6	10.6	10.6	3.5	3.5	3.5	3.5
G20	PB+To	0.1	0.1	0.1	0.1	6.1	6.1	6.1	6.1	6.1	6.1	0.1	0.1	0.1	0.1
G21	PB+To	1.2	1.2	1.2	1.2	1.6	1.6	1.6	1.6	1.6	1.6	1.2	1.2	1.2	1.2
G22	PB+To	-0.8	-0.9	2.8	1.7	26.7	13.6	5.6	16.4	18.4	11.7	-0.8	-0.9	2.8	1.7
G23	PB+To	1.0	0.9	4.6	3.5	22.8	11.4	4.9	13.7	15.4	9.8	1.0	0.9	4.6	3.5
G24	PB+To	1.7	1.6	5.3	4.2	21.9	8.0	0.5	11.6	13.6	6.8	1.7	1.6	5.3	4.2
G25	PB+To	-7.2	-7.5	0.3	-1.9	42.3	13.8	-1.2	22.1	26.2	12.2	-7.2	-7.5	0.3	-1.9
G26	PB+To	-7.5	-7.7	0.1	-2.1	38.6	9.2	-4.5	17.5	21.8	7.6	-7.5	-7.7	0.1	-2.1
G27	PB+To	-11.8	-12.1	-3.9	-6.2	34.3	1.7	-12.8	12.7	17.1	2.0	-11.8	-12.1	-3.9	-6.2
G28	PB+To	3.2	3.1	6.4	5.4	25.0	14.2	7.4	16.6	18.2	12.6	3.2	3.1	6.4	5.4
G29	PB+To	0.4	0.4	1.7	1.3	16.8	10.4	6.1	11.5	12.6	9.1	0.4	0.4	1.7	1.3
average		-2.6	-2.8	1.5	0.3	23.4	7.0	-1.2	11.7	14.1	6.2	-2.6	-2.8	1.5	0.3
range		15.3	15.6	10.4	11.6	44.3	24.6	25.9	28.6	31.2	23.2	15.3	15.6	10.4	11.6
st. deviation		4.2	4.3	2.9	3.1	12.2	7.5	8.1	7.5	8.3	6.7	4.2	4.3	2.9	3.1

APPENDIX V SUMMARY OF RESULTS OF THE NEW PROPOSALS

The final criteria selected are PZc (reported also as PZv2), PZd (PZ) and PCe (PC). Their columns are further darkened in order to enable their fast localisation. The numerical values in following tables concern directly ΔFI results of described groups or their statistical evaluation. All are expressed in %.

MATERIAL & LOAD TYPE – AVERAGE

case	ref.	loaded	tests	PZa	PZb	PZc	PZd	PCa	PCa2	PCb	PCc	PCd	PCe	PPa	PPb	PPc	PPd
hard steel	[13]	PB+To	10	3.9	3.9	3.9	3.9	10.5	10.5	10.5	10.5	10.5	10.5	6.5	6.5	6.5	6.5
mild steel	[13]	PB+To	8	4.4	4.4	4.4	4.4	14.9	14.9	14.9	14.9	14.9	14.9	7.5	7.5	7.5	7.5
hard steel	[52]	PB+To	10	1.6	1.6	1.6	1.6	8.7	8.7	8.7	8.7	8.7	8.7	4.0	4.0	4.0	4.0
42CrMo4	[52]	PB+To	9	-2.1	0.6	-0.7	-0.7	12.8	6.8	5.2	9.1	9.2	6.7	0.1	2.7	1.5	1.4
34Cr4	[52]	PB+To	14	-1.5	3.1	-0.8	-0.6	15.7	9.8	9.2	12.5	11.9	9.8	1.8	6.3	2.5	2.7
30NCD16	[22]	PB+To	13	-0.6	7.2	0.7	1.0	20.4	11.4	10.0	15.3	14.5	11.2	1.4	9.1	2.7	3.0
30NCD16	[5]	Rb+To	2	-3.6	-3.6	-3.6	-3.6	1.4	1.4	1.4	1.4	1.4	1.4	-3.6	-3.6	-3.6	-3.6
30NCD16	[5]	Ten	3	-3.9	-0.8	6.5	2.8	26.2	-2.6	-2.8	12.7	16.7	5.6	-3.9	-0.8	6.5	2.8
30NCD16	[5]	PB+To	26	-6.1	3.5	-4.6	-4.2	18.7	7.4	6.1	12.6	11.6	7.7	-4.3	5.2	-2.8	-2.4
XC18	[5]	PB+To	3	2.0	2.0	2.0	2.0	16.3	16.3	16.3	16.3	16.3	16.3	6.2	6.2	6.2	6.2
FGS800-2	[5]	PB+To	4	1.3	4.1	2.8	2.7	8.2	2.9	3.7	6.1	6.1	4.4	2.7	5.5	4.1	4.1
S65A	[29]	PB+To	27	-2.6	-2.8	1.5	0.3	23.4	7.0	-1.2	11.7	14.1	6.2	-2.6	-2.8	1.5	0.3
range				10.5	10.8	11.1	8.5	24.7	18.9	19.1	14.8	15.3	14.8	11.8	12.7	11.1	11.1
standard deviation				3.1	3.0	3.1	2.6	6.7	5.2	5.7	4.0	4.3	4.1	4.1	3.9	3.4	3.3

MATERIAL & LOAD TYPE – RANGE

case	ref.	loaded	tests	PZa	PZb	PZc	PZd	PCa	PCa2	PCb	PCc	PCd	PCe	PPa	PPb	PPc	PPd
hard steel	[13]	PB+To	10	4.3	4.3	4.3	4.3	6.5	6.5	6.5	6.5	6.5	6.5	7.8	7.8	7.8	7.8
mild steel	[13]	PB+To	8	9.0	9.0	9.0	9.0	11.2	11.2	11.2	11.2	11.2	11.2	17.1	17.1	17.1	17.1
hard steel	[52]	PB+To	10	3.9	3.9	3.9	3.9	7.2	7.2	7.2	7.2	7.2	7.2	8.8	8.8	8.8	8.8
42CrMo4	[52]	PB+To	9	21.1	23.0	21.7	21.6	30.6	16.5	15.0	20.5	20.8	16.1	20.3	19.6	19.5	19.5
34Cr4	[52]	PB+To	14	16.6	15.9	14.1	13.4	23.5	10.5	9.4	16.3	15.1	10.8	15.7	16.1	13.5	13.2
30NCD16	[22]	PB+To	13	13.9	18.3	13.7	13.7	21.2	17.5	16.4	15.5	15.6	16.2	14.3	13.9	14.1	14.0
30NCD16	[5]	Rb+To	2	3.3	3.3	3.3	3.3	0.0	0.0	0.0	0.0	0.0	0.0	3.3	3.3	3.3	3.3
30NCD16	[5]	Ten	3	11.9	9.0	2.5	5.7	16.6	13.5	10.4	4.7	8.3	2.5	11.9	9.0	2.5	5.7
30NCD16	[5]	PB+To	26	20.5	29.8	21.0	21.2	32.3	10.8	10.8	20.5	18.6	11.2	18.7	23.5	19.1	19.2
XC18	[5]	PB+To	3	4.0	4.0	4.0	4.0	2.3	2.3	2.3	2.3	2.3	2.3	7.6	7.6	7.6	7.6
FGS800-2	[5]	PB+To	4	18.4	7.1	12.6	12.7	15.6	12.0	8.6	7.0	7.1	6.2	23.9	12.7	18.2	18.3
S65A	[29]	PB+To	27	15.3	15.6	10.4	11.6	44.3	24.6	25.9	28.6	31.2	23.2	15.3	15.6	10.4	11.6
maximum				21.1	29.8	21.7	21.6	44.3	24.6	25.9	28.6	31.2	23.2	23.9	23.5	19.5	19.5
average				11.9	11.9	10.1	10.4	17.6	11.1	10.3	11.7	12.0	9.5	13.7	12.9	11.8	12.2

MATERIAL & LOAD TYPE - STANDARD DEVIATION

case	ref.	loaded	tests	PZa	PZb	PZc	PZd	PCa	PCa2	PCb	PCc	PCd	PCe	PPa	PPb	PPc	PPd
hard steel	[13]	PB+To	10	1.5	1.5	1.5	1.5	2.3	2.3	2.3	2.3	2.3	2.3	2.8	2.8	2.8	2.8
mild steel	[13]	PB+To	8	2.5	2.5	2.5	2.5	3.2	3.2	3.2	3.2	3.2	3.2	4.6	4.6	4.6	4.6
hard steel	[52]	PB+To	10	1.1	1.1	1.1	1.1	2.1	2.1	2.1	2.1	2.1	2.1	2.8	2.8	2.8	2.8
42CrMo4	[52]	PB+To	9	7.8	7.8	7.6	7.6	9.4	5.4	5.3	6.6	6.7	5.5	6.5	6.5	6.3	6.3
34Cr4	[52]	PB+To	14	3.9	5.1	3.6	3.5	8.9	3.3	2.9	5.7	5.1	3.4	4.1	4.9	3.7	3.7
30NCD16	[22]	PB+To	13	3.8	5.0	3.8	3.9	6.6	4.7	4.4	5.1	5.0	4.5	3.7	4.4	3.6	3.6
30NCD16	[5]	Rb+To	2	1.7	1.7	1.7	1.7	0.0	0.0	0.0	0.0	0.0	0.0	1.7	1.7	1.7	1.7
30NCD16	[5]	Ten	3	5.5	4.1	1.0	2.6	7.5	6.2	4.9	2.0	3.7	1.1	5.5	4.1	1.0	2.6
30NCD16	[5]	PB+To	26	5.1	6.1	4.8	4.8	8.0	3.4	3.1	5.0	4.6	3.3	4.7	5.3	4.3	4.3
XC18	[5]	PB+To	3	1.7	1.7	1.7	1.7	1.0	1.0	1.0	1.0	1.0	1.0	3.5	3.5	3.5	3.5
FGS800-2	[5]	PB+To	4	7.1	2.5	4.7	4.7	6.1	4.3	3.1	3.0	3.0	2.5	8.6	4.7	6.4	6.5
S65A	[29]	PB+To	27	4.2	4.3	2.9	3.1	12.2	7.5	8.1	7.5	8.3	6.7	4.2	4.3	2.9	3.1
maximum				7.8	7.8	7.6	7.6	12.2	7.5	8.1	7.5	8.3	6.7	8.6	6.5	6.4	6.5
average				3.8	3.6	3.1	3.2	5.6	3.6	3.4	3.6	3.7	3.0	4.4	4.1	3.6	3.8

PARTIAL EFFECTS - AVERAGE

case	tests	PZa	PZb	PZc	PZd	PCa	PCa2	PCb	PCc	PCd	PCe	PPa	PPb	PPc	PPd
All	129	-1.5	2.0	0.3	0.0	17.0	8.5	6.2	11.8	12.1	8.6	0.3	3.8	2.1	1.8
P	61	-1.1	1.1	1.2	0.7	18.6	8.4	4.4	11.8	12.6	8.1	-1.1	1.1	1.2	0.7
NP	55	-1.4	2.3	-0.7	-0.6	14.3	9.8	9.1	11.7	11.4	9.7	2.8	6.4	3.5	3.6
nMS	56	1.6	1.6	1.6	1.6	9.1	9.1	9.1	9.1	9.1	9.1	4.3	4.3	4.3	4.3
MS	73	-3.9	2.3	-0.8	-1.2	23.0	8.0	4.0	13.9	14.3	8.1	-2.8	3.4	0.4	0.0
P, nMS	23	2.3	2.3	2.3	2.3	8.3	8.3	8.3	8.3	8.3	8.3	2.3	2.3	2.3	2.3
NP, nMS	33	1.1	1.1	1.1	1.1	9.7	9.7	9.7	9.7	9.7	9.7	5.7	5.7	5.7	5.7
MS - torsion	12	-1.7	0.8	-0.3	-0.5	15.5	7.4	4.5	9.9	10.2	6.7	-0.5	2.0	0.9	0.8
MS - axial	44	-4.4	4.9	-1.5	-1.5	22.5	7.9	5.9	14.5	14.2	8.7	-2.9	6.2	-0.1	-0.1
NP - 90 deg	34	-2.3	1.9	-1.5	-1.3	14.5	9.3	8.5	11.6	11.2	9.3	2.7	6.8	3.5	3.6
NP - 90 deg, nMS	20	0.9	0.9	0.9	0.9	9.5	9.5	9.5	9.5	9.5	9.5	6.3	6.3	6.3	6.3
NP - not 90 deg	21	-0.3	2.6	0.1	0.2	14.1	10.7	10.1	12.1	11.8	10.6	3.1	5.9	3.5	3.7
NP - not 90 deg, nMS	13	1.4	1.4	1.4	1.4	10.0	10.0	10.0	10.0	10.0	10.0	4.7	4.7	4.7	4.7

PARTIAL EFFECTS - RANGE

case	tests	PZa	PZb	PZc	PZd	PCa	PCa2	PCb	PCc	PCd	PCe	PPa	PPb	PPc	PPd
All	129	24.6	31.1	23.5	23.1	46.1	27.1	33.9	28.6	31.2	24.0	29.6	31.1	27.8	27.5
P	61	21.6	25.4	18.9	19.0	44.3	24.6	32.6	28.6	31.2	23.2	21.6	25.4	18.9	19.0
NP	55	23.7	24.9	23.5	23.1	35.1	20.4	20.4	23.6	22.3	20.4	29.4	23.0	27.8	27.5
nMS	56	21.1	21.1	21.1	21.1	20.4	20.4	20.4	20.4	20.4	20.4	23.0	23.0	23.0	23.0
MS	73	23.7	31.1	23.5	23.1	44.3	27.1	30.9	28.6	31.2	23.2	21.9	31.1	21.6	21.1
P, nMS	23	15.1	15.1	15.1	15.1	15.9	15.9	15.9	15.9	15.9	15.9	15.1	15.1	15.1	15.1
NP, nMS	33	19.9	19.9	19.9	19.9	20.4	20.4	20.4	20.4	20.4	20.4	23.0	23.0	23.0	23.0
MS - torsion	12	19.5	19.6	19.5	19.5	26.3	20.0	21.2	23.0	21.4	20.5	19.5	19.6	19.5	19.5
MS - axial	44	20.5	26.9	21.0	21.2	26.5	24.7	30.9	22.9	21.8	22.5	20.4	26.9	20.1	20.0
NP - 90 deg	34	23.4	24.9	21.8	21.4	35.1	20.4	20.4	23.6	22.3	20.4	29.4	23.0	27.8	27.5
NP - 90 deg, nMS	20	19.9	19.9	19.9	19.9	20.4	20.4	20.4	20.4	20.4	20.4	23.0	23.0	23.0	23.0
NP - not 90 deg	21	14.8	14.1	13.3	12.9	21.5	11.7	13.0	15.6	14.7	11.7	20.3	13.5	18.8	18.5
NP - not 90 deg, nMS	13	7.8	7.8	7.8	7.8	10.3	10.3	10.3	10.3	10.3	10.3	7.7	7.7	7.7	7.7

PARTIAL EFFECTS - STANDARD DEVIATION

case	tests	PZa	PZb	PZc	PZd	PCa	PCa2	PCb	PCc	PCd	PCe	PPa	PPb	PPc	PPd
All	129	5.5	5.6	4.9	4.7	9.8	5.8	6.9	5.9	6.0	5.2	6.0	6.1	5.0	5.0
P	61	4.7	5.6	3.7	3.7	11.4	6.1	8.0	6.7	7.1	5.8	4.7	5.6	3.7	3.7
NP	55	6.0	5.0	5.5	5.4	7.7	4.3	4.5	5.3	5.0	4.4	6.2	5.0	5.7	5.6
nMS	56	4.2	4.2	4.2	4.2	4.6	4.6	4.6	4.6	4.6	4.6	4.5	4.5	4.5	4.5
MS	73	5.1	6.5	5.1	4.7	8.4	6.5	7.5	5.9	6.1	5.5	5.0	7.0	4.7	4.5
P, nMS	23	3.3	3.3	3.3	3.3	4.6	4.6	4.6	4.6	4.6	4.6	3.3	3.3	3.3	3.3
NP, nMS	33	4.7	4.7	4.7	4.7	4.5	4.5	4.5	4.5	4.5	4.5	4.8	4.8	4.8	4.8
MS - torsion	12	5.0	5.4	5.1	5.0	7.2	6.2	6.5	6.8	6.5	6.3	4.8	5.6	4.8	4.8
MS - axial	44	5.2	5.8	5.3	4.9	6.4	6.3	6.5	5.2	5.0	5.0	5.1	6.1	5.1	4.8
NP - 90 deg	34	6.7	5.7	6.1	6.0	8.4	4.8	5.0	5.9	5.6	4.9	7.1	5.7	6.5	6.4
NP - 90 deg, nMS	20	5.7	5.7	5.7	5.7	5.1	5.1	5.1	5.1	5.1	5.1	5.8	5.8	5.8	5.8
NP - not 90 deg	21	3.8	3.1	3.4	3.3	6.2	3.5	3.6	4.2	4.0	3.5	4.5	3.5	4.1	4.0
NP - not 90 deg, nMS	13	2.3	2.3	2.3	2.3	3.2	3.2	3.2	3.2	3.2	3.2	2.3	2.3	2.3	2.3

APPENDIX VI BRITTLE MATERIALS

GREY CAST IRON [13]

The grey cast iron referred has very dissimilar fatigue properties in comparison to the other tested materials (see Tab. 2) – namely the fatigue limits ratio κ which is close to one. Thus the behaviour of criteria is largely different. This applies mainly to integral criteria where either *a* or *b* parameter tends to be negative or even cannot be computed (KIA formula).

Although the CPA criteria do not have so large scatter, their trends are very similar. The only formula, which leads to distinctly other results, is the GAM criterion. It gives the best results available as well. The use of maximum principal stress in the criterion seems to work well here.

The two chosen criteria are the two more darkened – PZ4 is the carrier of the PZ and PZv2, whereas the PC4 is the carrier of PC formula. Results of the PC4 carrier are very satisfactorily, because they coincide well with the overall results. The integral method represented by carrier PZ4 cannot be used for the brittle material as is the grey cast iron here. Some reflection is required due to interesting behaviour of pairs {PZ4, PZ9} and {PP3, PP4} where the carriers with integration of N_{max} and with maximum hydrostatic stress are shown respectively. The maximum hydrostatic stress leads to much better results here, though they are still largely on conservative side. It can indicate possible usability of the integral criteria even in this category.

Unfortunately no results with mean loads were available. Since there are only 6 tests results for the only one material, further broader analysis in the area of brittle materials is necessary. This is the principal reason, why the analysis described is inserted in the appendix instead of the main report.

case	loaded	Sines	Cross	Ppd	FCS	KCP	KIA	McD	DV	Matake	Z&L	SpaM	GAM
CS24	PB+To	-36.0%	2.8%	2.8%	3.4%	3.4%	***	-32.1%	3.4%	3.4%	1.4%	3.1%	3.3%
CS25	PB+To	-30.2%	3.8%	3.8%	5.6%	5.6%	***	-25.1%	5.6%	5.7%	-2.0%	4.7%	5.4%
CS26	PB+To	-17.4%	5.6%	5.6%	8.4%	8.4%	***	-11.6%	8.4%	8.4%	-5.2%	5.9%	8.1%
CS28	PB+To	-34.0%	8.4%	12.6%	13.0%	13.0%	***	-29.6%	8.4%	12.5%	11.2%	11.0%	8.9%
CS29	PB+To	-38.5%	1.0%	20.9%	19.1%	19.1%	***	-25.6%	1.1%	48.9%	15.5%	14.2%	3.4%
CS30	PB+To	-5.6%	23.5%	33.7%	16.5%	16.5%	***	9.9%	29.5%	64.6%	21.6%	20.1%	3.8%
average		-27.0%	7.5%	13.2%	11.0%	11.0%	***	-19.0%	9.4%	23.9%	7.1%	9.8%	5.5%
range		32.9%	22.4%	30.9%	15.7%	15.7%	***	42.0%	28.4%	61.2%	26.8%	16.9%	5.6%
st. deviation		11.7%	7.5%	11.1%	5.7%	5.7%	***	14.5%	9.4%	23.8%	9.7%	6.0%	2.2%

case	loaded	PZ1	PZ3	PZ4	PZ9	PC4	PP1	PP2	PP3	PP4	PP5
CS24	PB+To	3.3	1.4	2.1	1.7	1.6	1.4	1.4	2.1	1.7	3.3
CS25	PB+To	8.4	-2.0	5.2	1.7	2.3	-2.0	-2.0	5.2	1.7	8.4
CS26	PB+To	23.7	-5.2	15.9	2.6	3.1	-5.2	-5.2	15.9	2.6	23.7
CS28	PB+To	13.6	10.0	9.3	7.3	5.9	10.9	10.9	10.3	8.3	15.1
CS29	PB+To	25.9	10.2	17.5	9.9	9.4	14.1	14.2	21.3	13.9	31.6
CS30	PB+To	56.7	15.3	38.1	20.5	15.2	19.9	20.0	42.0	24.9	62.0
average		21.9	5.0	14.7	7.3	6.3	6.5	6.6	16.1	8.8	24.0
range		53.3	20.5	36.0	18.8	13.7	25.1	25.2	39.9	23.2	58.7
st. deviation		17.4	7.3	11.8	6.7	4.8	9.1	9.1	13.2	8.4	19.4

APPENDIX VII PARAMETERS OF THE PZB FORMULA

FULLY REVERSED TORSION

The uniaxial test in fully reversed torsion is suitable for derivation of the *a* parameter. The three load components necessary in (132) can be derived from (18), (19) and (26):

$$\begin{aligned} N_a &= t_{-1}\cdot\sin(2\varphi)\sin^2\psi,\\ N_m &= 0,\\ C_a &= \sqrt{t_{-1}^2\cdot\left[\cos^2(2\varphi)\cdot\sin^2\psi+\frac{1}{4}\sin^2(2\varphi)\cdot\sin^2(2\psi)\right]}. \end{aligned} \qquad \text{(A1)}$$

Since the fatigue limit is examined the inequality in (132) becomes an equality. It can be integrated as:

$$\begin{aligned} f_{-1}^2 &= \frac{1}{4\pi}\int_\varphi\int_\psi\left(a\cdot C_a^2+b\cdot N_a+d\cdot N_m\right)\sin\psi d\psi d\varphi =\\ &= \frac{1}{4\pi}\int_\varphi\int_\psi\left\{at_{-1}^2\left[\cos^2(2\varphi)\sin^2\psi+\frac{1}{4}\sin^2(2\varphi)\sin^2(2\psi)\right]+bt_{-1}\sin(2\varphi)\sin^2\psi\right\}\sin\psi d\psi d\varphi =\\ &= \frac{1}{4\pi}\left\{at_{-1}^2\left[\frac{8}{5}\pi\right]+b\cdot 0\right\}=\frac{2}{5}at_{-1}^2. \end{aligned} \qquad \text{(A2)}$$

Thus the *a* parameter is:

$$a=\frac{5f_{-1}^2}{2t_{-1}^2}=\frac{5}{2}\kappa^2. \qquad \text{(A3)}$$

FULLY REVERSED AXIAL LOADING

Once the *a* parameter is set, the second fatigue limit in reversed loading leads to the other parameter of the basic PZ4 carrier. First the load components have to be derived:

$$\begin{aligned} N_a &= f_{-1}\cdot\cos^2\varphi\sin^2\psi,\\ N_m &= 0,\\ C_a &= \sqrt{\frac{f_{-1}^2}{4}\cdot\left[\sin^2(2\varphi)\cdot\sin^2\psi+\cos^4\varphi\cdot\sin^2(2\psi)\right]}. \end{aligned} \qquad \text{(A4)}$$

Then the equality comes to be:

$$\begin{aligned} f_{-1}^2 &= \frac{1}{4\pi}\int_\varphi\int_\psi\left(a\cdot C_a^2+b\cdot N_a+d\cdot N_m\right)\sin\psi d\psi d\varphi =\\ &= \frac{1}{4\pi}\int_\varphi\int_\psi\left\{\frac{af_{-1}^2}{4}\left[\sin^2(2\varphi)\sin^2\psi+\cos^4\varphi\sin^2(2\psi)\right]+bf_{-1}\cos^2\varphi\sin^2\psi\right\}\sin\psi d\psi d\varphi =\\ &= \frac{1}{4\pi}\left\{af_{-1}^2\left[\frac{8}{15}\pi\right]+bf_{-1}\frac{4\pi}{3}\right\}=\frac{2}{15}af_{-1}^2+\frac{1}{3}bf_{-1}=\frac{\kappa^2f_{-1}^2}{3}+\frac{bf_{-1}}{3}, \end{aligned} \qquad \text{(A5)}$$

which means that the value of *b* can be computed as:

$$b=3f_{-1}-\kappa^2f_{-1}=f_{-1}\left(3-\kappa^2\right). \qquad \text{(A6)}$$

REPEATED AXIAL LOADING

To get the last *d* parameter a fatigue limit of loading where the N_m component is non-zero is necessary. The fatigue limit in repeated axial loading is a suitable candidate:

$$\begin{aligned} N_a &= N_m = \frac{f_0}{2}\cdot\cos^2\varphi\sin^2\psi, \\ C_a &= \sqrt{\frac{f_0^2}{16}\cdot\left[\sin^2(2\varphi)\cdot\sin^2\psi+\cos^4\varphi\cdot\sin^2(2\psi)\right]}. \end{aligned} \qquad \text{(A7)}$$

The similarity between N_a and N_m components helps to solve the integration quickly:

$$\begin{aligned} f_{-1}^2 &= \frac{1}{4\pi}\int_\varphi\int_\psi\left(a\cdot C_a^2+b\cdot N_a+d\cdot N_m\right)\sin\psi d\psi d\varphi = \\ &= \frac{1}{4\pi}\int_\varphi\int_\psi\left\{\frac{af_0^2}{16}\left[\sin^2(2\varphi)\sin^2\psi+\cos^4\varphi\sin^2(2\psi)\right]+\frac{(b+d)}{2}f_0\cos^2\varphi\sin^2\psi\right\}\sin\psi d\psi d\varphi = \\ &= \frac{1}{4\pi}\left\{af_0^2\left[\frac{2}{15}\pi\right]+(b+d)f_0\frac{2\pi}{3}\right\} = \frac{1}{30}af_0^2+\frac{1}{6}(b+d)f_0 = \frac{\kappa^2 f_0^2}{12}+\frac{(b+d)f_0}{6}. \end{aligned} \qquad \text{(A8)}$$

The result directly follows to be:

$$d = f_0\left[6\left(\frac{f_{-1}}{f_0}\right)^2-\frac{\kappa^2}{2}-\frac{b}{f_0}\right]. \qquad \text{(A9)}$$

APPENDIX VIII PARAMETERS OF THE PCB FORMULA

FULLY REVERSED AXIAL LOADING

The load parameters are already summarised in (A4). Since the load is related directly to fatigue limit, the inequality in (120) becomes an equality:

$$f_{-1}^2 = aC_a^2 + bN_a + dN_m = \frac{af_{-1}^2}{4}\left[\sin^2(2\varphi_f)\sin^2\psi_f + \cos^4\varphi_f \sin^2(2\psi_f)\right] + bf_{-1}\cos^2\varphi_f \sin^2\psi_f . \quad \text{(A10)}$$

The index *f* put to the φ and ψ angles is related to the one direction where the equality is fulfilled. The criterion is defined as a maximum damage approach, which means that two derivations of the (A10) relation should be equal to zero at this position:

$$\frac{\partial f_{-1}}{\partial \varphi_f} = \frac{af_{-1}^2}{2}\sin(4\varphi_f)\sin^2\psi_f - af_{-1}^2\cos^3\varphi_f \sin\varphi_f \sin^2(2\psi_f) - bf_{-1}\sin(2\varphi_f)\sin^2\psi_f = 0 \quad \text{(A11)}$$

and

$$\frac{\partial f_{-1}}{\partial \psi_f} = af_{-1}^2 \sin^2(2\varphi_f)\sin(2\psi_f) + 2af_{-1}^2\cos^4\varphi_f \sin(4\psi_f) + bf_{-1}\cos^2\varphi_f \sin(2\psi_f) = 0 . \quad \text{(A12)}$$

The three equation (A10) – (A12) are described with the use of together 4 unknown parameters. These are *a*, *b*, φ_f and ψ_f. There is no other way how to solve it if another load condition is simultaneously used.

FULLY REVERSED TORSION

The load parameters were written in (A1). The final equality has a form:

$$f_{-1}^2 = at_{-1}^2\left[\cos^2(2\varphi_t)\sin^2\psi_t + \frac{1}{4}\sin^2(2\varphi_t)\sin^2(2\psi_t)\right] + bt_{-1}\sin(2\varphi_t)\sin^2\psi_t . \quad \text{(A13)}$$

In order to represent the MD approach, the partial derivations have to be zero:

$$\frac{\partial f_{-1}}{\partial \varphi_t} = -2at_{-1}^2\sin(4\varphi_t)\sin^2\psi_t + \frac{at_{-1}^2}{2}\sin(4\varphi_t)\sin^2(2\psi_t) + 2bt_{-1}\cos(2\varphi_t)\sin^2\psi_t = 0 , \quad \text{(A14)}$$

and

$$\frac{\partial f_{-1}}{\partial \psi_t} = at_{-1}^2\cos^2(2\varphi_t)\sin(2\psi_t) + \frac{at_{-1}^2}{2}\sin^2(2\varphi_t)\sin(4\psi_t) + bt_{-1}\sin(2\varphi_t)\sin(2\psi_t) = 0 . \quad \text{(A15)}$$

COMPLETION

The system of 6 non-linear equations with 6 unknown *a*, *b*, φ_f, ψ_f, φ_t and ψ_t was solved with a polytop optimisation algorithm by minimization of a sum of squares of equations' deviations from the equality. All materials mentioned in this report were tested. Results of several parameters could be unambiguously detected to be:

$$b = f_{-1}; \qquad \varphi_f = 0; \qquad \psi_f = \psi_t = \frac{\pi}{2}. \quad \text{(A16)}$$

Although only one unknown (*a* parameter) rests in the system of equations (A10) - (A12), the equations cannot be used for its derivation, because they all lead to multivalent solutions. The use of the second triad is necessary. Precisely the first two equations (A13) and (A14) lead to:

$$f_{-1}^2 = at_{-1}^2\left[\cos^2(2\varphi_t) + 0\right] + f_{-1}t_{-1}\sin(2\varphi_t) = at_{-1}^2\left[1 - \sin^2(2\varphi_t)\right] + f_{-1}t_{-1}\sin(2\varphi_t) \quad \text{(A17)}$$

and

$$\frac{\partial f_{-1}}{\partial \varphi_t} = -2at_{-1}^2 \sin(4\varphi_t) + 2f_{-1}t_{-1}\cos(2\varphi_t) = 0 \tag{A18}$$

If the (A18) relation is divided by $\cos(2\varphi_t)$:

$$-4at_{-1}^2 \sin(2\varphi_t) + 2f_{-1}t_{-1} = 0\,, \tag{A19}$$

it allows substituting the $\sin(2\varphi_t)$ in the (A17) relation. It becomes:

$$f_{-1}^2 = at_{-1}^2\left[1-\left(\frac{f_{-1}}{2at_{-1}}\right)^2\right] + f_{-1}t_{-1}\frac{f_{-1}}{2at_{-1}}\,. \tag{A20}$$

The resulting quadratic equation has two roots:

$$a_{1,2} = \frac{\kappa^2}{2} \pm \frac{\sqrt{\kappa^4-\kappa^2}}{2}\,, \tag{A21}$$

but only that with positive sign leads to positive values of *a*. Then it follows to be:

$$a = \frac{\kappa^2}{2} + \frac{\sqrt{\kappa^4-\kappa^2}}{2}\,. \tag{A22}$$

Results of the derived formula perfectly coincide with results obtained from the polytop method.

REPEATED AXIAL LOADING

Once the *a* and *b* parameters are set, the last parameter can be derived similarly from the maximization of left hand side of the (120) formula:

$$f_{-1}^2 = \frac{af_0^2}{16}\left[\sin^2(2\varphi_r)\sin^2\psi_r + \cos^4\varphi_r\sin^2(2\psi_r)\right] + (b+d)\frac{f_0}{2}\cos^2\varphi_r\sin^2\psi_r\,. \tag{A23}$$

$$\frac{\partial f_{-1}}{\partial \varphi_r} = \frac{af_0^2}{8}\sin(4\varphi_r)\sin^2\psi_r - \frac{af_0^2}{4}\cos^3\varphi_r\sin\varphi_r\sin^2(2\psi_r) - \frac{(b+d)}{2}f_0\sin(2\varphi_r)\sin^2\psi_r = 0 \tag{A24}$$

$$\frac{\partial f_{-1}}{\partial \psi_r} = \frac{af_0^2}{16}\sin^2(2\varphi_r)\sin(2\psi_r) + \frac{af_0^2}{8}\cos^4\varphi_r\sin(4\psi_r) + \frac{(b+d)}{2}f_0\cos^2\varphi_r\sin(2\psi_r) = 0\,. \tag{A25}$$

The optimization of solution so that all three non-linear equations can hold trrue is used. Its use on the material parameters of all materials evaluated here leads to the same solution of angles of the critical plane:

$$\varphi_r = 0; \qquad \psi_r = \frac{\pi}{2}. \tag{A26}$$

In order to get the *d* parameter, the (A23) equation should be further analyzed:

$$\begin{aligned} f_{-1}^2 &= (b+d)\frac{f_0}{2}, \\ d &= f_{-1}\left[2\frac{f_{-1}}{f_0}-1\right] \end{aligned} \tag{A27}$$

APPENDIX IX SPECIFICATION OF THE PCB EXTREMES

In order to reach really a maximum of damage in the given directions φ and ψ, the conditions given in (146) and (147) has to be fulfilled.

FULLY REVERSED AXIAL LOADING

The second derivations are computed as follows:

$$\frac{\partial^2 f_{-1}}{\partial \varphi_f^2} = 2a\cos(4\varphi_f)\sin^2\psi_f + (4\sin^2\varphi_f - 1)a\cos^2\varphi_f\sin^2(2\psi_f) - \frac{2b}{f_{-1}}\cos(2\varphi_f)\sin^2\psi_f$$
$$\frac{\partial^2 f_{-1}}{\partial \varphi_f^2} = 2a - \frac{2b}{f_{-1}}, \qquad \text{(A28)}$$

$$\frac{\partial^2 f_{-1}}{\partial \psi_f^2} = \frac{a}{2}\sin^2(2\varphi_f)\cos(2\psi_f) + 2a\cos^4\varphi_f\cos(4\psi_f) + \frac{2b}{f_{-1}}\cos^2\varphi_f\cos(2\psi_f) = 2a - \frac{2b}{f_{-1}}. \qquad \text{(A29)}$$

and

$$\frac{\partial^2 f_{-1}}{\partial \varphi_f \partial \psi_f} = \frac{a}{2}\sin(4\varphi_f)\sin(2\psi_f) - 2a\cos^3\varphi_f\sin\varphi_f\sin(4\psi_f) - \frac{b}{f_{-1}}\sin(2\varphi_f)\sin(2\psi_f) = 0. \qquad \text{(A30)}$$

Here the angles φ_f and ψ_f determined in the Appendix VIII were introduced. The condition (146) can be rewritten as:

$$\left(2a - \frac{2b}{f_{-1}}\right)^2 > 0. \qquad \text{(A31)}$$

which is satisfied automatically thanks to the square. Both derivations (A28) and (A29) have the same form of results. If the maximum of the f_{-1} equation (A10) is located according to the φ_f and ψ_f angles, the inequality has to be obeyed:

$$2a < \frac{2b}{f_{-1}} \qquad \text{(A32)}$$

The a and b parameters were quantified in (A16) and (A22). When introduced, they give:

$$\kappa < \frac{2}{\sqrt{3}} = 1.1547 \qquad \text{(A33)}$$

If the extreme found has to be a maximum, the method can be applied only to materials with as low κ ratio as corresponds e.g. to grey cast iron here or to brittle material generally.

FULLY REVERSED TORSION

The technique is the same:

$$\frac{\partial^2 t_{-1}}{\partial \varphi_t^2} = -8a\cos(4\varphi_t)\sin^2\psi_t + 2a\cos(4\varphi_t)\sin^2(2\psi_t) - \frac{4b}{t_{-1}}\sin(2\varphi_t)\sin^2\psi_t = -8a + 2\frac{\kappa^2}{a}, \qquad \text{(A34)}$$

$$\frac{\partial^2 t_{-1}}{\partial \psi_t^2} = 2a\cos^2(2\varphi_t)\cos(2\psi_t) + 2a\sin^2 2\varphi_t\cos(4\psi_t) + \frac{2b}{t_{-1}}\sin(2\varphi_t)\cos(2\psi_t) = -2a, \qquad \text{(A35)}$$

$$\frac{\partial^2 t_{-1}}{\partial \varphi_t \partial \psi_t} = -2a\sin(4\varphi_t)\sin(2\psi_t) + a\sin(4\varphi_t)\sin(4\psi_t) - \frac{2b}{t_{-1}}\cos(2\varphi_t)\sin(2\psi_t) = 0. \qquad \text{(A36)}$$

All the necessary conditions (146) and (147) are fulfilled for any material with $\kappa > 1$.

REPEATED AXIAL LOADING

The three second derivations are:

$$\frac{\partial^2 f_{-1}}{\partial \varphi_r^2} = \frac{a}{2}\cos(4\varphi_r)\sin^2\psi_r + \left(4\sin^2\varphi_r - 1\right)\frac{a}{4}\cos^2\varphi_r \sin^2(2\psi_r) - \frac{b+d}{f_0}\cos(2\varphi_r)\sin^2\psi_r$$
$$\frac{\partial^2 f_{-1}}{\partial \varphi_r^2} = \frac{a}{2} - \frac{b+d}{f_0}, \qquad \text{(A37)}$$

$$\frac{\partial^2 f_{-1}}{\partial \psi_f^2} = \frac{a}{2}\sin^2(2\varphi_f)\cos(2\psi_f) + 2a\cos^4\varphi_f\cos(4\psi_f) + \frac{b+d}{f_0}\cos^2\varphi_f\cos(2\psi_f) = 2a - \frac{b+d}{f_0}, \qquad \text{(A38)}$$

$$\frac{\partial^2 f_{-1}}{\partial \varphi_f \partial \psi_f} = \frac{a}{8}\sin(4\varphi_f)\sin(2\psi_f) - \frac{a}{2}\cos^3\varphi_f \sin\varphi_f \sin(4\psi_f) - \frac{b+d}{2f_0}\sin(2\varphi_f)\sin(2\psi_f) = 0. \qquad \text{(A39)}$$

The three resulting conditions are:

$$a^2 - 5a\left(\frac{f_{-1}}{f_0}\right)^4 + 4\left(\frac{f_{-1}}{f_0}\right)^4 > 0 \quad \ldots\text{to find an extreme from (146),} \qquad \text{(A40)}$$

$$a < \left(\frac{2f_{-1}}{f_0}\right)^2 \text{ and } a < \left(\frac{f_{-1}}{f_0}\right)^2 \quad \ldots\text{to satisfy the conditions of maximum (147).} \qquad \text{(A41)}$$

The three conditions together are not fulfilled for any of materials presented here.